JAERI-M

91-104

EVALUATION REPORT ON SCTF CORE-III TEST S3-22

(INVESTIGATION OF WATER BREAK-THROUGH AND CORE COOLING BEHAVIORS UNDER ALTERNATE ECC WATER DELIVERY FROM HOT LEGS TO UPPER PLENUM DURING REFLOODING IN PWRS WITH COMBINED-INJECTION TYPE ECCS)

July 1991

Tsutomu OKUBO, Tadashi IGUCHI, Takamichi IWAMURA
Hajime AKIMOTO, Akira OHNUKI, Yutaka ABE
Hiromichi ADACHI* and Yoshio MURAO

日本原子力研究所
Japan Atomic Energy Research Institute

編集兼発行　日本原子力研究所
印　　刷　㈱原子力資料サービス

Evaluation Report on SCTF Core-III Test S3-22

(Investigation of Water Break-through and Core Cooling Behaviors under Alternate ECC Water Delivery from Hot Legs to Upper Plenum during Reflooding in PWRs with Combined-injection Type ECCS)

Tsutomu OKUBO, Tadashi IGUCHI, Takamichi IWAMURA
Hajime AKIMOTO, Akira OHNUKI, Yutaka ABE
Hiromichi ADACHI* and Yoshio MURAO

Department of Reactor Engineering
Tokai Research Establishment
Japan Atomic Energy Research Institute
Tokai-mura, Naka-gun, Ibaraki-ken

(Received June 5, 1991)

During the reflood phase of the loss-of-coolant accident (LOCA) in a German type Pressurized Water Reactor (GPWR) with a combined-injection type Emergency Core Cooling System (ECCS), the ECC water injected into the hot legs is considered to be delivered to the upper plenum. Although this water delivery was considered to be steady, there is some information which shows that the ECC water delivery to the upper plenum is not steady but alternate and intermittent due to condensation in the hot legs. One is based on recent test results from Upper Plenum Test Facility (UPTF) in Germany, and another is calculational results with TRAC codes developed in the USA.

Based on the information, two tests (Tests S3-20 and S3-22) were conducted with JAERI's Slab Core Test Facility (SCTF) Core-III in order to investigate water break-through and core cooling behaviors under the intermittent ECC water delivery from the hot legs to one location in the upper plenum and the alternate ECC water delivery to two locations in the upper

* Yamagata University

plenum during reflooding, respectively. Results of Test S3-20 (the intermittent case) were already analyzed and reported, and this report presents an analysis on Test S3-22 (the alternate case). In this test, subcooled ECC water was injected alternately just above the upper core support plate above Bundles 7 and 8 and Bundles 3 and 4. The total injection rate from both injection ports was set to be the same as that in SCTF Test S3-20 and Test S3-13, which was conducted with continuous ECC water injection under the Evaluation Model (EM) conditions.

Analyzing the test data together with those of Tests S3-13 and S3-20 the following has been found:

(1) Alternate break-through occurred immediately corresponding to the alternate ECC water injection except for one period, during which no break-through was observed. However, there observed a difference in break-through behavior that break-through was strong above the low power region, whereas weak above the high power region. The above-mentioned period with no break-through was one of periods with water injection above the high power region.

(2) Although its break-through behavior was different, nearly the same core cooling as in the continuous (Test S3-13) or intermittent (Test S3-20) ECC water delivery case was observed except for the period around quench (*i.e.* after about 75 s).

(3) Around quench time, degraded core cooling comparing to the continuous or intermittent ECC water delivery case was observed. That is, quench time at the midplane level of the present test was 35 s later than in the continuous case. This is considered to result from decrease in core water inventory caused by water sealing at the cross-over leg, which occurred at 76 s.

keywords : Reactor Safety, PWR, LOCA, Combined-injection Type ECCS, Reflood Experiments, Break-through, Core Cooling, SCTF, Heat Transfer Two-phase Flow

SCTF 第3次炉心試験 S3 － 22 評価報告書
（複合注水型 ECCS 付 PWR の再冠水時に於けるホットレグから上部プレナムへの ECC 水の交互流入下でのブレークスルー及び炉心冷却挙動の検討）

日本原子力研究所東海研究所原子炉工学部
大久保　努・井口　　正・岩村　公道・秋元　　肇
大貫　　晃・阿部　豊・安達　公道*・村尾　良夫

（1991 年 6 月 5 日受理）

複合注水型緊急炉心冷却系（ECCS）を備えたドイツ型加圧水型原子炉（GPWR）に於ける冷却材喪失事故（LOCA）時の再冠水過程では，ホットレグに注入された ECC 水は上部プレナムに供給されると考えられている。この供給は安定的に行われると考えられていたが，ホットレグ内での凝縮の為，安定的ではなく各ループから交互にかつ間欠的に行われるとの情報が存在する。その１つは，ドイツの上部プレナム試験装置（UPTF）による最近の実験結果であり，また他のものは，米国で開発された TRAC コードによる計算結果である。

これらの情報に基づいて，原研の平板炉心試験装置（SCTF）第 3 次炉心を用いて 2 回の試験（試験 S3 － 20 及び S3 － 22）を実施した。これらの試験では再冠水時に上部プレナムへの ECC 水の供給を 1 ヶ所に間欠的に及び 2 ヶ所に交互に行い，それぞれの場合に於けるブレークスルー及び炉心冷却挙動を検討した。試験 S3 － 20（間欠的なケース）の結果は既に解析されて報告されており，本報告書では試験 S3 － 22（交互のケース）に関する報告をする。本試験では，サブクール ECC 水をバンドル 7 と 8 の上方及びバンドル 3 と 4 の上方の上部炉心板直上に交互に供給した。注水流量の全体値は，平板炉心試験 S3 － 20 や評価モデル（EM）条件下で連続的に注水を実施した試験 S3 － 13 と同一に設定した。

本試験のデータを試験 S3 － 13 及び S3 － 20 のデータも含めて検討して，以下の事柄が明かとなった。

(1)　ブレークスルーが観測されなかった 1 つの期間を除いて，ECC 水の交互注入に即応してブレークスルーが 2 ヵ所に交互に発生した。しかし，ブレークスルーは炉心出力が低い領域の上方では強く，高い領域の上方では弱いという差がみられた。上述のブレークスルーの観測されない期間は，高出力領域上方への注水期間の一つであった。

(2)　本試験でのブレークスルー挙動は，ECC 水の供給が連続的（試験 S3 － 13）又は間欠的

東海研究所：〒 319-11 茨城県那珂郡東海村白方字白根　2 － 1
＊　山形大学工学部

（試験 S3 － 20）な場合とは異なっていたが，炉心冷却はクエンチ時期の近く（即ち，80 秒以降）を除いてそれらの試験とほぼ同じであった。

(3) クエンチ時期の近くでは，ECC 水の供給が連続的又は間欠的な場合と比較して炉心冷却が劣化していた。即ち，炉心中央高さ位置でのクエンチ時間は連続注水の場合に比べて 35 秒遅れた。これは，76 秒に生じたクロスオーバレグの封水により炉心の水のインベントリが減少したことによると考えられる。

目　　次

Contents

Table list

Figure list

1. Introduction

A Slab Core Test Facility (SCTF) test program is a part of a large scale reflood test program together with a Cylindrical Core Test Facility (CCTF) test program[1], which are performed by Japan Atomic Energy Research Institute (JAERI) under contract with Atomic Energy Bureau of Science and Technology Agency of Japan. The SCTF test program is also one of the research activities based on the trilateral agreement among JAERI, the United States Nuclear Regulatory Commission (USNRC) and the Federal Minister for Research and Technology (BMFT) of Federal Republic of Germany (FRG).

There are three test series (Core-I, -II and -III) in the SCTF test program. The SCTF Core-I[2] and Core-II[3] test series were already performed mainly to investigate two-dimensional thermal hydraulic behavior in the core during the reflood phase of a loss-of-coolant accident (LOCA) of a Westinghouse type (US/J-type) pressurized water reactor (PWR). On the other hand, one of the major objectives of the SCTF Core-III[4] test series was to investigate the effectiveness of the combined-injection type emergency core cooling system (ECCS) in a German type PWR (GPWR). In addition, simulation tests for a US/J-type PWR were also performed with the SCTF Core-III.

Reflood phenomena for PWRs with combined-injection type ECCS have been investigated mainly in FRG, since PWRs of such type are manufactured only there. However, test facilities used for the investigation are rather small in comparison with GPWRs, and it is considered to be necessary to investigate them further with a large scale facility. Therefore, tests to study the reflood phenomena for PWRs with the combined-injection type ECCS have been performed with the SCTF, because it has a large scale full radius core.

According to the previous information, the ECC water injected into the hot legs was considered to be delivered stably to the upper plenum during reflooding of a GPWR large-break LOCA. However, some information shows the delivery is not steady but alternate and intermittent. One is based on test results[5] from Upper Plenum Test Facility (UPTF) in FRG, and another is calculational results[6] with the TRAC codes developed in the USA.

Based on the information, one test was performed in order to investigate break-through and core cooling behaviors during the reflood phase of a GPWR under the evaluation model (EM) conditions with intermittent ECC water delivery to the upper plenum. This test was named Test S3-20 (Run 724)[7]. In this test, immediate break-through of ECC water was observed corresponding to each intermittent ECC water injection. However, results of another SCTF test (Test S3-8)[8] showed rather long delay (about 70 s) to establish stable break-through in saturated two-phase up-flow region. A reason for the difference between these two test results was considered to be almost doubly higher ECC water injection rate in Test S3-20 (intermittent injection though). Therefore, a test with better simulation of the alternate ECC water delivery to the upper plenum was proposed to clarify the unresolved issue mentioned above, and Test S3-22 was performed. The background for Test S3-22 is described more in detail in Chap. 3. This report describes the major results of this test and discussion on them.

A brief description of the SCTF Core-III is presented in Appendix A. Some selected data obtained in Test S3-22 are presented in Appendix B for better understanding of the test.

A brief information on the test is presented in the following:

1) Test name :

GPWR simulation integral EM test

where, GPWR : German type PWR with combined-injection type ECCS
EM : Evaluation model

2) Test number :

S3-22 (Run 726)

where, S : SCTF
3 : Core-III
22 : Sequential number of main tests

3) Objectives of test :

i) To investigate the break-through phenomena during the reflood phase in a GPWR under alternate ECC water delivery from the hot legs to the upper plenum

ii) To investigate core cooling phenomena during the reflood phase in a GPWR under alternate ECC water delivery to the upper plenum

4) Type of test :

Refill and reflood integral test simulating a GPWR under EM conditions

2. Test Description

2.1 Test Facility[4]

The SCTF was originally designed to study two-dimensional effects on thermal hydraulics during the reflood phase in a PWR core with full length radius[2],[3]. A flow diagram of the SCTF is shown in Fig. 2.1. The SCTF is simulating a 200% cold-leg-large-break with a simplified primary system and can be operated at system pressure less than 0.6 MPa. It consists of a pressure vessel, a combined intact loop, a broken loop at pressure vessel side, and a broken loop at steam-water separator side.

Figure 2.2 shows a vertical cross section of the pressure vessel. The pressure vessel includes a simulated core, an upper plenum with its internals, a lower plenum, a core baffle region and a downcomer. The configurations of the upper plenum structure and the end box simulate those of a 1,300 MWe class GPWR as practically as possible.

The core is full-height, full-radius and one-bundle width one. Core flow area scaling ratio is 1/24 to a typical 1,300 MWe class GPWR. 1,888 electrical heater rods to simulate fuel rods are installed in the core. Dimensions of a heater rod is 10.7 mm in diameter and 3,613 mm in heated length simulating those of PWRs. The maximum available power supplied to the core is 10 MW.

The heater rods are assembled in a 16 x 16 square array bundle being positioned with grid spacers. Eight bundles are installed in a row in the core, as shown in Fig. 2.2. In the SCTF, the leftmost bundle in the figure is named Bundle 1 and orderly to the right direction the bundles are named Bundle 2, 3, ..., 8. Since the downcomer and the hot leg are connected to Bundle 8 side, Bundle 1 and 8 sides are corresponding to the central and the peripheral sides of PWRs, respectively.

The ECC water can be injected into the lower plenum, the cold leg and the upper plenum in the SCTF. Since the SCTF has no injection port in the hot leg, the hot leg injection of the ECC water in PWRs with combined-injection type ECCS was substituted by the upper plenum injection. The ECC water can be injected into the upper plenum from both top and side (just above the upper core support plate (UCSP)) walls.

The core and the upper plenum are enveloped by honeycomb thermal insulators with wall plates to minimize the wall thermal effects.

Description of the SCTF Core-III is presented more in detail in Appendix A.

2.2 Test Conditions and Sequence

Test conditions were selected to simulate the refill and reflood phenomena under the EM conditions for a GPWR 200% cold-leg-large-break LOCA. The bases for the test conditions are summarized in Sec. 2.3. Table 2.1 gives planned and the measured test conditions.

Figure 2.3 shows the conceptual initial set-up of the facility for Test S3-22. The ECC water was injected alternately from injection ports located just above the UCSP (side injection ports named UCSP1 and UCSP3) and at the cold leg. The ports UCSP1 and UCSP3 are located above Bundles 7 and 8 and Bundles 3 and 4 of the core, respectively. Although ECC water injection into the upper plenum was alternate, total value for all ports was set to be the same as that for SCTF Test S3-13[9], which is an integral test performed under the EM conditions, and Test S3-20[7].

Orifice diameters for the steam-water separator side broken cold leg, the intact cold leg and the pump simulator were 75.1, 164.5 and 173.7 mm, respectively. No orifice was inserted in the pressure vessel side broken cold leg. Water in the steam-water separator was set to be drained to the containment tank II to keep the maximum water level in the steam-water separator at 1.1 m. Differences in test conditions between Tests S3-22 and S3-13 were the upper plenum water injection sequence (alternate *vs.* steady) and the loop flow resistance, small difference though. The difference between Tests S3-22 and S3-20 was only the upper plenum water injection sequence (alternate *vs.* intermittent).

Figure 2.4 shows sequence of Test S3-22. In this figure, the time when the maximum clad temperature reached 700 ^{o}C is defined as 0 s. Pressure in the containment tank II was kept constant at 0.3 MPa by controlling discharge rate of steam through the blow valve to the atmosphere after 0 s. The ECC water was injected both into the cold leg and the upper plenum after 0 s. ECC water injection rate into the upper plenum was oscillatory as show in Fig. 2.4. Water temperature for this was set to 35 ^{o}C. Injection rate from the cold leg was decreased monotonously. Temperature of the water was also 35 ^{o}C. Core power was initially set at 7.5 MW and was decreased to simulate decay as shown in Fig. 2.4.

2.3 Bases for Test Conditions

Bases for the test conditions are summarized in Table 2.2. A brief explanation is as follows:

(1) Pressure

According to TRAC calculations for the GPWR large-break LOCA, pressure in the pressure vessel is about 0.3 MPa during the reflood period. Accordingly, pressure in the containment tank II was determined to be 0.3 MPa and was intended to be kept constant during the reflood phase. However, the initial pressure in the primary system was set at 0.6 MPa and decreased to 0.3 MPa after 0 s by opening the blowdown valves (*i.e.* V1 and V2 in Fig. 2.3) in order to simulate the end of the blowdown and refill phases.

(2) Core power

Core power for the present test was determined by the following equation:

$$P_{SCTF} = P_{o\ GPWR} \times S_F \times (\text{Old ANS} \times 1.03 + \text{Act.})$$

(t s after scram)

where, $P_{o\ GPWR} = 3765$ MW

$$S_F = \text{Scaling ratio} = \frac{\text{SCTF core volume}}{\text{GPWR core volume}} = \frac{0.8931}{21.5} = \frac{1}{24.07}$$

$t = 25$ s

As a result,

$$P_{SCTF} = 7.5 \text{ MW}$$

(3) Power profile

Radial power ratio in the present test at given radius F(r) was determined to simulate that in a GPWR. Namely,

$$F(r)_{SCTF} = k \cdot F(r)_{GPWR}$$

where, $F(r)_{SCTF}$ is based on the slab geometry, while $F(r)_{GPWR}$ is based on the sector or circular geometry. The constant k was determined to achieve

$$(F(r)_{SCTF})_{Average} = 1.0$$

(4) Initial clad temperature

Initial clad temperature was determined to simulate the stored energy of rods at pressure of 0.6 MPa. The referred data base is the test result of PKL-IIB-2 performed in FRG.

(5) Mode of ECC injection

Since the present test is an integral test to investigate effects of alternate ECC water delivery to the upper plenum on water break-through and core cooling behaviors, the ECC water was injected at the cold leg and on the UCSP of the upper plenum instead of the hot leg. Injection locations on the UCSP were corresponding location above Bundles 7 and 8 and Bundles 3 and 4.

Selection base for the ECC injection mode is the same as in Tests S3-13 and S3-20 and summarized in Table 2.2. This is one of the EM conditions and based on the following situation proposed by FRG:

(i) The ECC water injected into the broken cold leg is not effective

(ii) One Low Pressure Coolant Injection (LPCI) pump is not working

(iii) One Accumulator (Acc) in the hot leg is under repair

(iv) One valve in the hot leg injection line is closed as an assumption of the single failure.

(6) ECC injection rate and temperature

According to the mode of the ECC injection presented above, the injection rates are determined as:

3 Acc + 2.6 LPCI (cold leg)
2 Acc + 1.4 LPCI (upper plenum)

2.4 Measured Boundary Conditions

Major measured test conditions are listed in Table 2.1. Table 2.3 shows the chronology of events occurred during the test. Figures 2.5 to 2.10 show the measured boundary conditions of the test.

There observed no significant differences between the planned and the measured except for the pressure in the upper plenum. The pressure was controlled at 0.3 MPa by venting the excessive steam. However, the control was not accurate enough to keep the pressure at 0.3 MPa because of oscillatory steam generation and condensation due to alternate subcooled ECC water injection, so that the pressure decreased oscillatory, as shown in Fig. 2.5.

Table 2.1 Conditions for Test S3-22

Item	Planned	Measured
Pressure (MPa)		
Containment tank	0.3	0.29 ~ 0.39
Pressure vessel	0.6 → 0.3	0.6 → 0.29 ~ 0.39
Power		
Initial power (MW)	7.5	7.48
Decay curve	ANS x 1.03 + Act.	ANS x 1.03 + Act.
Time after scram (s)	25	25
Radial profile	1.04:1.08:1.08:1.04 :1.04:1.04:0.97:0.71	1.05:1.08:1.08:1.04 :1.04:1.04:0.97:0.71
Peak clad temperature at ECC water injection initiation (K)	973	1032
ECC water injection location	UCSP1, UCSP3 and cold leg	UCSP1, UCSP3 and cold leg
UCSP injection		
Injection rate (kg/s)	As specified	See Fig. 2.6
Water temperature (K)	308	310
Cold leg injection		
Injection rate (kg/s)	As specified	See Fig. 2.7
Water temperature (K)	308	310

Table 2.2 Summary of bases of test conditions

Pressure		
in PV	0.6 MPa → 0.3 MPa	Blowdown from 0.6 MPa
in CT II	0.3 MPa	TRAC calculation
Power		
Initial power	7.5 MW	Scaled value (following Eq.)
Decay curve	P_o x (Old ANS x 1.03+ Act.)	Similar to GPWR-EM
Timing at 0.6 MPa 25 s after scram		
Power profile	1.04:1.08:1.08:1.04 :1.04:1.04:0.97:0.71	Preserved GPWR power profile against radius
Clad temperature		
Initial PCT (0.6 MPa, GPWR profile)	973 K	-Preserved GPWR initial stored energy -Referred to PKL-IIB-2 result
ECC mode		
CL	3 Acc + 2.6 LPCI	-ECC into broken cold leg is not considered
HL	2 Acc + 1.4 LPCI	-One HL valve is on single failure -One LPCI pump and one hot leg Acc are under repair

Timing equation:

$$P_{SCTF} = P_{o\ GPWR} \times S_F \times (\text{Old ANS} \times 1.03 + \text{Act.}), \quad \text{after t sec}$$

$P_{o\ GPWR}$ = 3765 MW

S_F = 0.8931/21.5 = 1/24.07

t = 25 s

* Note

PV : pressure vessel

PCT: peak clad temperatture

HL : hot leg

CT : containment tank

CL : cold leg

Table 2.3 Chronology of events for Test S3-22

Item	Time (s)
Core power "ON"	0
System depressurization initiation	108.0
Core power decay initiation	108.0
UCSP injection initiation	108.0
Cold leg injection initiation	108.0
BOCREC	124.0
Whole core quench	282.5

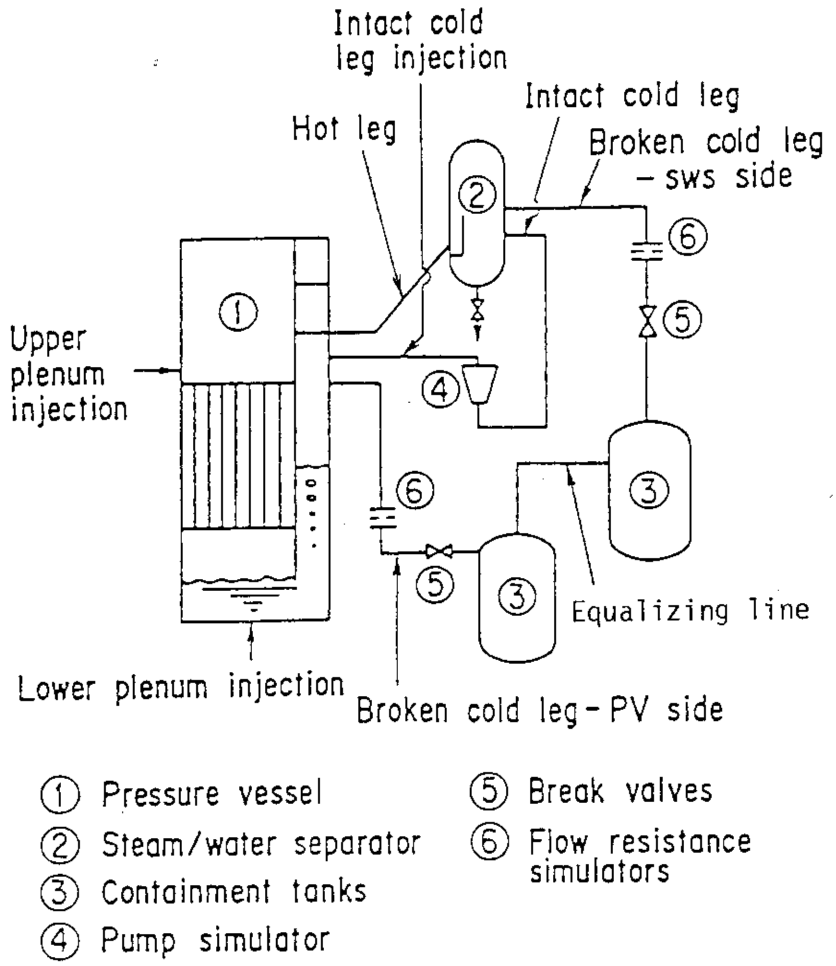

Fig. 2.1 Flow diagram of SCTF

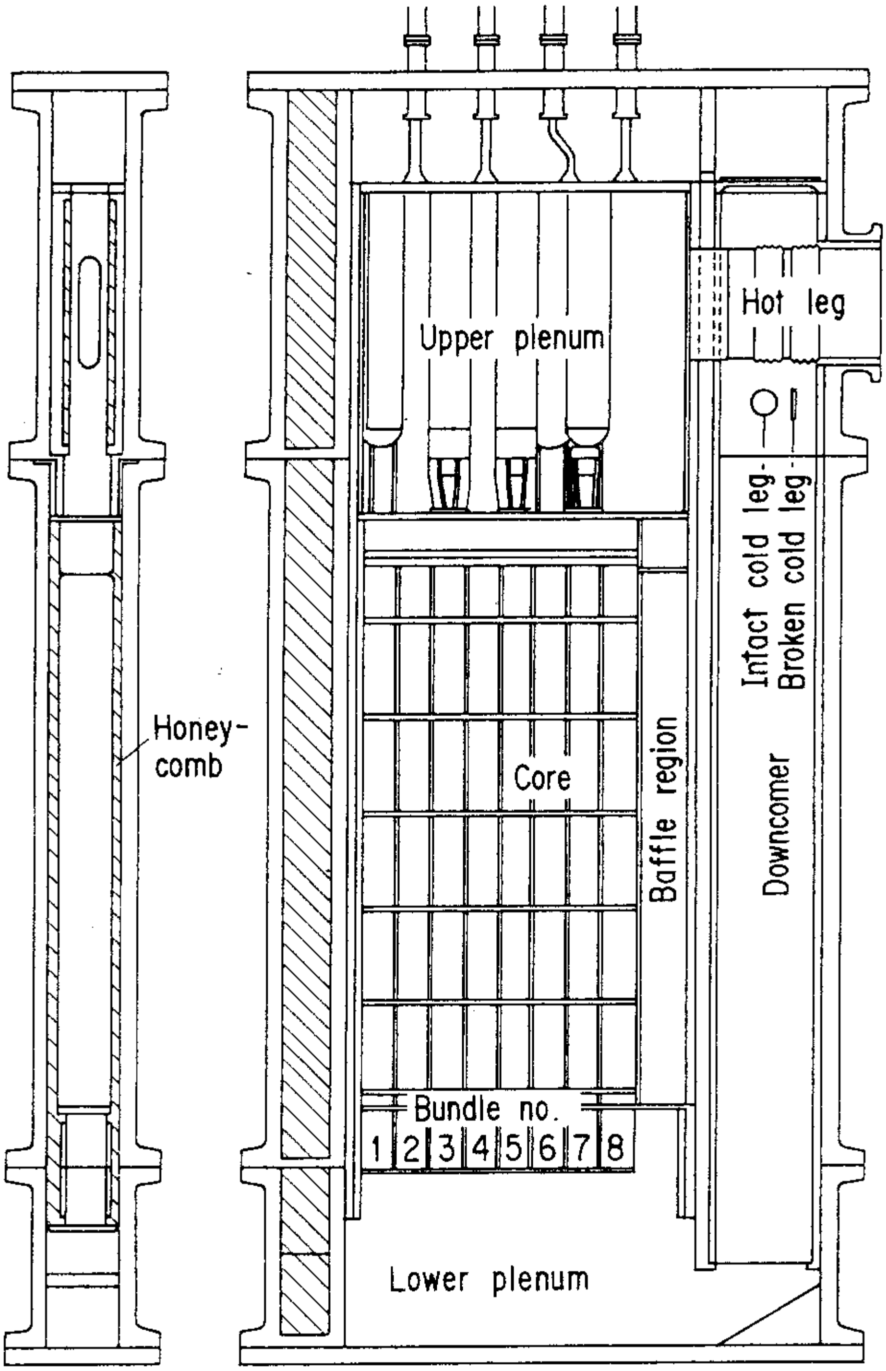

Fig. 2.2 Vertical cross section of pressure vessel

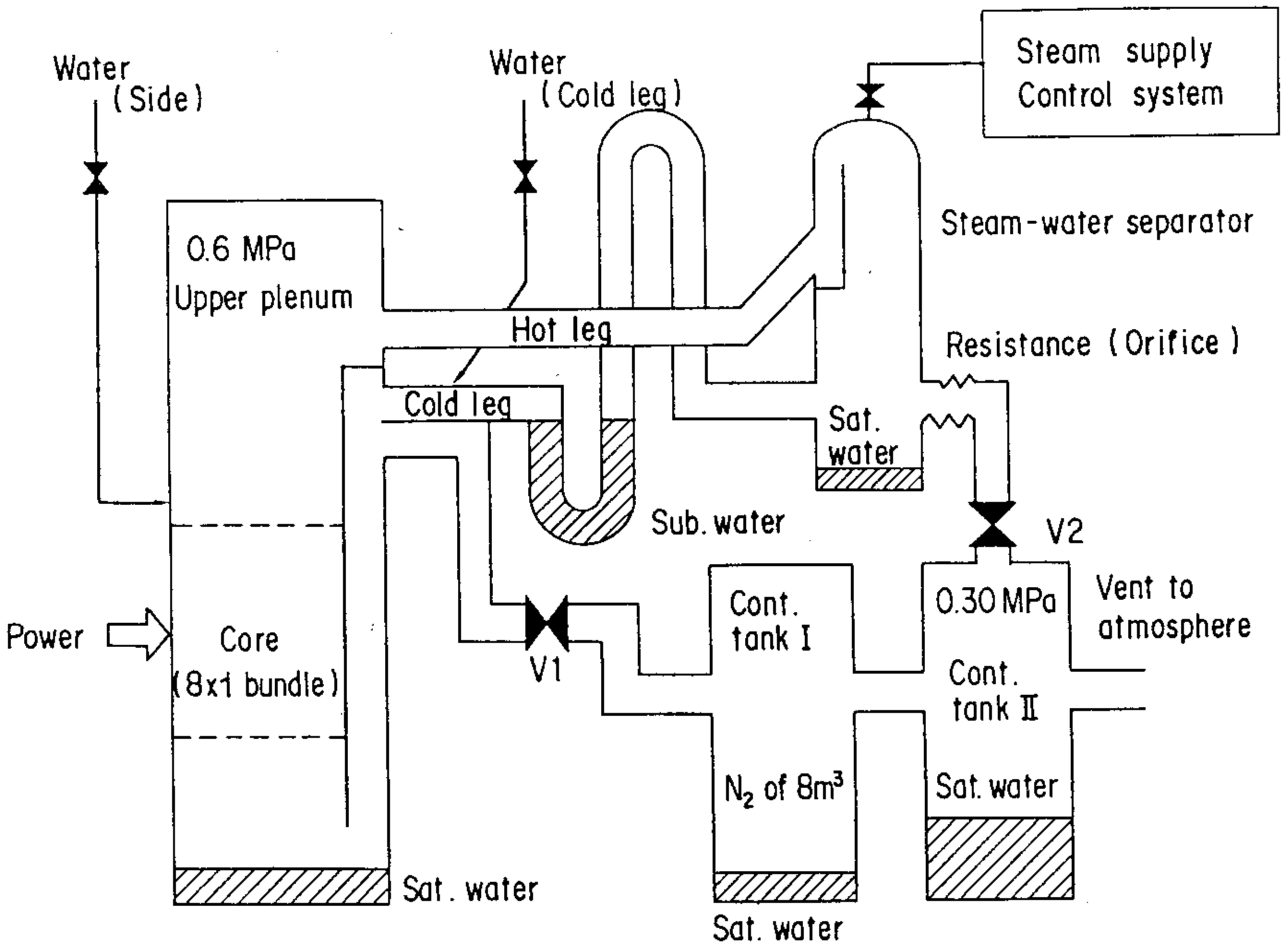

Fig. 2.3 Initial set-up of Test S3-22

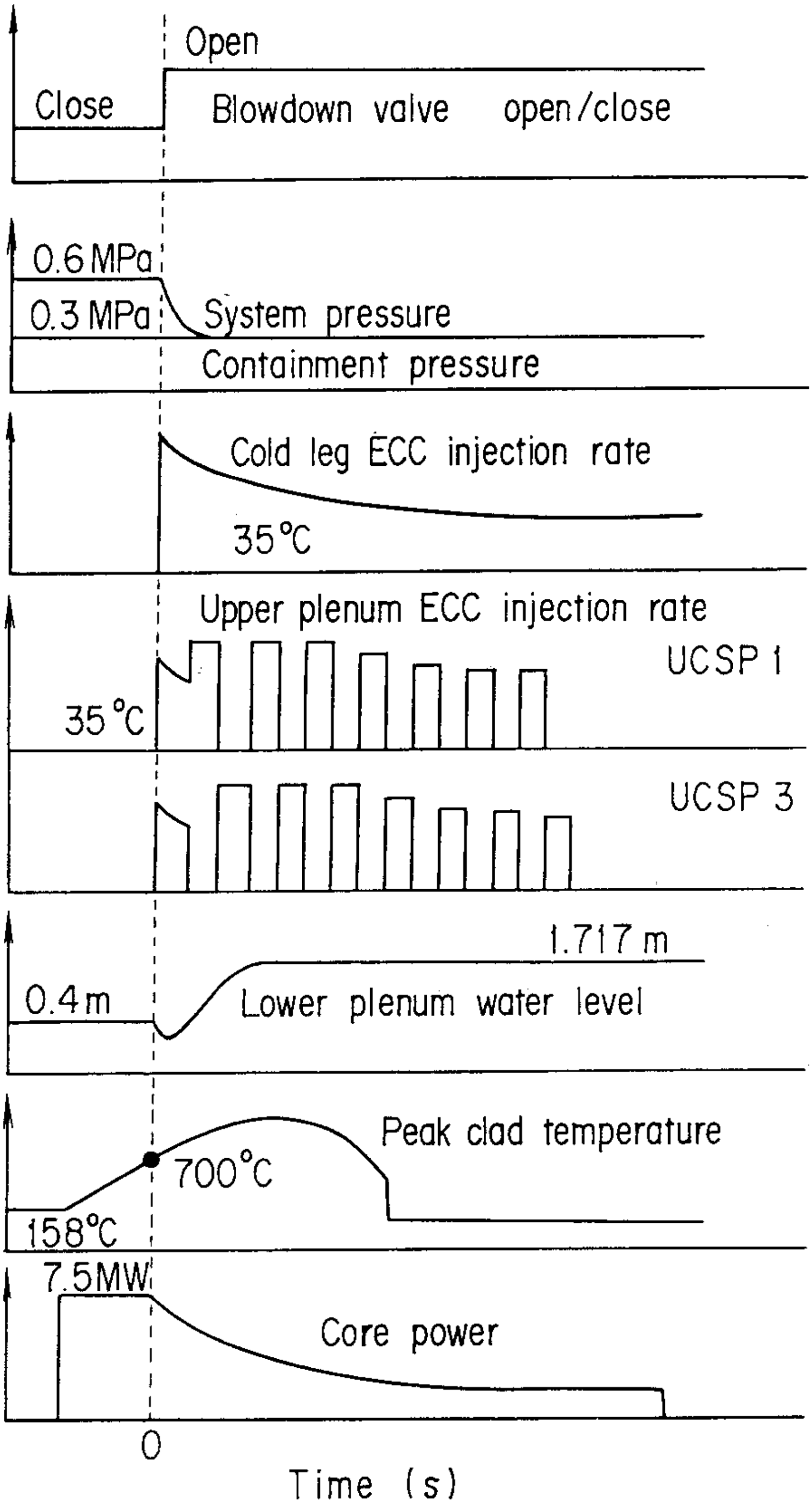

Fig. 2.4 Sequence for Test S3-22

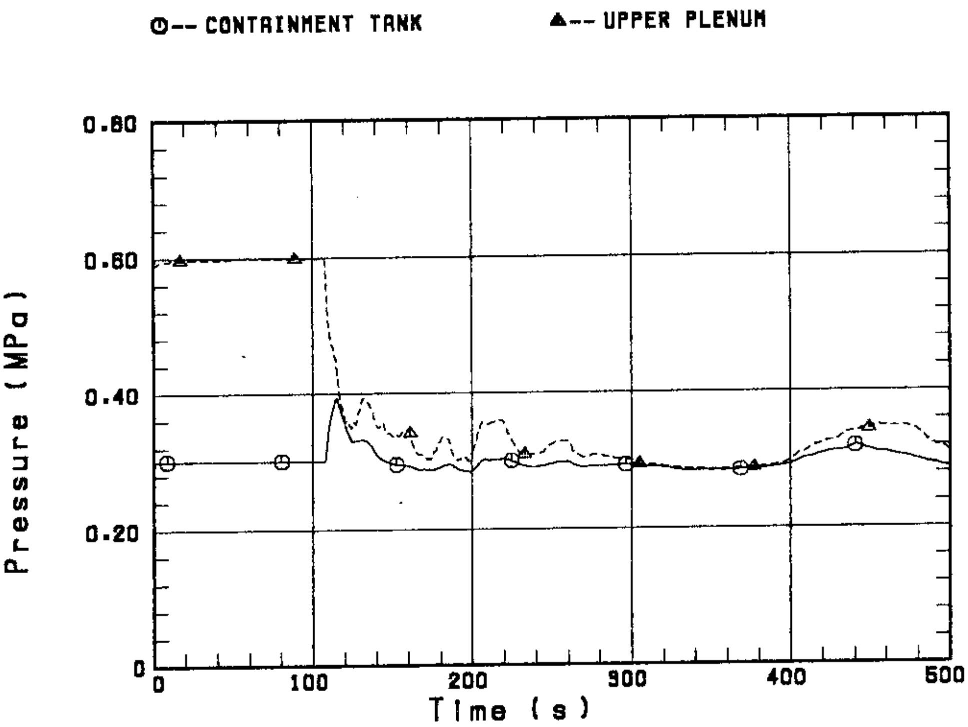

Fig. 2.5 Pressures of containment tank II and upper plenum

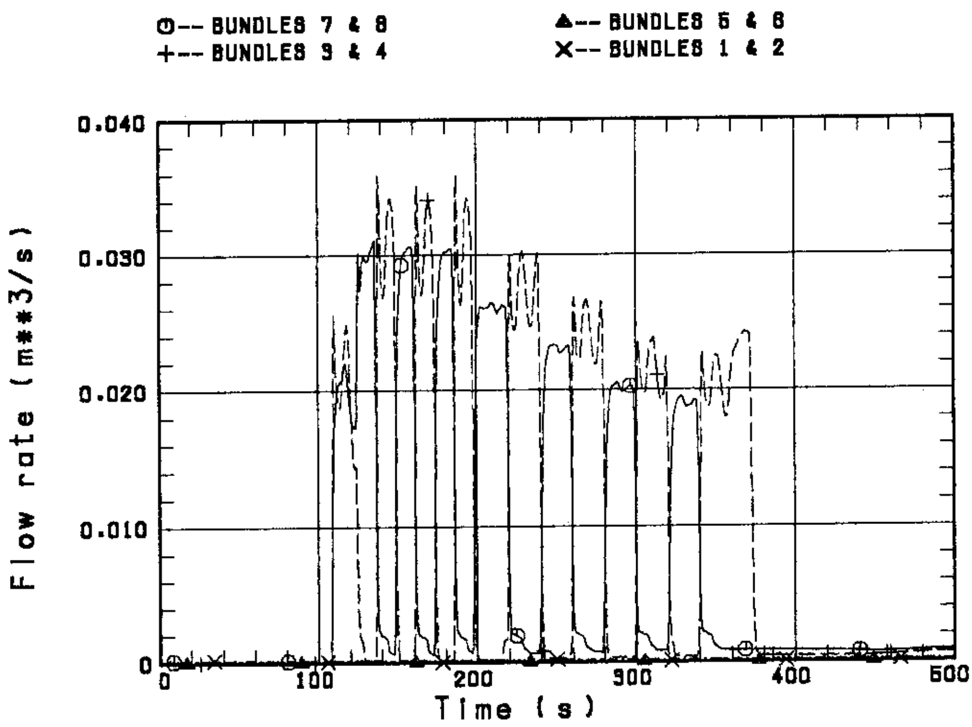

Fig. 2.6 ECC injection rate into upper plenum

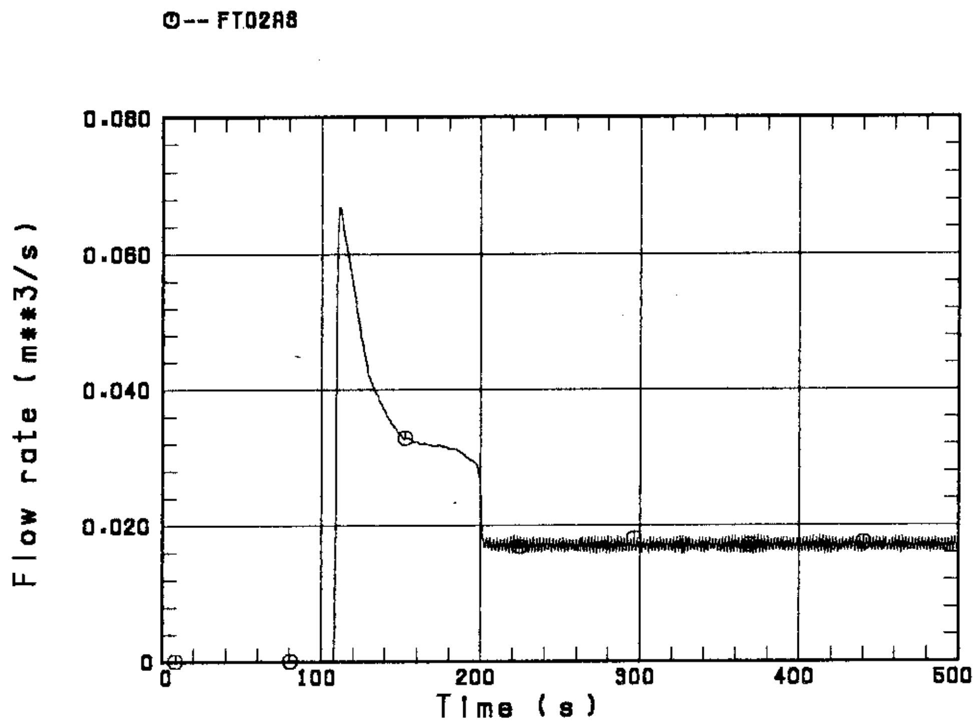

Fig. 2.7 ECC injection rate into cold leg

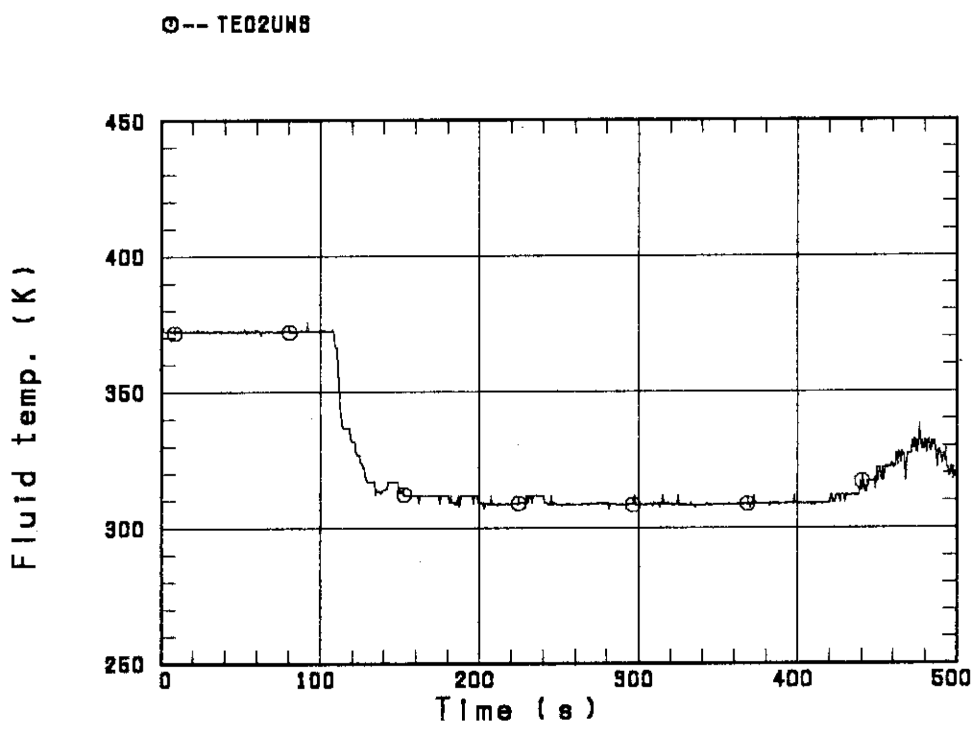

Fig. 2.8 Water temperature of upper plenum injection

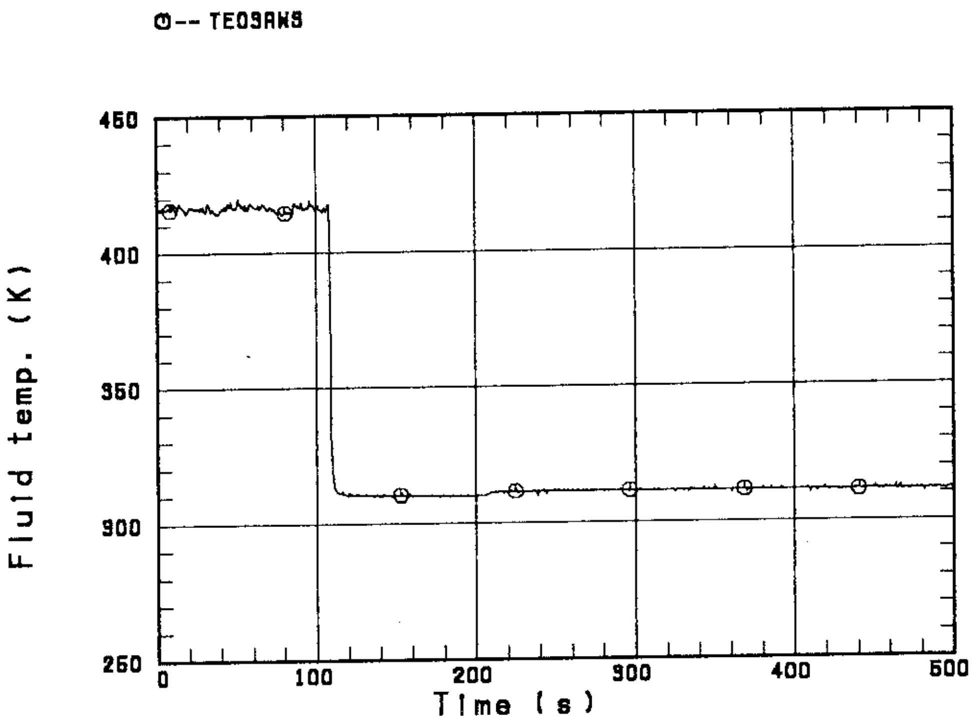

Fig. 2.9 Water temperature of cold leg injection

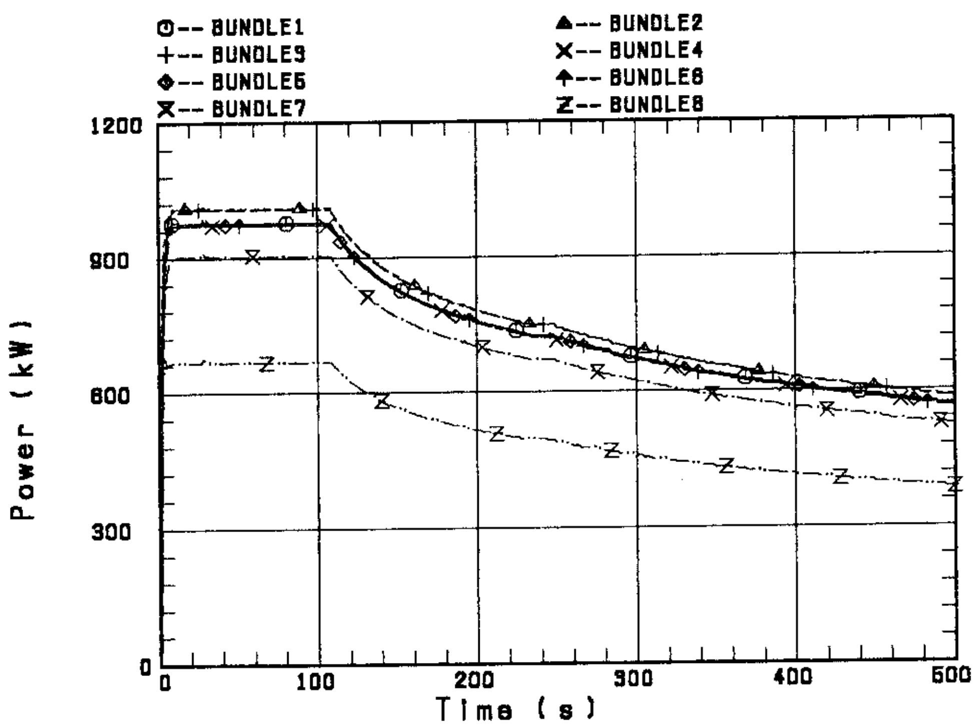

Fig. 2.10 Supplied core power

3. Background of Test

In order to understand purposes of the present test well, background of the test is described in the following. As mentioned in Chap. 1, water delivery from the hot legs to the upper plenum was considered to be steady during reflooding of a large-break LOCA in a GPWR. However, some recent information shows that the water delivery is not steady but alternate and intermittent. One is recent test results[5] from the UPTF in FRG, and another is calculational results[6] with TRAC codes. According to the information, the ECC water injected into the hot legs (two hot legs out of four under the EM condition) are delivered to the upper plenum intermittently. This is explained due to condensation induced oscillation in the hot legs. Furthermore, phase of the oscillations in the different hot legs are opposite. Therefore, the ECC water delivery from the hot legs to the upper plenum is alternate. That is, the ECC water is delivered to the upper plenum from one of the two hot legs for some time, and then the delivery stops and the delivery from the other hot leg starts. In this manner the water delivery from the hot legs to the upper plenum takes place alternately.

Based on the information above, a SCTF test (Test S3-20[7]) was performed under the intermittent ECC water delivery to the upper plenum (Fig. 3.1). In this test, only the intermittent rather than the alternate ECC water delivery to the upper plenum was separately investigated. That is, as shown in Fig. 3.1 the ECC water was injected intermittently above Bundles 7 and 8 at the rate of about 50 kg/s, which is about twice of the rate for the continuous ECC water delivery test (Test S3-13[9]). Results of the test showed intermittent break-through corresponding to the intermittent ECC water injection as shown in Fig. 3.2, and oscillatory core cooling shown in Fig. 3.3. However, on the other hand, results of another SCTF test (Test S3-8[8]) showed that change of the ECC water injection location resulted in some delay (about 65 s) in establishing stable break-through as shown in Fig. 3.4, and hence, degraded core cooling comparing to the corresponding continuous injection case (Test S3-SH1[10]) as shown in Fig. 3.5. This delay in establishing break-through is considered[8] to be caused as follows: Before the change of the ECC water injection location, non-break-through region (Bundle 4) was full of saturated water. Therefore, even the subcooled ECC water was changed to be injected above Bundle 4, it took some time for the subcooled water to swap with the saturated water. In this way, it took some time in establishing stable break-through above Bundle 4.

The above results suggested that when the ECC water delivery was intermittent, there was a possibility that break-through would not occur intermittently. This was because temperature of the water above the UCSP becomes saturated when the ECC water injection stopped, and hence, the situation became similar to that in Test S3-8. However, results of Test S3-20 showed immediate break-through after the corresponding intermittent ECC water injection as shown in Fig. 3.2. A reason for this immediate break-through occurrence was considered to be the high (almost twice) ECC water delivery rate in Test S3-20. In the real situation, delivery of the ECC water to one specified region of the upper plenum is expected to be around 25 kg/s and the location of the ECC water delivery is different from time to time corresponding to the active hot leg location, in which the ECC water is injected. Under the injection rate of about 25 kg/s, the similar delay in break-through to that in Test S3-8 was considered to take place. Based on the consideration above, it was considered to be meaningful to investigate break-through and core cooling behaviors under more realistic alternate ECC water injection condition, and hence, Test S3-22 was performed as the last test with the SCTF Core-III test facility.

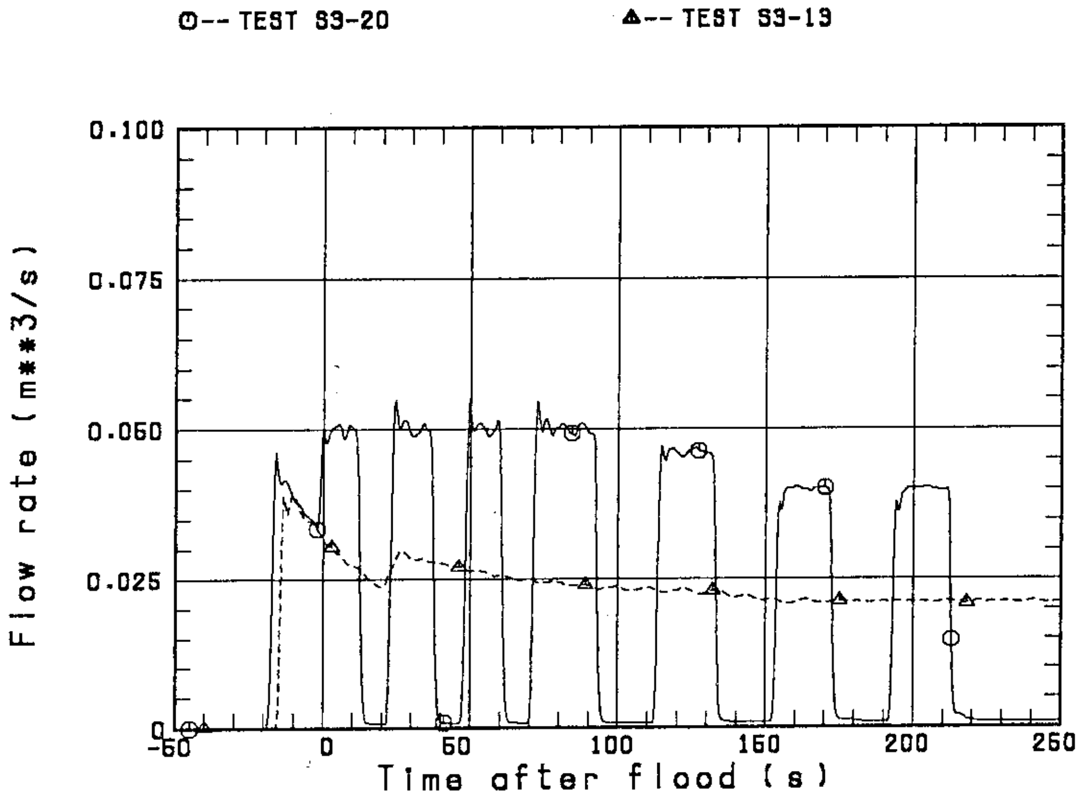

Fig. 3.1 ECC water injection rate into upper Plenum in Test S3-20 compared with that in Test S3-13

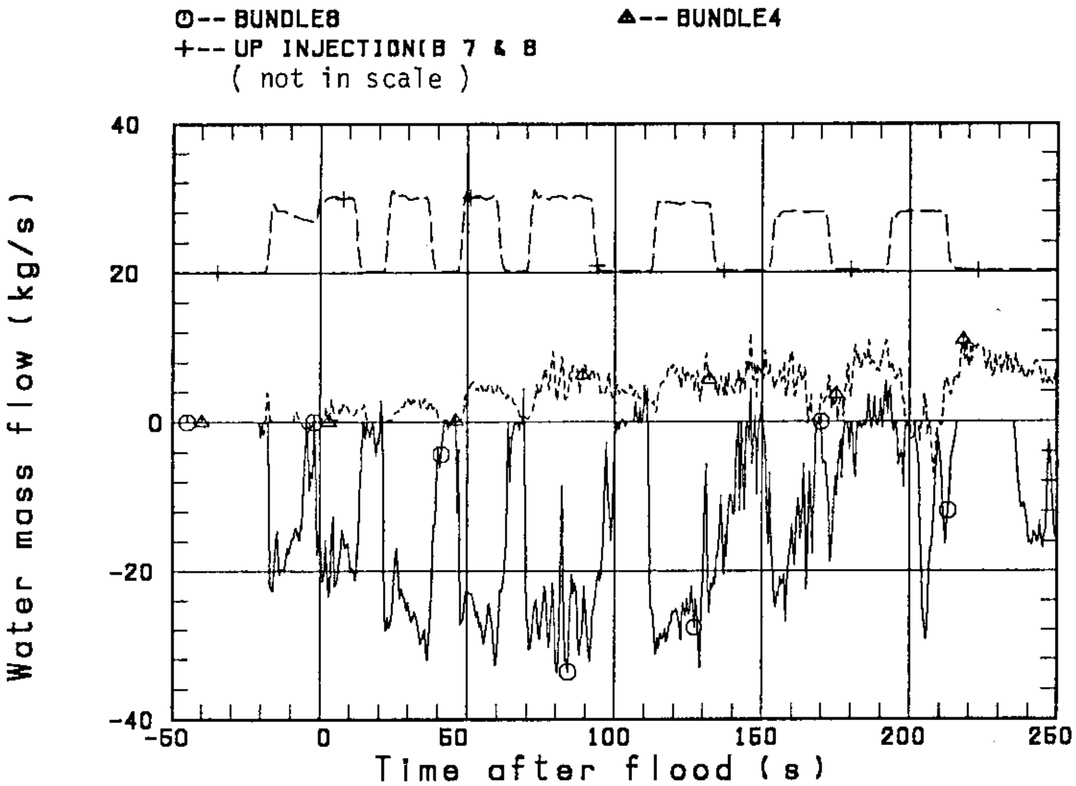

Fig. 3.2 Tie plate water mass flow rates in Test S3-20

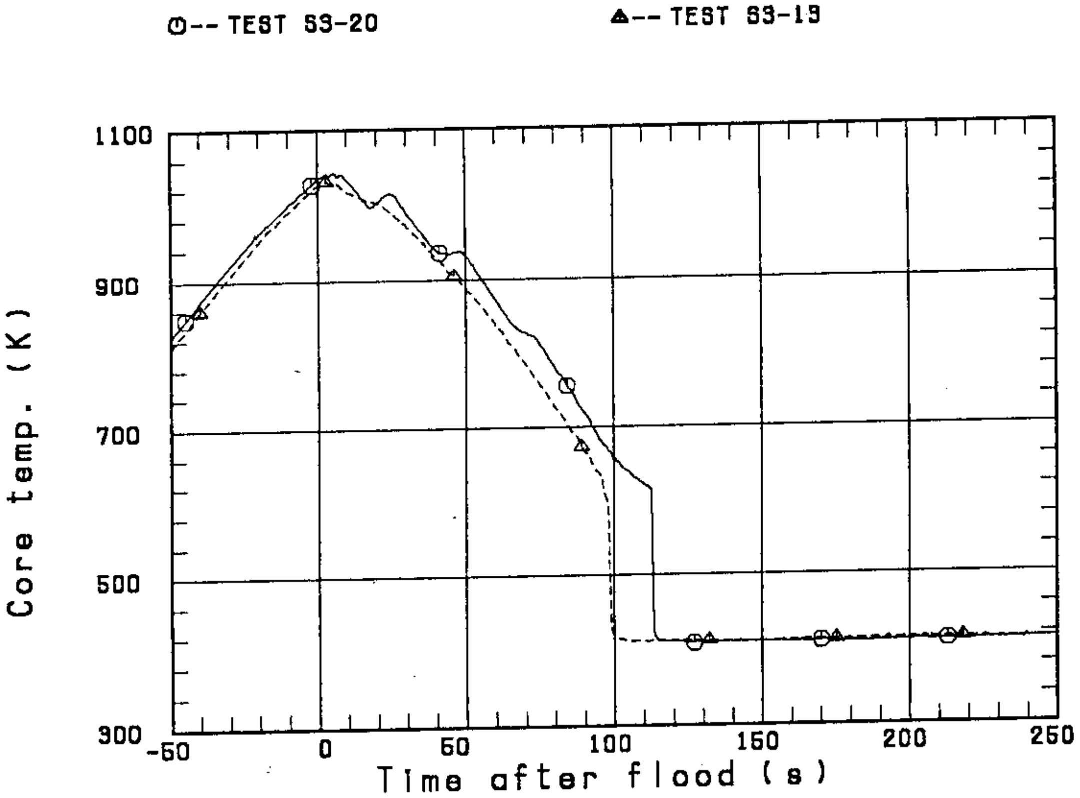

Fig. 3.3 Clad surface temperature at 1,905 m elevation in Test S3-20 compared with that in Test S3-13

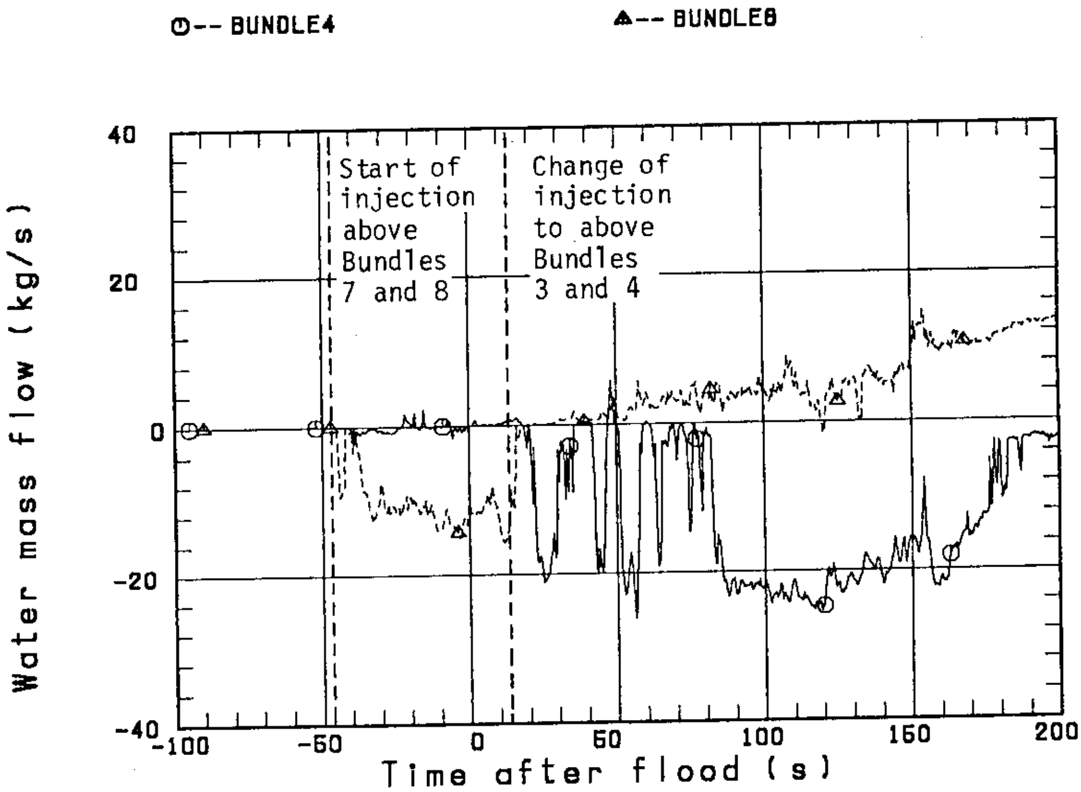

Fig. 3.4 Tie plate water mass flow rates in test S3-8

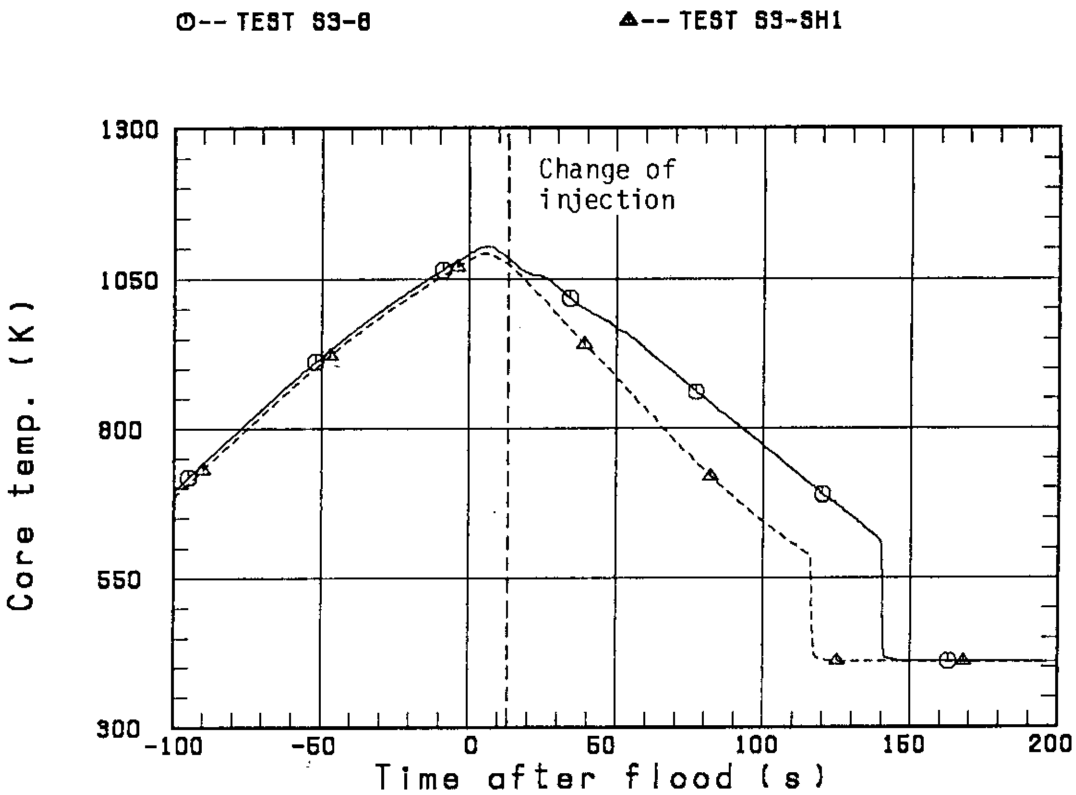

Fig. 3.5 Clad surface temperature at 1,905 m elevation in Test S3-8 compared with that in Test S3-SH1

4. Test Results and Discussion

4.1 Break-through Behavior

ECC water injection rate into the upper plenum is shown in Fig. 4.1 together with that for Test S3-13. There are seven oscillations in injection rate. Although total value from all injection ports were set to be the same as that for Test S3-13, it is larger in the present test. Duration of injection was set to 12 s for the initial three, 21 s for the fourth and 20 s for the rest. Time-integrations of measured injection rates are not the same and that for the present test is larger by about 11% at 283 s, by when whole core quench was attained.

Figure 4.2 shows differential pressures across the tie plate. ECC water injection rate into the upper plenum is also shown in the figure to compare relation among them. The differential pressures above Bundles 7 and 8 become negative corresponding to the increase in the water injection rate above those bundles except for the last one, indicating occurrence of break-through. For the last injection period, there observed no break-through. This is because the core was completely filled with water by that time, and hence, break-through was not possible any more. When the injection decreases, the differential pressures become zero or positive, indicating stop of break-through. Above Bundles 3 and 4, the differential pressure above Bundle 3 shows negative value only during the initial two injection periods, whereas above Bundle 4 it shows negative value except the third one and the last two ones. Since the core had a radial power profile in the three concerned tests and the power ratio for Bundles 3, 4, 7 and 8 were 1.08, 1.04, 0.97 and 0.71, respectively (see Table 2.1), the test results indicate that break-through was strong above the low power region but weak above the high power region.

It should be noted that break-through was observed in the present test except only one time period. This is a different tendency from expected based on the results of Test S3-8 as discussed in Chap. 3. Main reason for the difference in break-through characteristic is considered to be the alternate ECC water delivery. In the alternate ECC water delivery case, the cold ECC water is injected into the same location just 10 to 20 s before. Therefore, the local average temperature of water accumulating in the upper plenum around the ECC water delivery location is considered to be lower than in the case of Test S3-8, and hence, break-through to occur more easily. This would be a general explanation for the occurrence of break-through in the alternate ECC water delivery case.

Figure 4.3 shows fluid temperatures just below the tie plate holes. Except only one time period (the third injection period above Bundles 3 and 4), the temperatures become lower corresponding to increases in water injection rate, suggesting occurrence of break-through. Water mass flow rates at the tie plate shown in Fig. 4.4, which were measured with the advanced two-phase flow instrumentation provided by USNRC, also indicate that break-through occurred above Bundle 8 corresponding to the increase in the injection rate and it stopped corresponding to the decrease in the injection rate. Above Bundle 4, on the other hand, there observed no break-through during the third injection period and weaker break-through than above Bundle 8 was observed during the initial 100 s. Break-through mass flow rate was about 20 kg/s per bundle above Bundle 8 and is much higher than the water injection rate (about 10 ~ 15 kg/s per bundle). This indicates more water than injected fell down above Bundle 8, suggesting the effect of the core radial power distribution mentioned above.

4.2 Core Water Accumulation and System Behaviors

Figure 4.5 shows the core differential pressure compared with that for Test S3-13. The data for the present test experience small oscillation and become much smaller after about 75 s. Although the small oscillation did not influence core cooling, the smaller differential pressure after about 75 s gave a remarkable effect on core cooling as shown later. Figure 4.6 shows the intact loop differential pressure compared with the core differential pressure. As recognized from these data, when the core differential pressure is smaller after 75 s, the intact loop differential pressure becomes larger. Accordingly, it is inferred that the increase in intact loop differential pressure resulted in the decrease in core differential pressure. In general, intact loop differential pressure decreases gradually as the reflooding goes on due to the core power decay. Therefore, the observed increase in intact loop differential pressure after 75 s in the present test is unique, and hence, the reason for this is investigated in the following.

Figures 4.7 through 4.9 show differential pressures in the intact cold leg. Measurement locations of them are illustrated in Fig. 4.10. An orifice with rather high flow resistance is included in the measuring section for the differential pressure of DT01CS. The other sections only consist of pipes, and hence, flow resistance is small. As shown in Fig. 2.3, the cross-over leg was initially filled with subcooled water. Therefore, these differential pressures initially give the water head. During depressurization (starts at -16 s after flood) the water head decreased and the cross-over leg became empty until 76 s as shown in Figs 4.7 and 4.8. Figure 4.9 does not only give water head but gives frictional pressure drop across the orifice, and hence, gives positive value until 76 s. Around 76 s, these differential pressures increased significantly suggesting loop seal of the cross-over leg with the ECC water from the cold leg injection port. As illustrated in Fig. 4.10, pipe in the steam/water separator side was only partially filled, judging from data in Fig. 4.7, and this resulted in the rather high intact loop differential pressure shown above.

Figures 4.11(a) through (c) show fluid temperatures at three locations illustrated in Fig. 4.10. From these data, subcooled water came to the pump exit at 70 s (see Fig. 4.11(a)), and then reached pump bottom at 74 s (see Fig. 4.11(b)), and finally arrived at bottom of the cross-over leg at 76 s (see Fig. 4.11(c)) establishing the loop seal.

The reason for occurrence of the loop seal is considered to be the low loop steam mass flow rate around 70 s shown in Fig. 4.12. As described above, the reversal flow from the ECC port to the cross-over leg was observed first at 70 s. Therefore, it is inferred that steam mass flow rate in the primary loop decreased and could not obstruct any more the flow reversal of the cold leg ECC water to the cross-over leg at 70 s.

There are two possible reasons for the decrease in the loop steam mass flow rate around 70 s mentioned above. One is significant decrease in core outlet steam mass flow rate around 70 s shown in Fig. 4.13, which were evaluated with steam mass flow rate measured with the tie plate "flow modules" provided by USNRC. The other is significant increase in upper plenum water level around 70 s shown in Fig. 4.14, which is considered to decrease steam mass flow rate due to steam condensation. Increase in upper plenum water level corresponds to weak or no water break-through above Bundles 3 and 4 as shown in Fig. 4.2 or 4.4.

The decrease in core outlet steam mass flow rate around 70 s shown in Fig. 4.13 is explained as follows. Figure 4.15(a) and (b) show evaluated fluid temperature distributions in the core with contour lines at two times. Contour line 7 gives the saturation temperature and contour lines 6, 5, ..., 1 give subcooling of 10 K, 20 K, ..., 60 K, respectively. At 55 s, fluid temperature distribution is almost the same in both tests and subcooled water exists only around Bundles 7 and 8. However, at 70 s, the distribution is different between the two tests. Subcooled water exists both around Bundles 7 and 8 and Bundles 3 and 4 in the present test, whereas only around Bundles 7 and 8 in Test S3-13. That is, in the late period of reflooding, region of subcooled water is larger in the alternate injection case than in the continuous injection case. This is considered to be because subcooled water can spread more when the break-through location is more and simultaneously the core power is rather small. Anyway, the larger is the subcooled water region, the smaller is expected to be the core outlet steam mass flow rate.

From above discussion, it is expected that, in the alternate ECC water delivery case, steam flow rate in the primary loop becomes very small in a late period and results in loop seal at cross-over leg. However, the applicability of the present test results to the PWR under the alternate ECC water delivery will be further discussed later in Section 4.4.

4.3 Core Cooling Behavior

Figure 4.16 shows the clad surface temperatures at 1.905 m elevation, which is close to the midplane level of the core. Corresponding heat transfer coefficients are presented in Fig. 4.17. Quenching occurred significantly early in Bundle 8, then Bundle 4, and then Bundle 7, and finally the other bundles. As recognized from Fig. 4.17, core cooling started before the reflood initiation in Bundles 3, 4, 7 and 8, indicating the effect of break-through. In the other Bundles, it started after the reflood initiation. At about 75 s, heat transfer coefficients started to decrease as shown in Fig. 4.17. This is considered to result from the decrease in core water inventory described in the previous section.

Figures 4.18 and 4.19 show comparisons of clad surface temperatures at 1.905 m elevation and the corresponding heat transfer coefficients, respectively, among Tests S3-22, S3-13 and S3-20. Although the present test gave the worst results after about 75 s (resulting in later quench time by 35 s at the midplane level than in the continuous case) comparing to the other two tests, core cooling of the three tests were very good and almost the same during the major period. This is considered to be because the amount of break-through water was almost the same, and hence, the core water inventory was almost the same among these tests until about 75 s.

4.4 Discussion on Application of Present Test Results to PWR

Based on the available experimental results, there are two possible ways of the ECC water delivery to the upper plenum in a PWR with the combined injection type ECCS. One is continuous delivery as observed in the CCTF experiments[11],[12], and the other is the intermittent delivery as observed in the UPTF tests[5]. Although it has not been clarified that which is typical for the PWR with the combined injection type ECCS, the following discussion will be based on the alternative case because the conditions of the present test are based on it.

From the discussion in Section 4.2, it is generally expected that the loop seal at the cross-over leg occurs in a late period, when the ECC water delivery to the upper plenum is alternative. Therefore, the loop seal at the cross-over leg is expected to occur also in the PWR. However, in the SCTF test, only the way of the ECC water delivery was simulated and the dynamic system response, which produced the alternate delivery, was not necessarily simulated. That is, for instance, although there observed water plug formation in the hot and cold legs, loop seal at the cross-over legs and water evaporation effect in the steam generators in the UPTF tests, these were not simulated in the SCTF test due to the difference in its system components from those of the PWR. The loop seal was repeatedly observed in the UPTF test from the early period of the transient. However, at every time, the loop seal was cleared in a short time resulting in the water delivery to the upper plenum in the UPTF test. This is considered to be due to steam injection to its steam generator simulators, which was intended to simulate water evaporation in the steam generators of the PWR when the water plug moves into them. Therefore, in the alternate ECC water delivery case, the loop seal would not be kept for a long time. Also, in the alternate ECC water delivery case, the loop seal occurred out of phase in each loop. At this situation, the core cooling is not expected to be degraded and to be similar to that in the continuous delivery case.

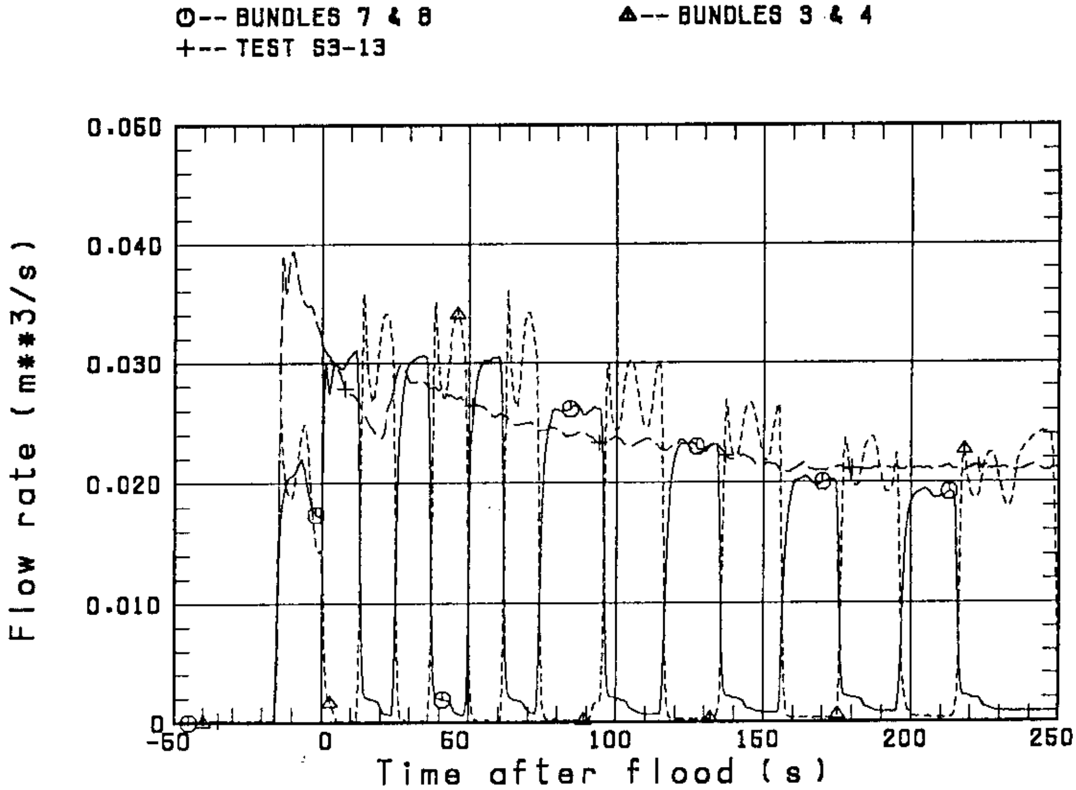

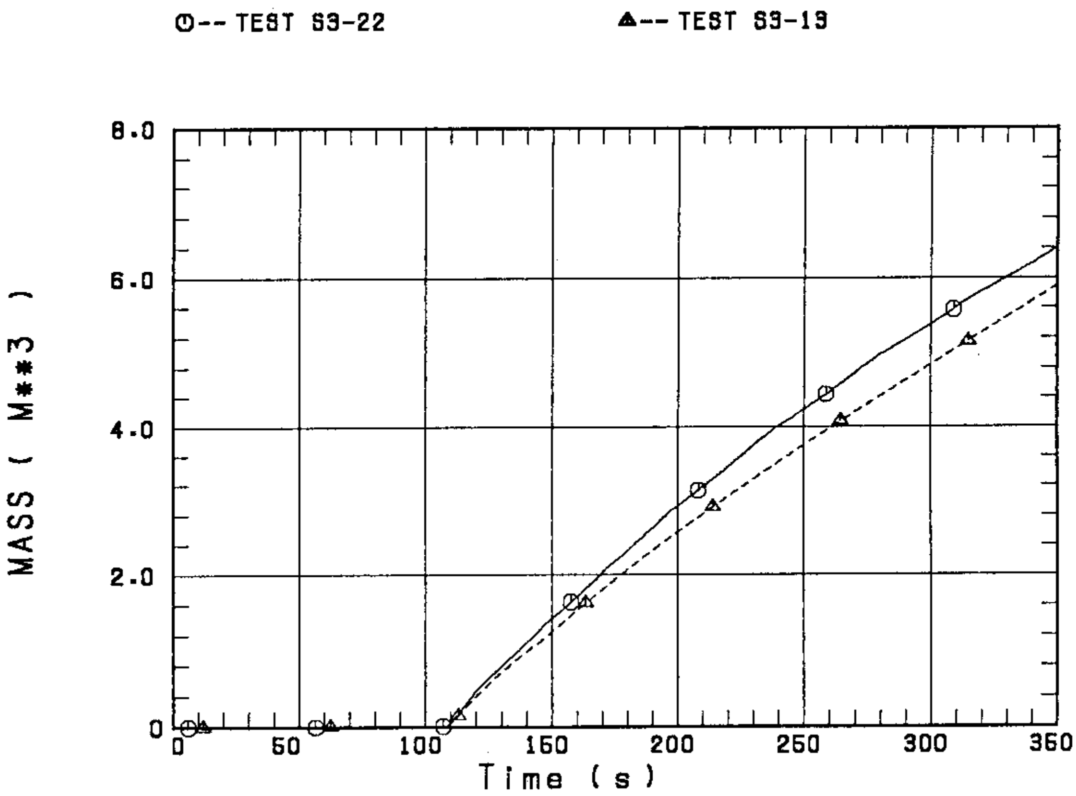

Fig. 4.1 ECC water injection rates into upper plenum and their time-integrations

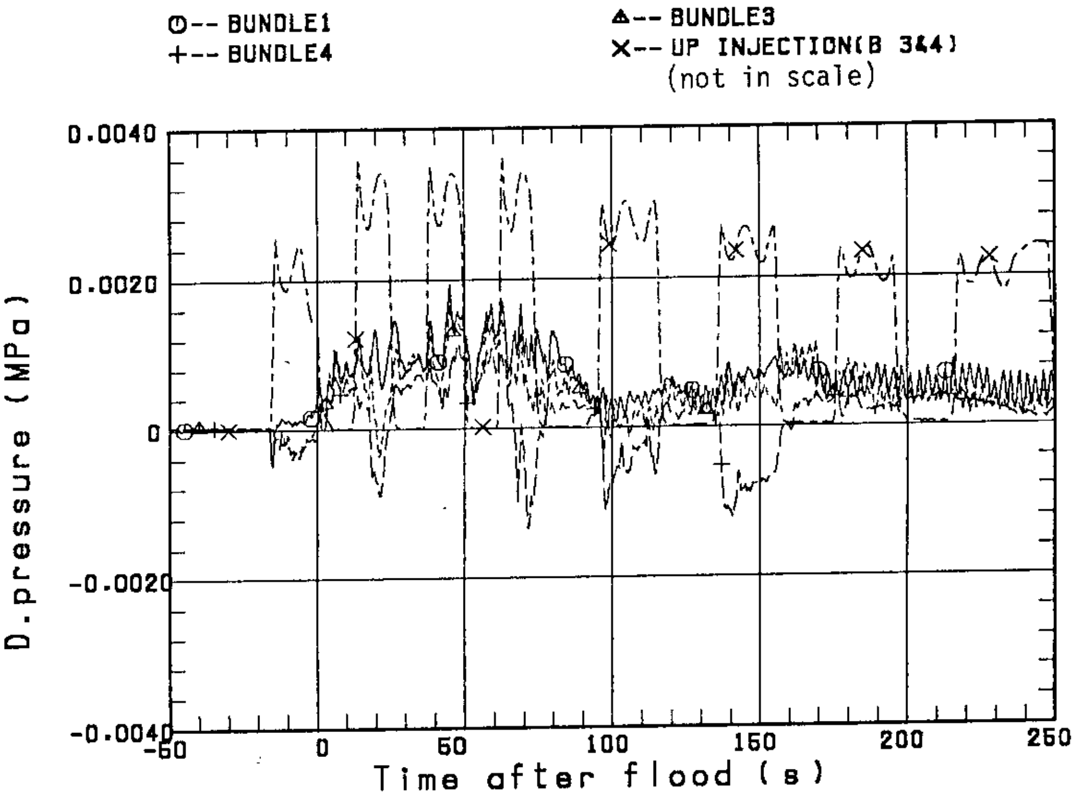

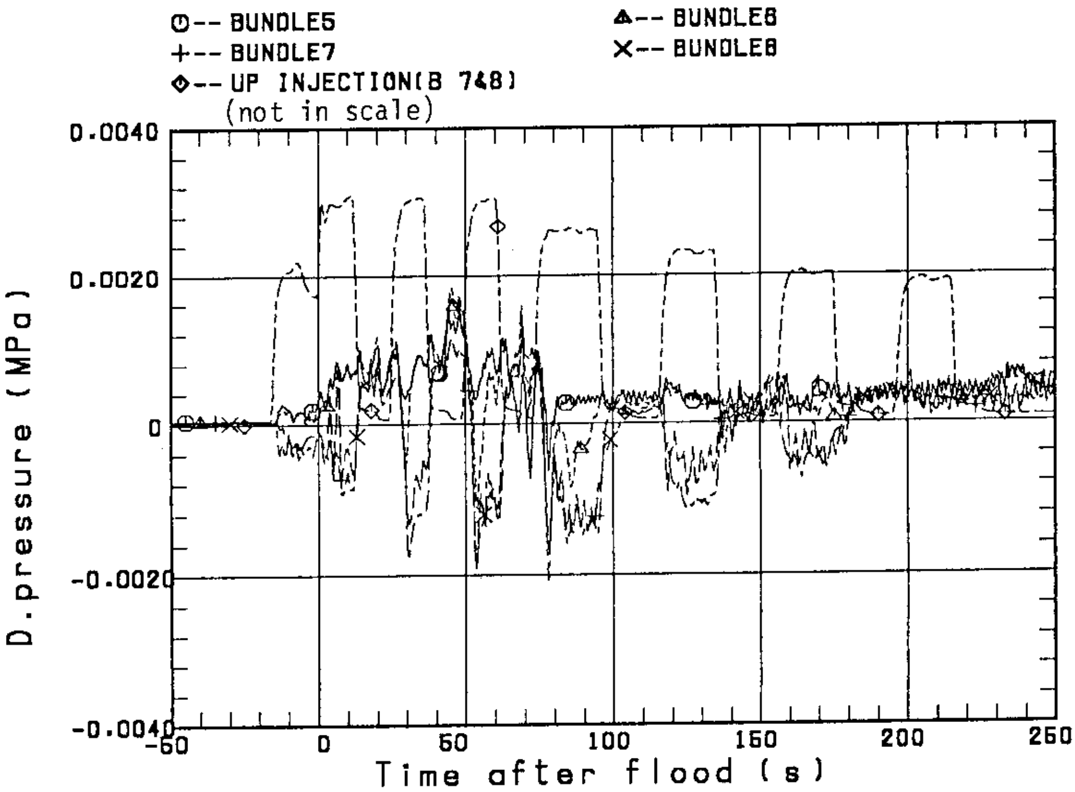

Fig. 4.2 Differential pressures across tie plate

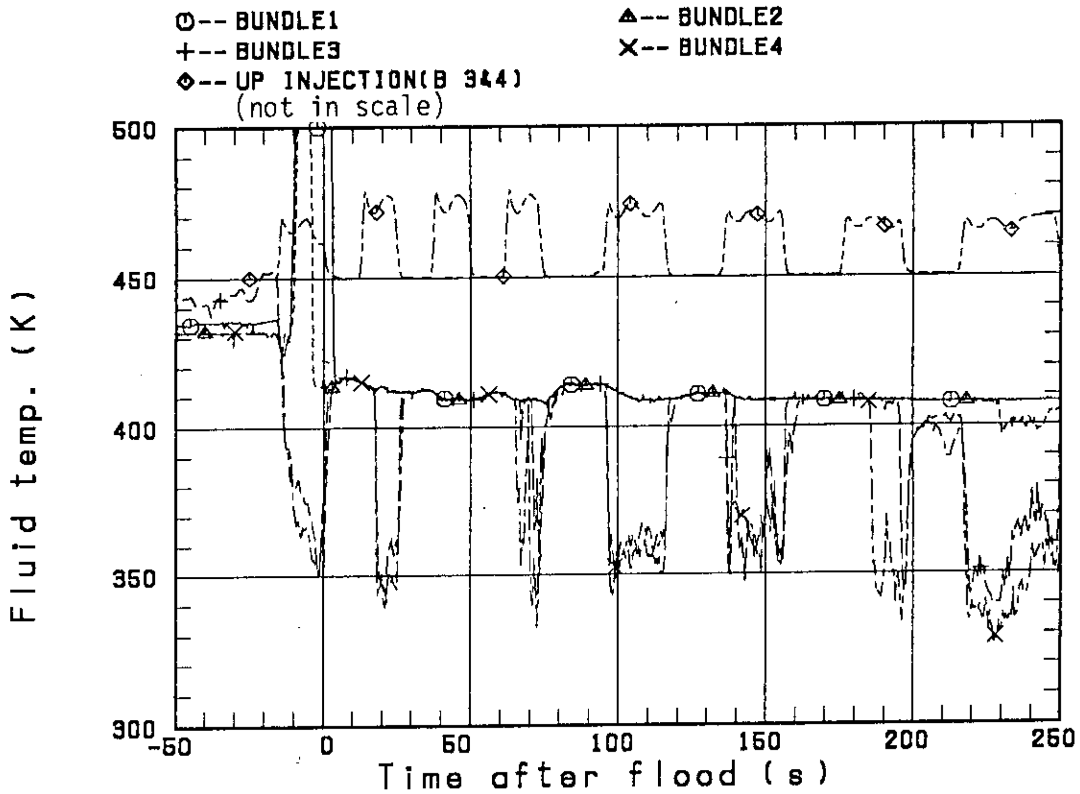

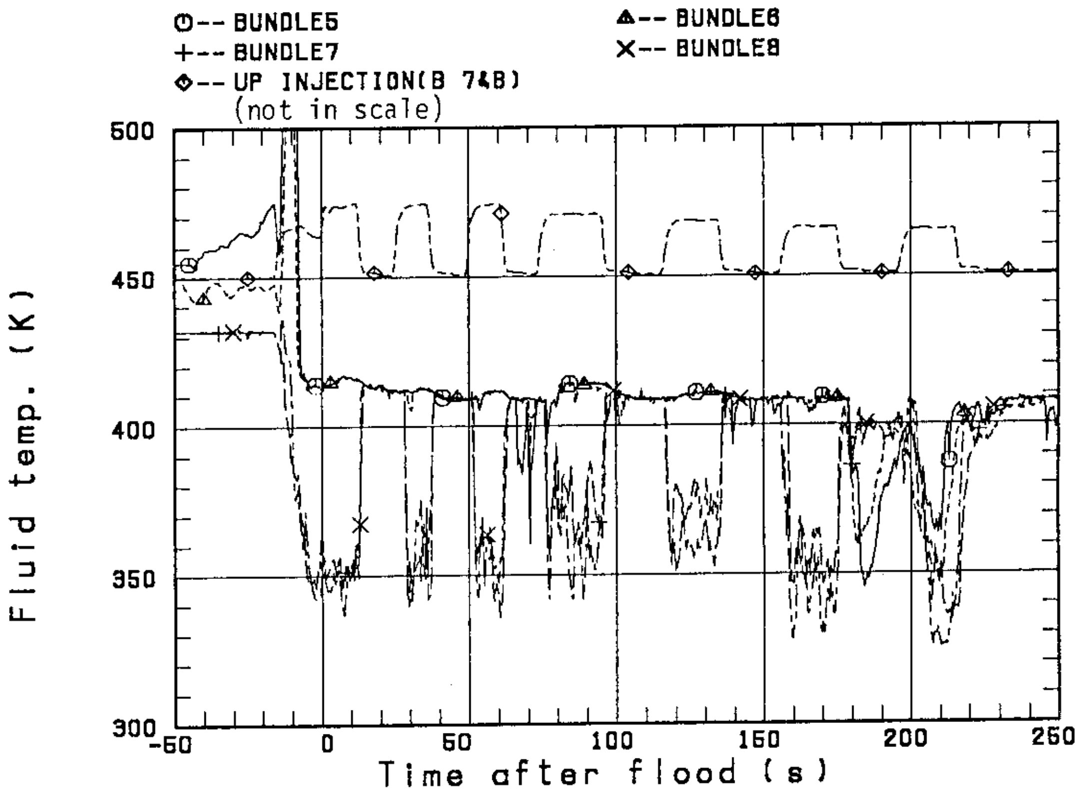

Fig. 4.3 Fluid temperatures just below tie plate holes

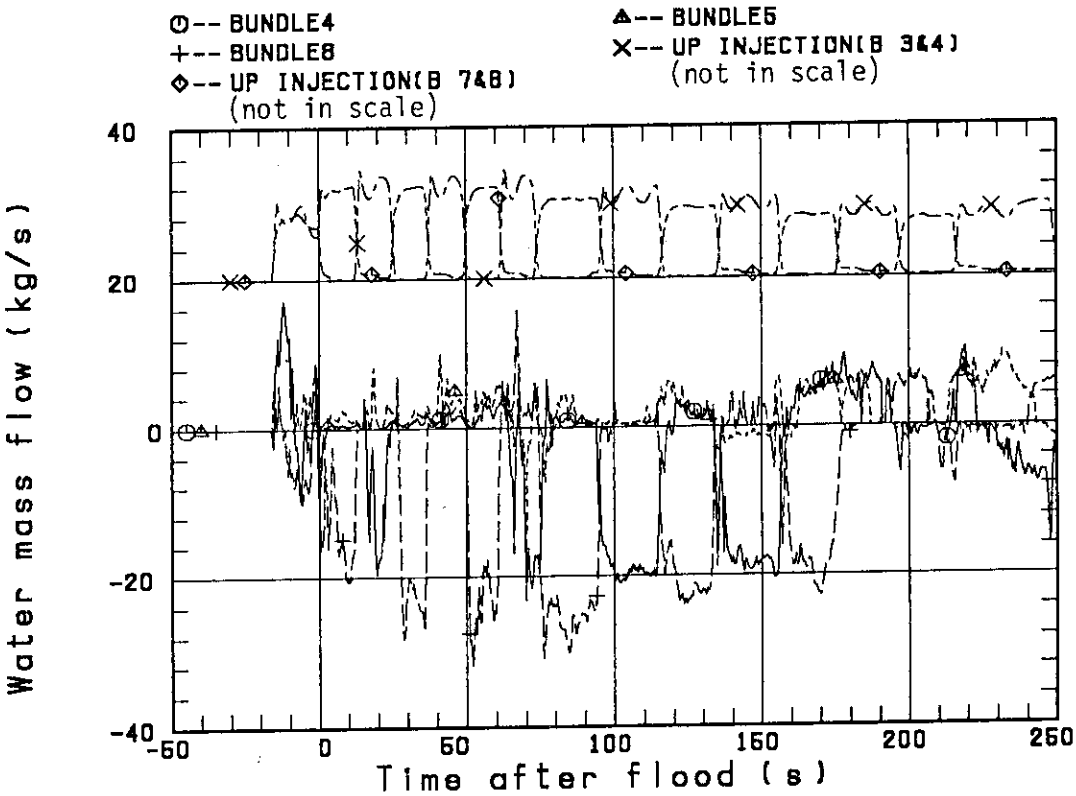

Fig. 4.4 Water mass flow rates at tie plate

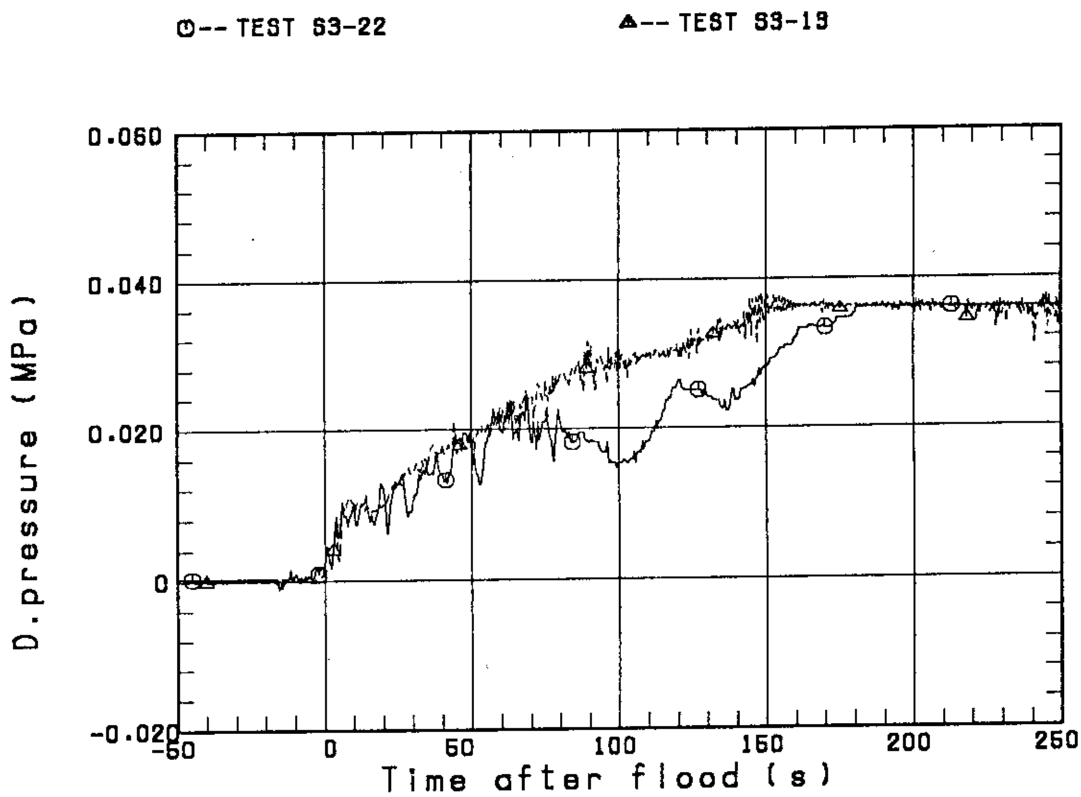

Fig. 4.5 Comparison of core differential pressures

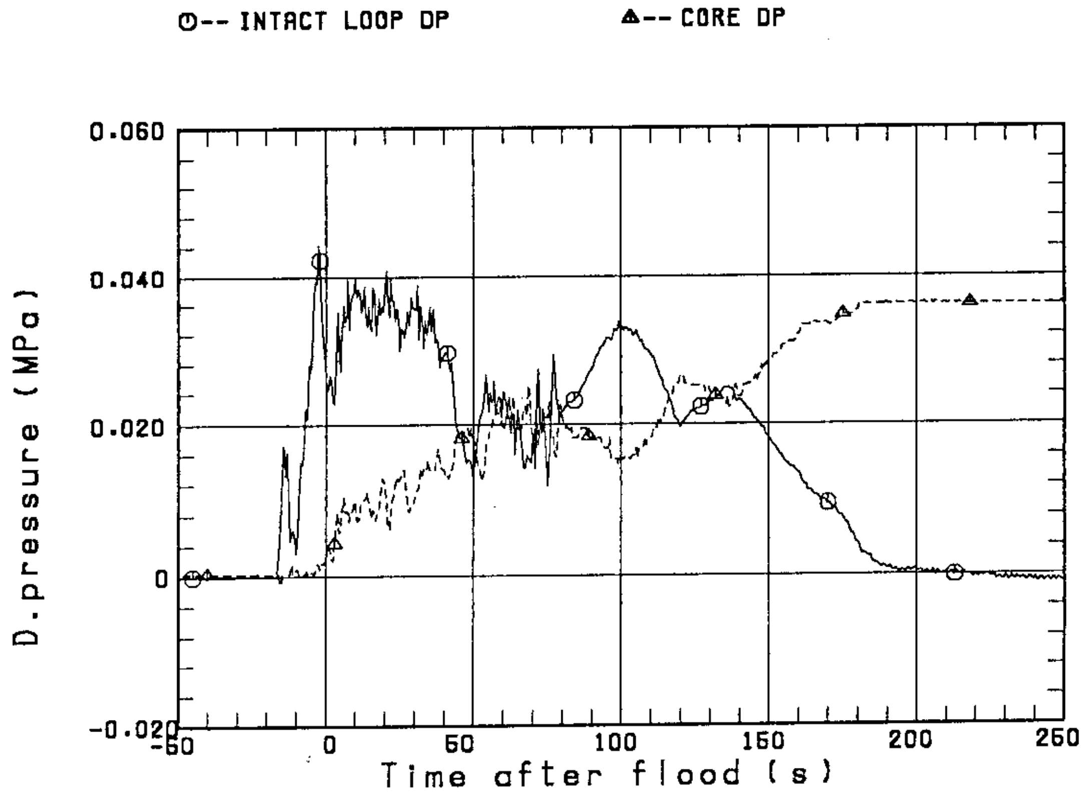

Fig. 4.6 Comparison of intact loop differential pressure with core differential pressure

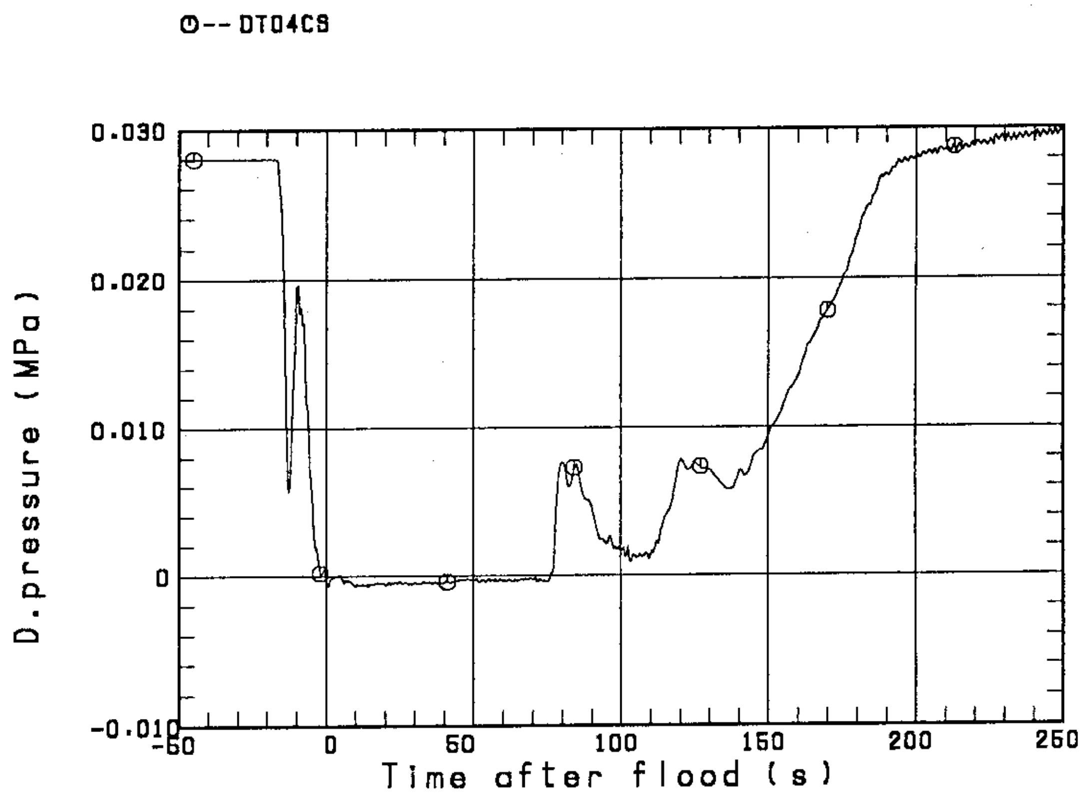

Fig. 4.7 Differential pressure between top and bottom of cross-over leg (Steam/water separator side)

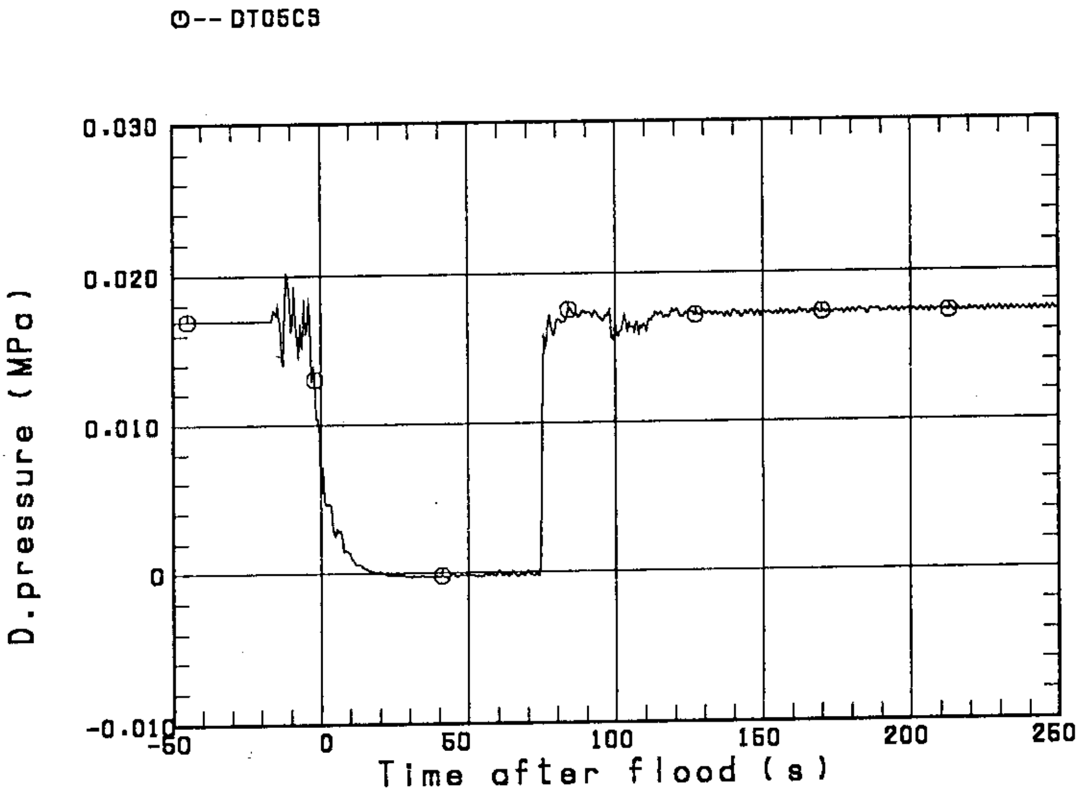

Fig. 4.8 Differential pressure between bottom of coross-over leg and pump inlet

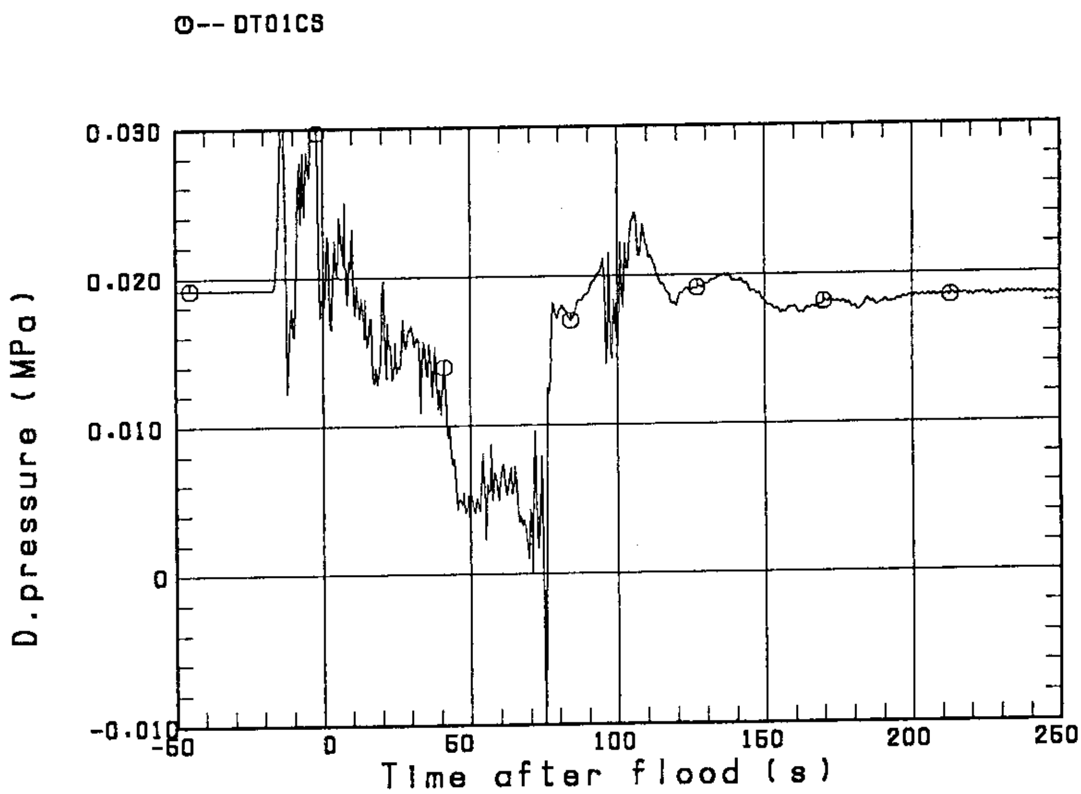

Fig. 4.9 Differential pressure across pump simulator

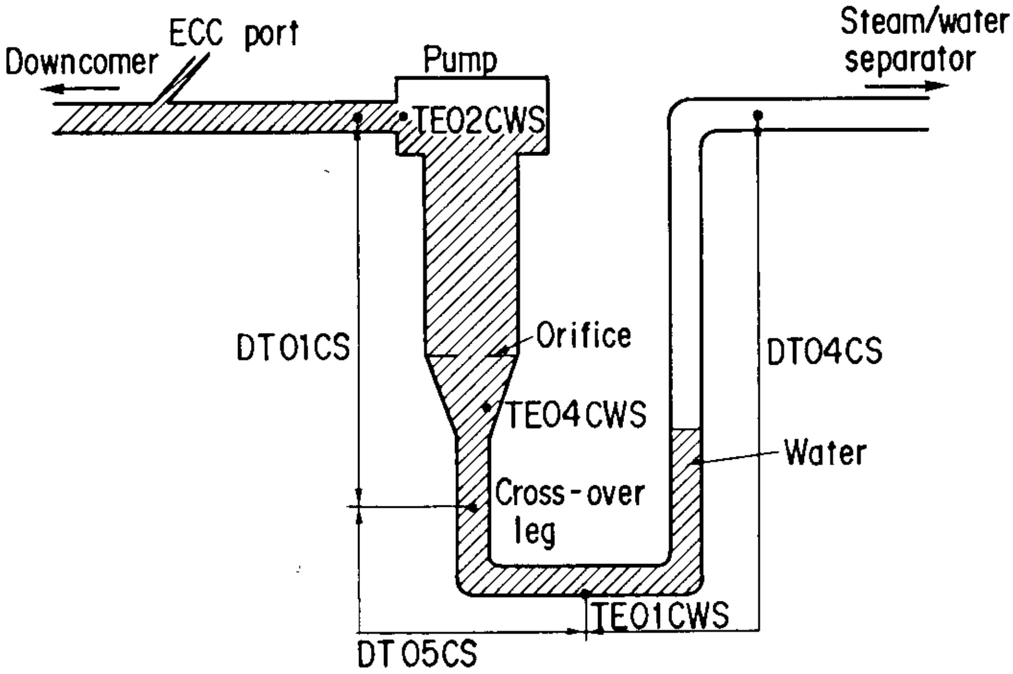

Fig. 4.10 Measurement locations of differential pressure and fluid temperature around cross-over leg

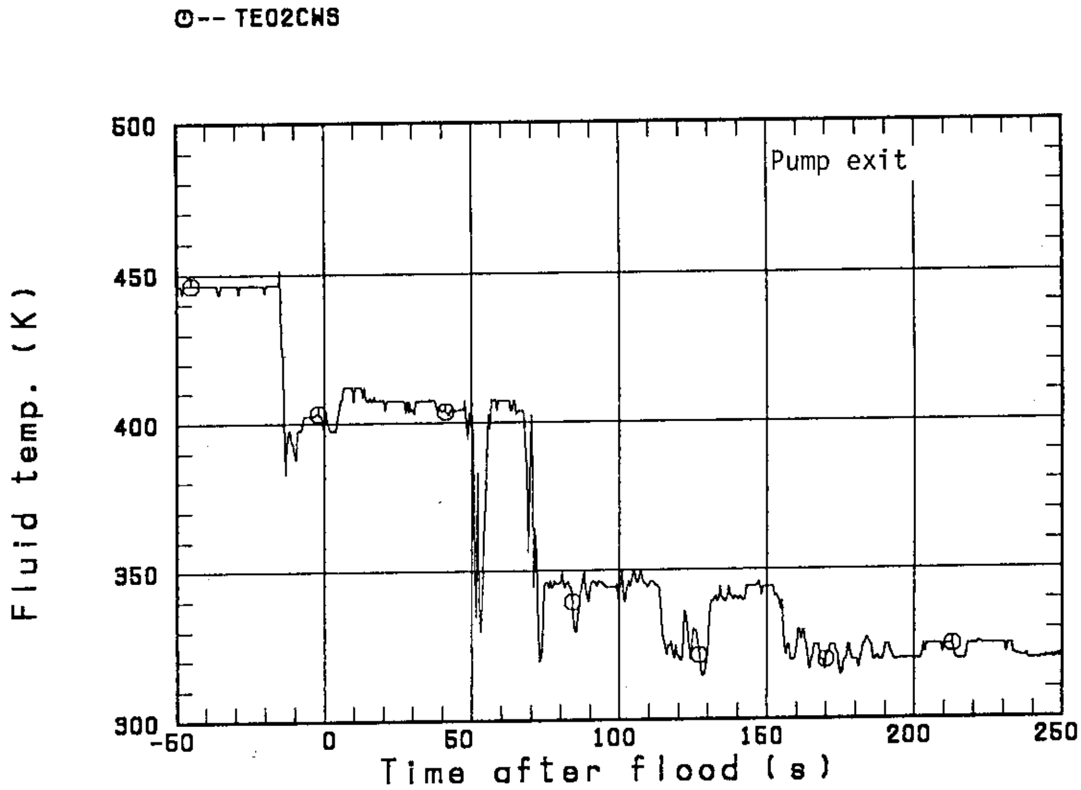

Fig. 4.11(a) Fluid temperature at pump exit

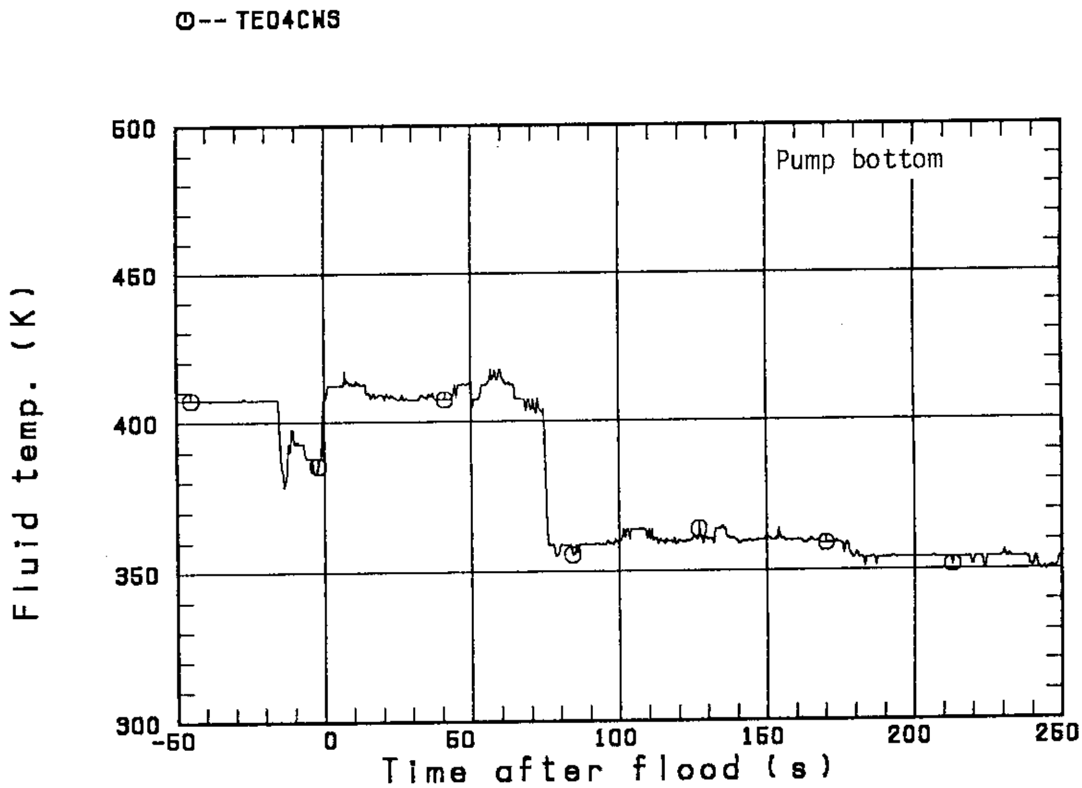

Fig. 4.11(b) Fluid temperature at pump bottom

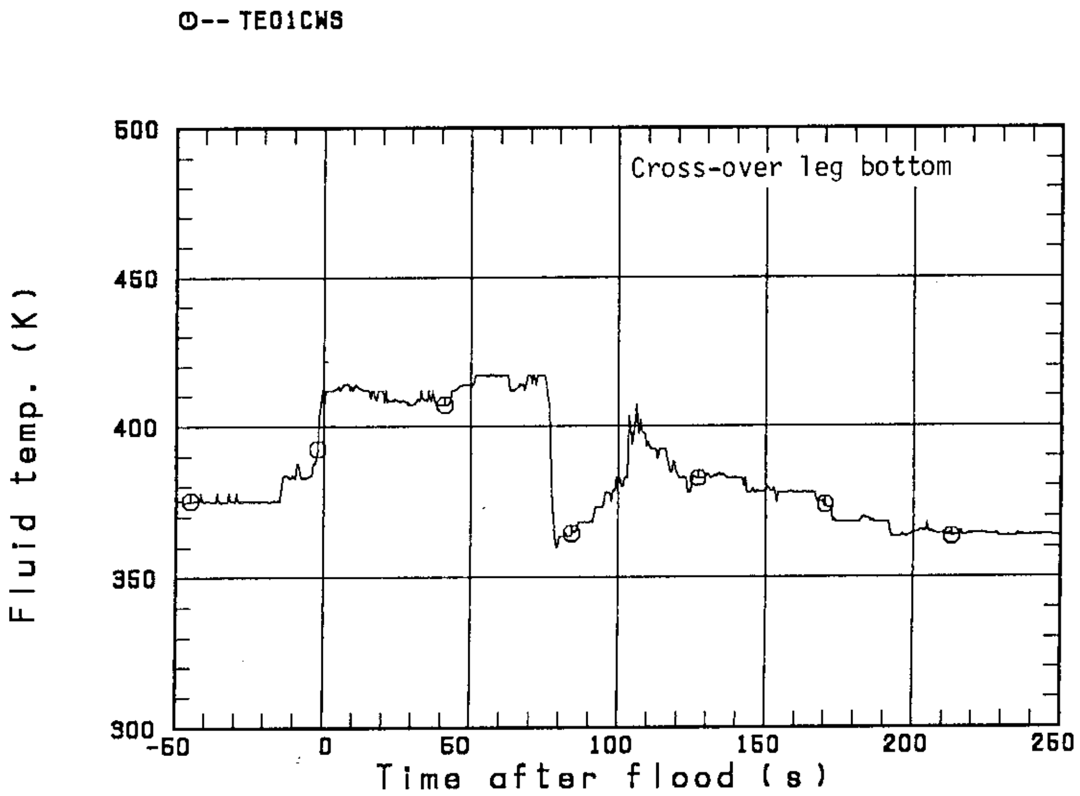

Fig. 4.11(c) Fluid temperature at bottom of cross-over leg

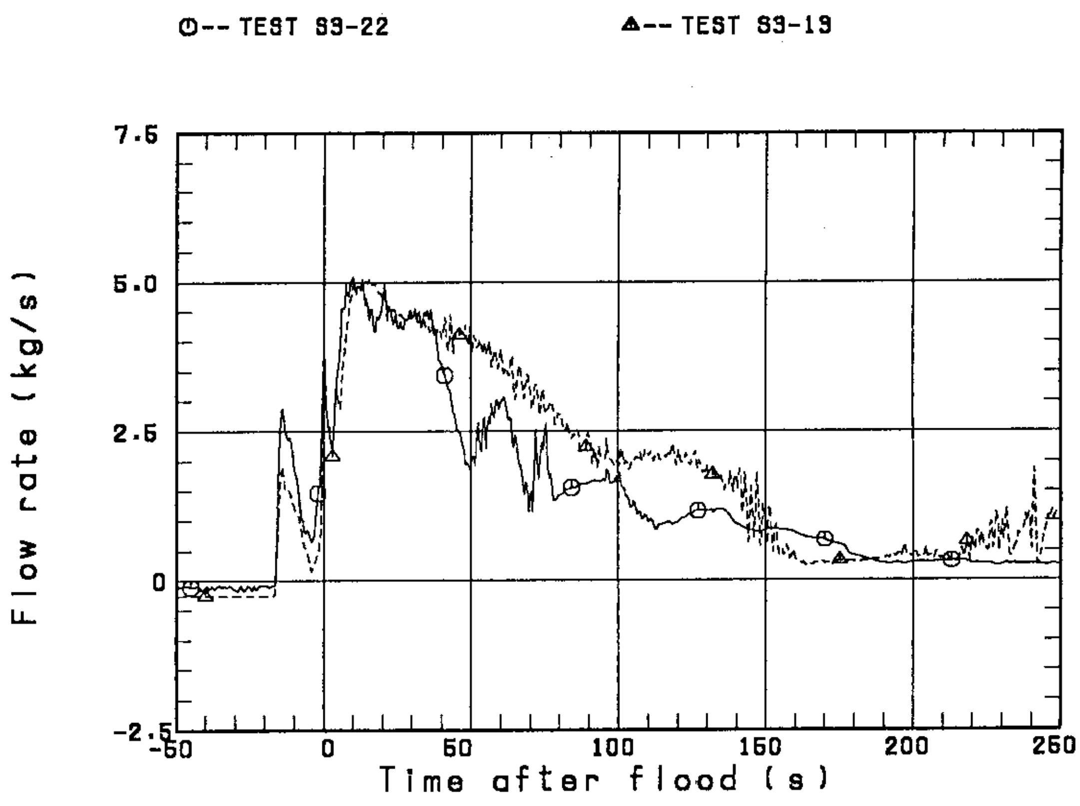

Fig. 4.12 Steam mass flow rates in primary loop

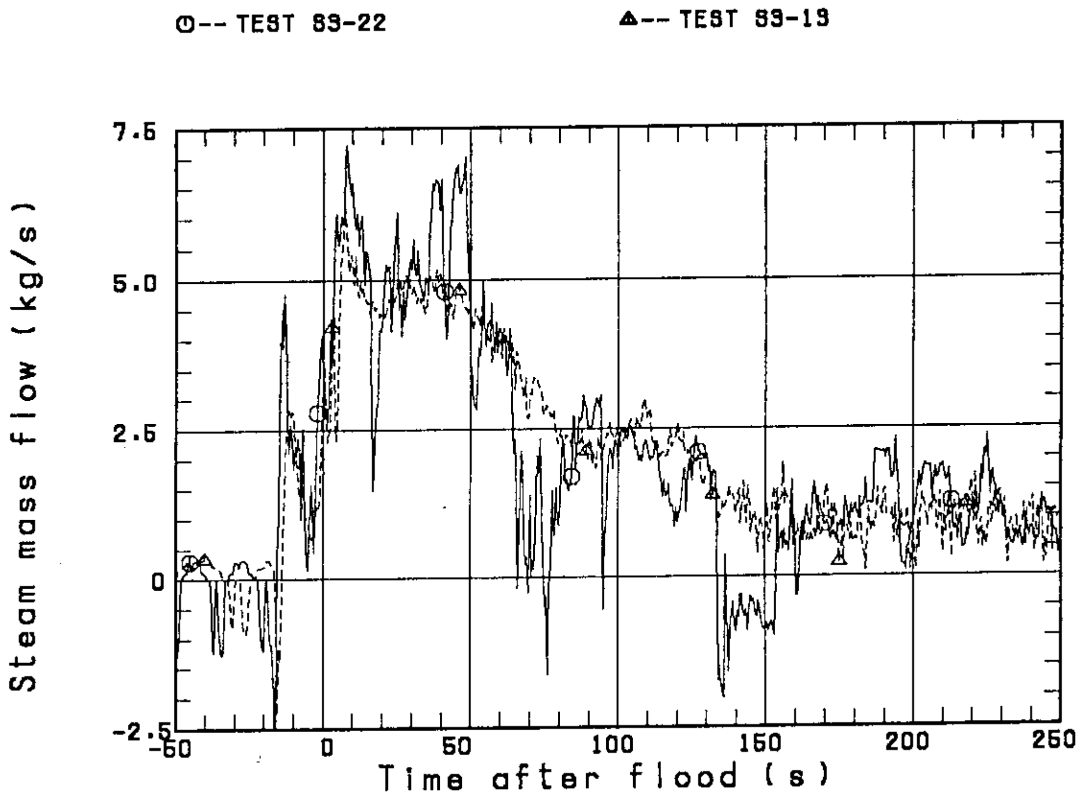

Fig. 4.13 Core outlet steam mass flow rates evaluated with tie plate flow module data

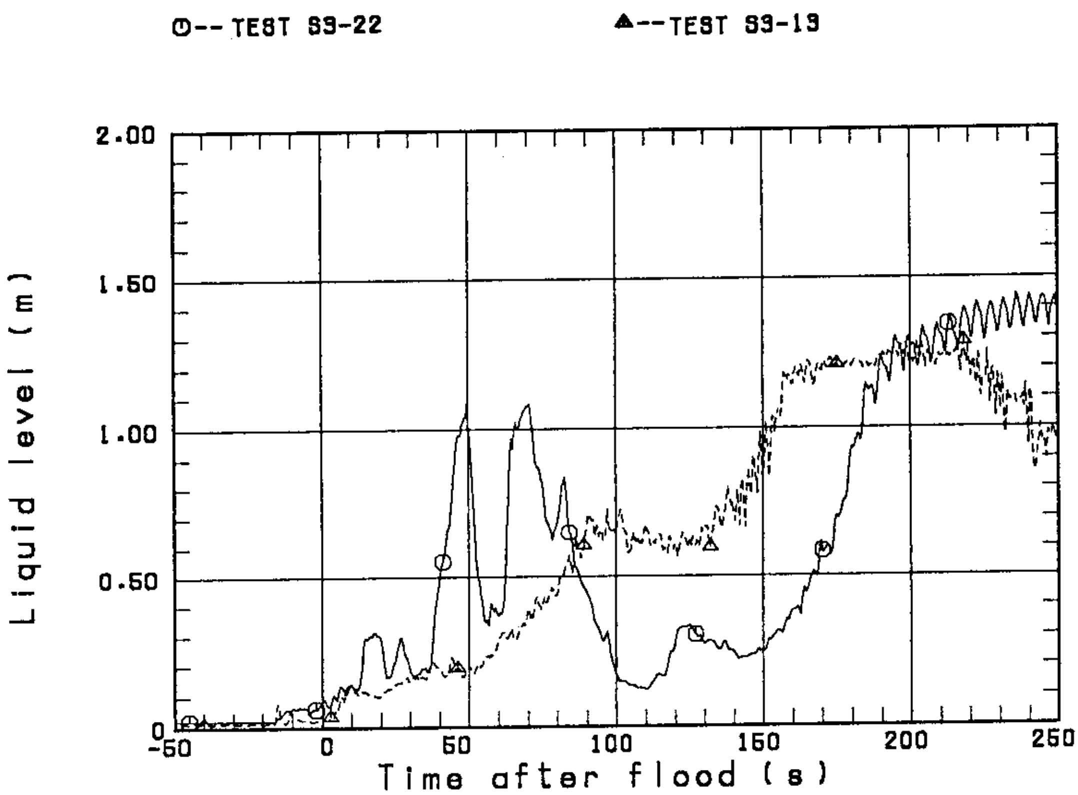

Fig. 4.14 Upper plenum water levels

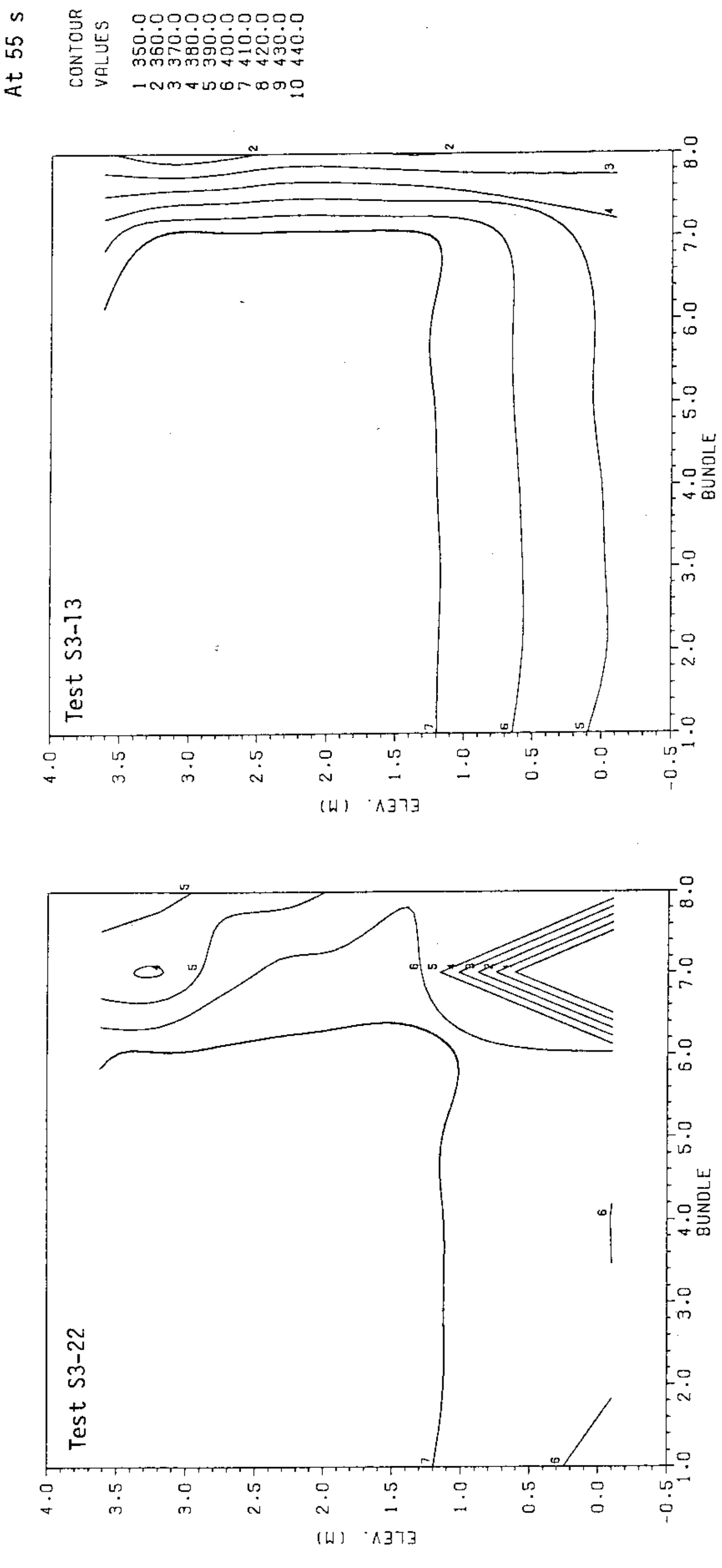

Fig. 4.15(a) Evaluated fluid temperature distributions in core at 55 s

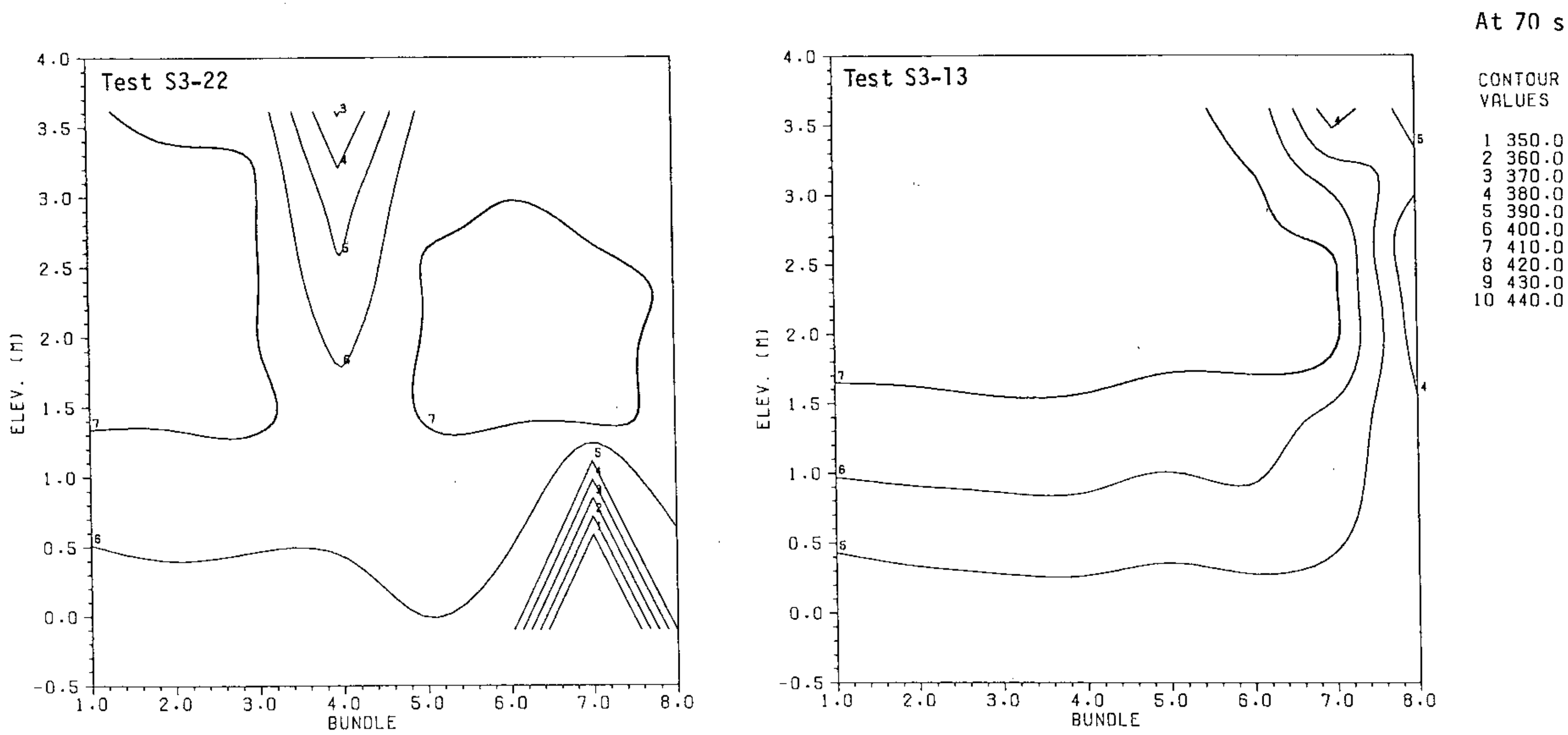

Fig. 4.15(b) Evaluated fluid temperature distributions in core at 70 s

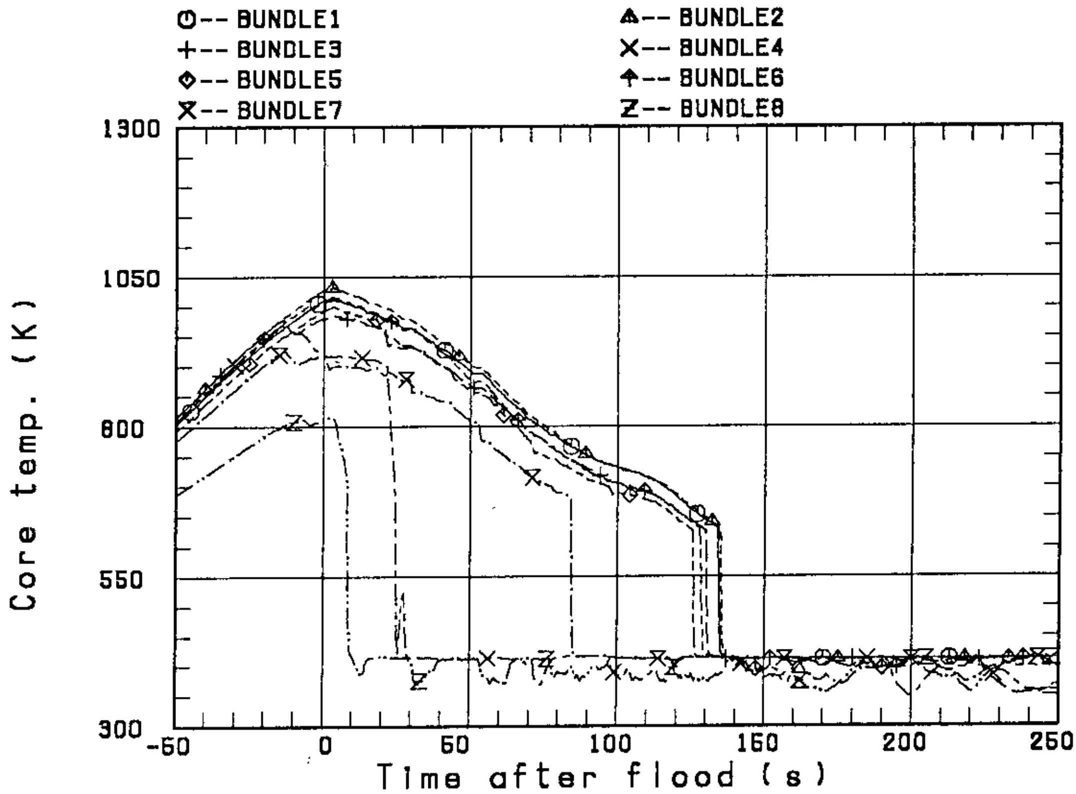

Fig. 4.16 Clad surface temperatures at 1.905 m elevation

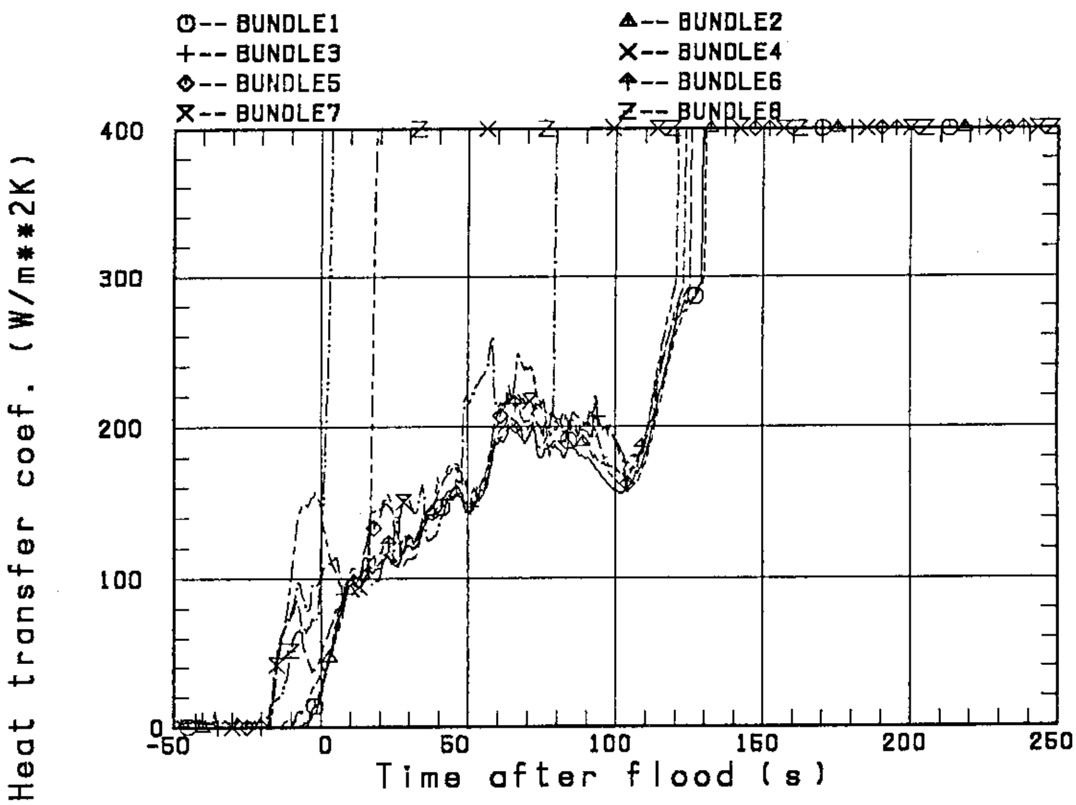

Fig. 4.17 Heat transfer coefficients at 1.905 m elevation

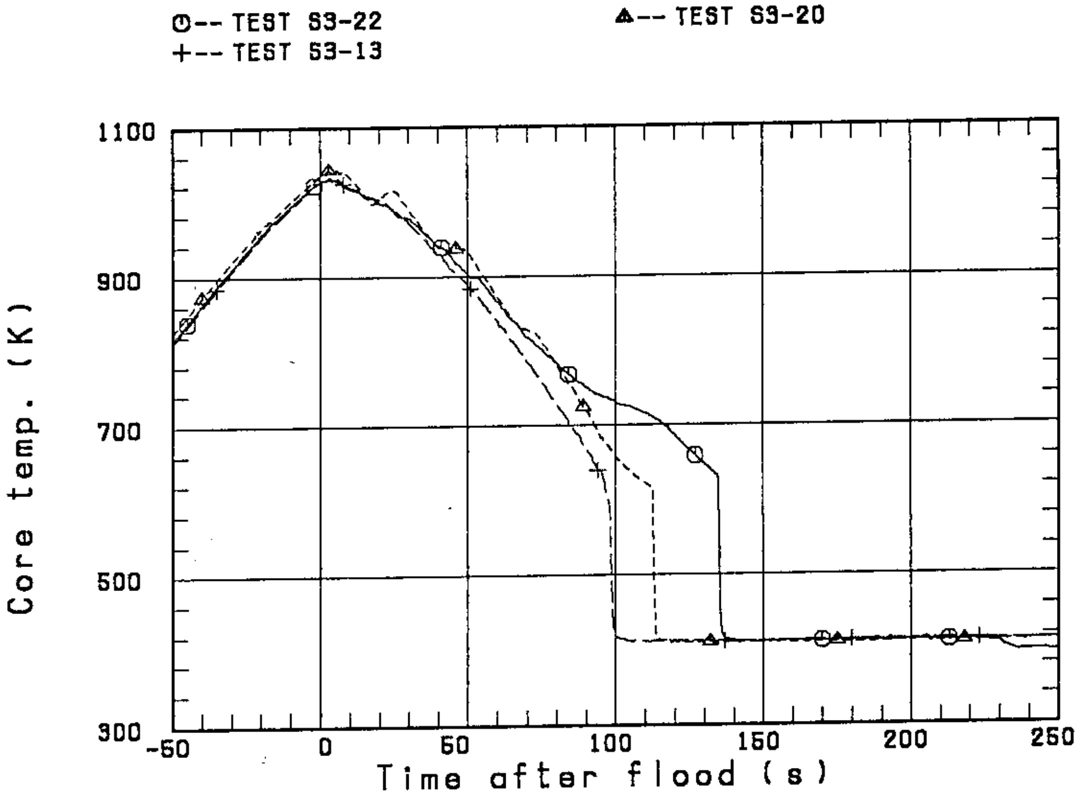

Fig. 4.18 Comparison of clad surface temperature at 1.905 m elevation in Bundle 2 among Tests S3-22, S3-20 and S3-13

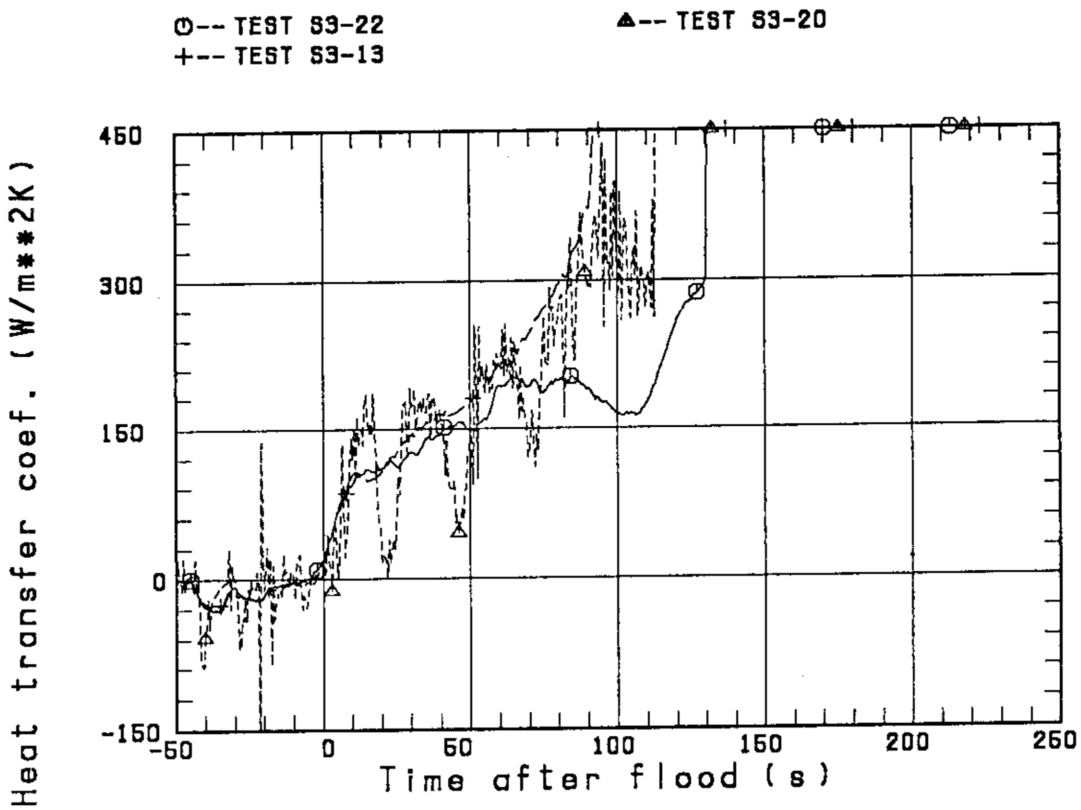

Fig. 4.19 Comparison of heat transfer coefficient at 1.905 m elevation in Bundle 2 among Tests S3-22, S3-20 and S3-13

5. Conclusions

Analyzing data of Test S3-22 together with those of Tests S3-13 and S3-20, the following conclusions are obtained:

(1) Alternate break-through occurred immediately corresponding to the alternate ECC water injection except for one period, during which no break-through was observed. However, there observed difference in break-through behavior that break-through was strong above the low power region of the core, whereas weak above the high power region. The above-mentioned period with no break-through was one of periods with water injection above the high power region.

(2) Although its break-through behavior was different, nearly the same core cooling as in the continuous or intermittent ECC water delivery case was observed except for the period around quench (*i.e.* after about 75 s). This is considered to be because amount of break-through water was almost the same, and hence, core water inventory was almost the same among these three tests until about 75 s.

(3) Around quench time, degraded core cooling comparing to the continuous or intermittent ECC water delivery case was observed. That is, quench time at the midplane level of the present test was 35 s later than in the continuous case. This is considered to result from decrease in core water inventory caused by loop seal at the cross-over leg, which occurred at 76 s.

(4) However, under the alternate ECC water delivery case, the system response in the PWR is considered to be different from that observed in the present test and the loop seal would not be kept for a long time. Also, in the alternate delivery case, the loop seal occurs out of phase in each loop. At this situation, the core cooling is not expected to be degraded and to be similar to that in the continuous delivery case.

Acknowledgment

The authors would like to express their appreciation to Messrs. A. Kamoshida, T. Oyama, Y. Niitsuma, K. Nakajima, T. Chiba, K. Komori, H. Sonobe and A. Owada for their contribution to the test conduction. They also wish to express their application to the 2D/3D project members of Japan, the USA and FRG for valuable discussion.

This work was performed under a contract with the Atomic Energy Bureau of Science and Technology Agency of Japan.

References

[1] Hirano, K. and Murao, Y.: "Large Scale Reflood Test", Nihon-Genshiryoku-Gakkai Shi (J. At. Energy Soc. Jpn.) [in Japanese], 22[10], 681(1980).

[2] Adachi, H. *et al.*: "Design of Slab Core test Facility (SCTF) in Large Scale Reflood Test Program, Part I: Core-I", JAERI-M 83-080 (1983).

[3] Sobajima, M. *et al.*: "Design of Slab Core Test Facility (SCTF) in Large Scale Reflood Test Program, Part II: Core-II", To be published as a JAERI-M report.

[4] Adachi, H. *et al.*: "Design of Slab Core Test Facility (SCTF) in Large Scale Reflood Test Program, Part III: Core-III", To be published as a JAERI-M report.

[5] Weiss, P.A. and Hertlein, R.J.: "UPTF First Integral Test with Combined ECC Injection", NUREG/CP-0091, Vol. 4 (1988)

[6] Cappiello, M.W.: Private communication.

[7] Okubo, T. *et al.*: "Evaluation Report on SCTF Core-III Test S3-20 (Investigation of Water Break-through and Core Cooling Behaviors under Intermittent ECC water Delivery to Upper Plenum during Reflooding in PWRs with Combined-Injection-Type ECCS)", JAERI-M 90-080 (1990).

[8] Okubo, T. *et al.*: "Evaluation Report on SCTF Core-III Tests S3-7 and S3-8 (Investigation of Tie Plate Water Temperature Distribution Effects on Water Break-through and Core Cooling during Reflooding in PWRs with Combined-Injection-Type ECCS)", JAERI-M 90-035 (1990).

[9] Iguchi, T. *et al.*: "Evaluation Report on SCTF Core-III Test S3-13", To be published as a JAERI-M report.

Acknowledgment

The authors would like to express their appreciation to Messrs. A. Kamoshida, T. Oyama, Y. Niitsuma, K. Nakajima, T. Chiba, K. Komori, H. Sonobe and A. Owada for their contribution to the test conduction. They also wish to express their application to the 2D/3D project members of Japan, the USA and FRG for valuable discussion.

This work was performed under a contract with the Atomic Energy Bureau of Science and Technology Agency of Japan.

References

[1] Hirano, K. and Murao, Y.: "Large Scale Reflood Test", Nihon-Genshiryoku-Gakkai Shi (J. At. Energy Soc. Jpn.) [in Japanese], 22[10], 681(1980).

[2] Adachi, H. *et al.*: "Design of Slab Core test Facility (SCTF) in Large Scale Reflood Test Program, Part I: Core-I", JAERI-M 83-080 (1983).

[3] Sobajima, M. *et al.*: "Design of Slab Core Test Facility (SCTF) in Large Scale Reflood Test Program, Part II: Core-II", To be published as a JAERI-M report.

[4] Adachi, H. *et al.*: "Design of Slab Core Test Facility (SCTF) in Large Scale Reflood Test Program, Part III: Core-III", To be published as a JAERI-M report.

[5] Weiss, P.A. and Hertlein, R.J.: "UPTF First Integral Test with Combined ECC Injection", NUREG/CP-0091, Vol. 4 (1988)

[6] Cappiello, M.W.: Private communication.

[7] Okubo, T. *et al.*: "Evaluation Report on SCTF Core-III Test S3-20 (Investigation of Water Break-through and Core Cooling Behaviors under Intermittent ECC water Delivery to Upper Plenum during Reflooding in PWRs with Combined-Injection-Type ECCS)", JAERI-M 90-080 (1990).

[8] Okubo, T. *et al.*: "Evaluation Report on SCTF Core-III Tests S3-7 and S3-8 (Investigation of Tie Plate Water Temperature Distribution Effects on Water Break-through and Core Cooling during Reflooding in PWRs with Combined-Injection-Type ECCS)", JAERI-M 90-035 (1990).

[9] Iguchi, T. *et al.*: "Evaluation Report on SCTF Core-III Test S3-13", To be published as a JAERI-M report.

[10] Iwamura, T. *et al.*: "Evaluation Report on SCTF Core-III Test S3-SH1 (Effect of Hot Leg Injection on Core Thermal-hydraulics for PWR's with a Combined Injection Type ECCS)", JAERI-M 88-125 (1988).

[11] Sugimoto, J. *et al.*: "Evaluation Report on CCTF Core-II Reflood Test C2-19 (Run 79) -- Combined Injection Mode under EM Condition -- ", To be published as a JAERI-M report.

[12] Sugimoto, J. *et al .*: "Evaluation Report on CCTF Core-II Reflood Tests C2-20 (Run 80) and C2-21 (Run 81) -- BE Condition and Effect of Hot Leg ECC Flow Rate under Combined Injection Mode -- ", To be published as a JAERI-M report.

Appendix A Description of SCTF Core-III

A.1 Test Facility

The overall schematic diagram of SCTF is shown in Fig. A-1. The principal dimensions of the facility is shown in Table A-1, and the comparison of dimensions between SCTF and the reference PWR is shown in Fig. A-2.

A.1.1 Pressure Vessel

The pressure vessel is of slab geometry as shown in Fig. A-3. The height of the components in the pressure vessel is almost the same as the reference reactor's, and the flow area and the fluid volume of each component are scaled down based on the nominal core flow area scaling, 1/21.

The core consists of 8 bundles arranged in a row and each bundle includes heater rods and non-heated rods with 16×16 array. The core is enveloped by the honeycomb thermal insulator which is attached on the back surface of core wall plate.

The downcomer is located at one end of the pressure vessel which corresponds to the periphery of the actual reactor pressure vessel. The core baffle region located between the core and the downcomer is isolated for Core-III to minimize uncertainty in actual core flow. The cross sections of the pressure vessel at the upper head, upper plenum, core and lower plenum are shown in Fig. A-4.

A.1.2 Interface between Core and Upper Plenum

The interface between the core and the upper plenum consists of upper core support plate (UCSP), end box and various structures in the end box such as control rod spider which is paired with the control rod guid assembly (CRGA) and its support column bottom and special baffle plate spider which is paired with the hold-down bridge. These structures are exactly the same as those for a German PWR except some minor modifications.

Figure A-5 shows arrangement of the UCSP, the end box and the top grid spacer. The configuration of the end box is shown in Fig. A-6.

Detail of the end boxes with drag transducer device and other internals is shown in Fig. A-7. The UCSP shown in Fig. A-8 has two kinds of holes, i.e., the square holes correspond to the end boxes with control rod spider and the circular holes correspond to the end boxes with special baffle plate spider.

A.1.3 Upper Plenum and Upper Head

The vertical and horizontal cross sections of the upper plenum are shown in Figs A-9 and A-4, respectively. In the SCTF Core-III, the slab cut of the upper plenum of a German (KWU) PWR is simulated. The splitted and staggered arrangement of the CRGA support columns was chosen to make good simulation of horizontal flow in the upper plenum.

As shown in Fig. A-10, there are three kinds of CRGA support column. Support column-1 is installed above Bundles 3 and 5 and connected to the CRGA support column bottom with the transition cone. Cross section of the CRGA support calumn changes from a circle to a half circle in this transition cone. Support column 2 is installed above Bundles 6 and 7 and the bottom is closed with the half conical bottom seal plate with many flow holes. Support column 3 is essentially the same as support column 2 but the edge of one side is cut off in order to install above Bundle 1. Each CRGA support column has ten or eleven baffle plates with flow holes. Top flow paths to the upper head bottom and to the upper plenum top are also provided.

Figure A-11 shows vertical cross section of the bottom part of the upper plenum and the interface between the core and the upper plenum. There are eight side flow injection nozzles and eight side flow extraction nozzles just at the opposite side of the upper plenum bottom, corresponding to each bundle.

The upper plenum is separated from the upper head by an upper support plate. Four top injection nozzles penetrate the upper head and open the top of upper plenum as shown in Fig. A-12. Outlet part of the top injection nozzle has a rectangular cross section and double mesh screen with 45 degree cross angle is attached at the mouth.

A.1.4 Simulated Core

The simulated core for the SCTF Core-III consists of 8 heater rod bundles arranged in a row. Each bundle has 236 electrically heated rods and 20 non-heated rods. The arrangement of rods in a bundle is shown in Fig. A-13. The dimensions of the heater rods are based on 15×15 fuel rods bundle for a PWR and the heated length and the outer diameter of each heater rod are 3.613 m and 10.7 mm, respectively. A heater rod consists of a nichrome heater element, boron nitride (BN) or magnesium oxide (MgO) depending on elevation in the heated zone and Nichrofer 7216 (equivalent to Inconel 600) sheath. The sheath thickness is about 1.0 mm and is thicker than the actual fuel cladding because of the requirements for thermocouple installation. The heater element is a helical coil and has a 17 step chopped cosine axial power profile as shown in Fig. A-14. The peaking factor is 1.4.

Non-heated rods are either pipes or solid rods of stainless steel with 13.8 mm O.D. The heater rods and non-heated rods are fixed at the top of the core allowing downward expansion. In Fig. A-15, relative elevation of rods and spacers is shown.

For better simulation of flow resistance in the lower plenum, the simulated fuel rods end in the lower plenum and do not penetrate through the bottom plate of the lower plenum as shown in Fig. A-15.

A.1.5 Primary Loops

Primary loops consist of a hot leg equivalent to four hot legs in area, a steam/water separator for simulating single steam phase flow downstream of the steam generator and for measuring flow rate of carry over water, an intact cold leg equivalent to three intact loops, a broken cold leg on the pressure vessel side and a broken cold leg on the steam/water separator side. These two broken cold legs are connected to two containment tanks through break valves, respectively. The arrangement of the primary loops is shown in Fig. A-16. The flow area of each loop is scaled down based on the core flow area scaling, 1/21. It should be emphasized that the cross section of the hot leg is an elongated circle with an actual height to realize proper flow pattern in the hot leg. The steam/water separator has a steam generator inlet plenum simulator to correctly simulate the flow characteristics of carryover water into the U-tubes. The cross section of the hot leg and the configuration of the steam genrator inlet plenum simulator are shown in Fig. A-17.

A pump simulator and a loop seal part are provided for the intact cold leg. The arangement of the intact cold leg is shown in Fig. A-18. The pump simulator consists of the casing and duct simulators and an orifice plate as shown in Fig. A-19. The loop resistance is adjusted with the orifice plates attached to the intact cold leg, the steam/ water separator side and pressure vessel side broken cold legs and the pump simulator.

A.1.6 ECC Water Injection System

Three kinds of ECCSs are provided, i.e., the accumulator injection system (Acc), low pressure coolant injection system (LPCI) and combined injection system. Available injection locations for the former two are the intact and broken cold legs, the hot leg, the lower plenum and the downcomer. On the other hand, those for the last one are the top and bottom-side of the upper plenum and the intact and broken cold legs.

A.1.7 Containment Tanks and Auxiliary System

Two containment tanks are provided to SCTF. The containment tank-I is connected with the downcomer through the pressure vessel side broken cold leg and the containment tank-II is connected with the steam/water separator through the steam/water separator side broken cold leg. Especially in the containment tank-I, carryover water from the downcomer is measured by the differentiation of the liquid level. These containment tanks and auxiliary system such as a pressurizer for injecting water from the Acc tanks, etc. are shared with CCTF.

A.2 Instrumentation

The instrumentation in SCTF has been provided both by JAERI and USNRC. The JAERI-provided instrumentation includes the measurement of temperatures, pressures, differential pressures, liquid levels, flow velocities, and heating powers. USNRC has provided film probes, impedance probes, string probes, liquid level detectors (LLDs), fluid distribution grids (FDGs), turbine meters, drag disks, densitometers, spool pieces, drag bodies, break through detectors and video optical probes. Locations of the JAERI-provided instruments are shown in Figs. A-20 through A-43.

Table A-1 Principal Dimensions of the SCTF

1. Core Dimension	
(1) Quantity of Bundle	8 Bundles
(2) Bundle Array	1 × 8
(3) Bundle Pitch	230 mm
(4) Rod Array in a Bundle	16 × 16
(5) Rod Pitch in a Bundle	14.3 mm
(6) Quantity of Heater Rod in a Bundle	236 rods
(7) Quantity of Non-Heated Rod in a Bundle	20 rods
(8) Total Quantity of Heater Rods	236×8=1,888 rods
(9) Total Quantity of Non-Heated Rods	20×8=160 rods
(10) Effective Heated Length of Heater Rod	3613 mm
(11) Diameter of Heater Rod	10.7 mm
(12) Diameter of Non-Heated Rod	13.8 mm
2. Flow Area & Fluid Volume	
(1) Core Flow Area	0.25 m^2
(2) Core Fluid Volume	0.903 m^3
(3) Baffle Region Flow Area (isolated)	(0.096) m^2
(4) Baffle Region Fluid Volume (nominal)	0.355 m^3
(5) Cross-Sectional Area of Core Additional Fluid Volumes Including Gap between Core Barrel and Pressure Vessel Wall and Various Penetration Holes	0.07 m^2 ~ 0.10 m^2
(6) Downcomer Flow Area	0.158 m^2
(7) Upper Annulus Flow Area	0.158 m^2
(8) Upper Plenum Horizontal Flow Area (max.)	0.541 m^2
(9) Upper Plenum Vertical Flow Area	0.525 m^2
(10) Upper Plenum Fluid Volume	1.156 m^3
(11) Upper Head Fluid Volume	0.86 m^3
(12) Lower Plenum Fluid Volume (excluding below downcomer)	1.305 m^3
(13) Steam Generator Inlet Plenum Simulator Flow Area	0.626 m^2
(14) Steam Generator Inlet Plenum Simulator Fluid Volume	0.931 m^3
(15) Steam Water Separator Fluid Volume	5.3 m^3
(16) Flow Area at the Top Plate of Steam Generator Inlet Plenum Simulator	0.195 m^2
(17) Hot Leg Flow Area	0.0826 m^2

Table A-1 (continue)

(18)	Intact Cold Leg Flow Area (Diameter = 297.9 mm) Inverted U-Tube with 0.0314 m^2 Cross-Sectional Area (Diameter = 200 mm) and 10 m Height from the Top of Steam Generator Inlet Plenum Simulator Can Be Added As an Option.	0.0697	m^2
(19)	Broken Cold Leg Flow Area (Diameter = 151.0 mm)	0.0197	m^2
(20)	Containment Tank-I Fluid Volume	30	m^3
(21)	Containment Tank-II Fluid Volume	50	m^3
(22)	Flow Area of Exhausted Steam Line from Containment Tank-II to the Atmosphere	see Fig. 3-63	

3. Elevation & Height

(1)	Top Surface of Upper Core Support Plate (UCSP)	0	mm
(2)	Bottom Surface of UCSP	- 40	mm
(3)	Top of the Effective Heated Length of Heater Rod	- 444	mm
(4)	Bottom of the Effective Heated Length of Heater Rod	-4,057	mm
(5)	Bottom of the Skirt in the Lower Plenum	-5,270	mm
(6)	Bottom of Intact Cold Leg	+ 724	mm
(7)	Bottom of Hot Leg	+1,050	mm
(8)	Top of Upper Plenum	+2,200	mm
(9)	Bottom of Steam Generator Inlet Plenum Simulator	+1,933	mm
(10)	Centerline of Loop Seal Bottom	-2,281	mm
(11)	Bottom Surface of End Box	- 263	mm
(12)	Top of Upper Annulus of Downcomer	+2,234	mm
(13)	Height of Steam Generator Inlet Plenum Simulator	1,595	mm
(14)	Height of Loop Seal	3,140	mm
(15)	Inner Height of Hot Leg Pipe	737	mm
(16)	Bottom of Lower Plenum	-5,772	mm
(17)	Top of Upper Head	+2,887	mm

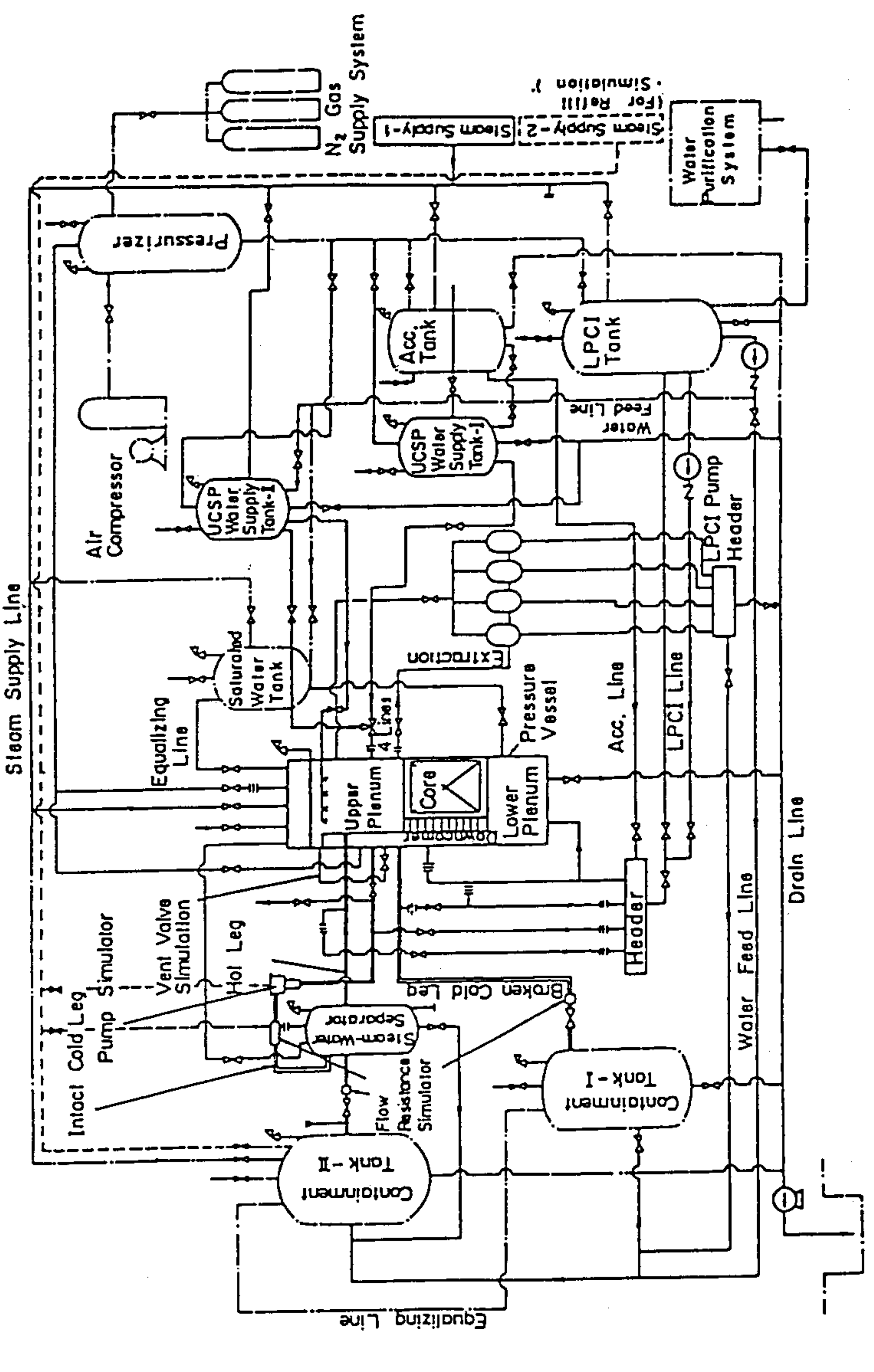

Fig. A-1 Schematic diagram of slab core test facility

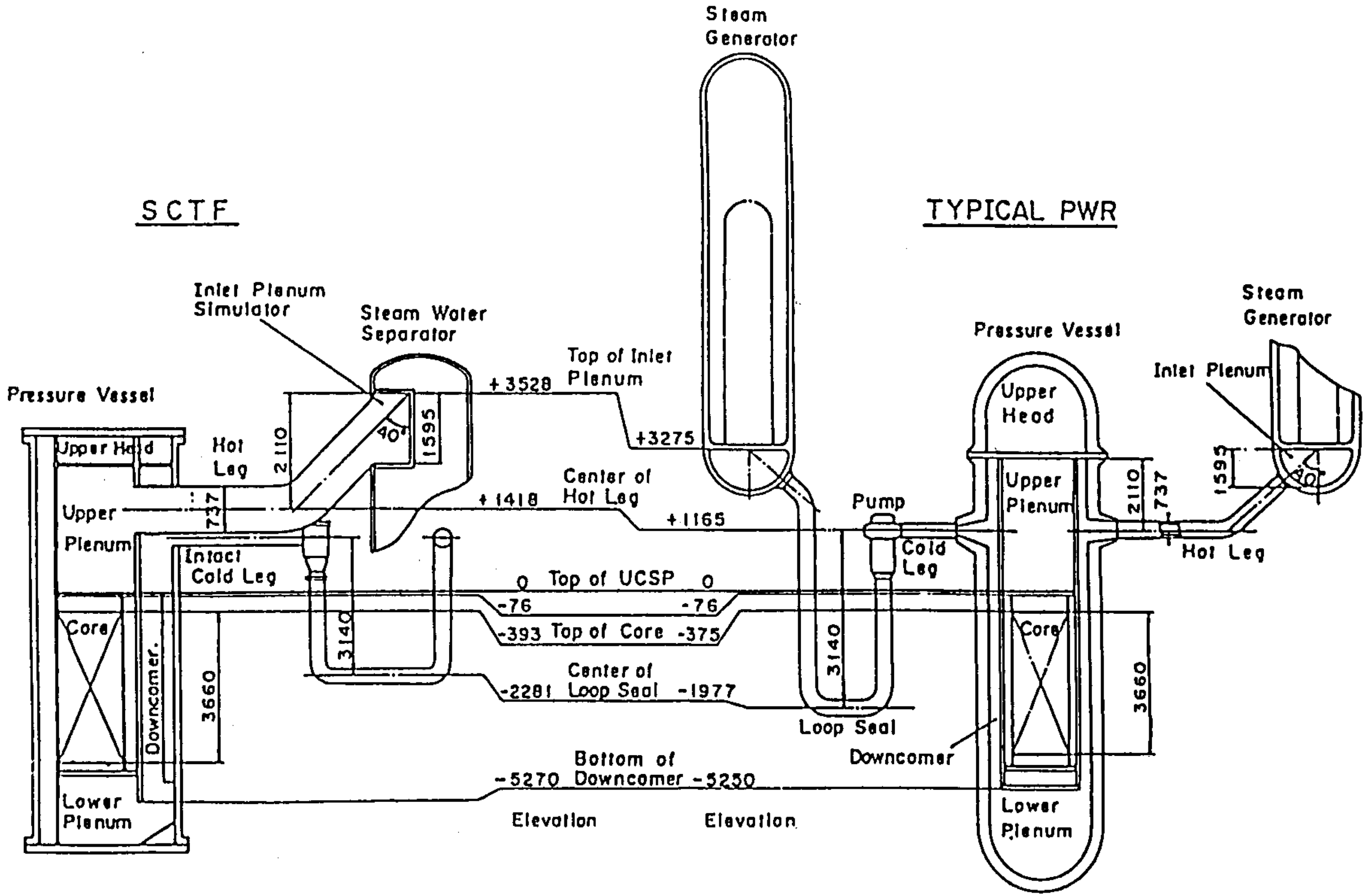

Fig. A-2 Comparison of dimensions between SCTF and a reference PWR

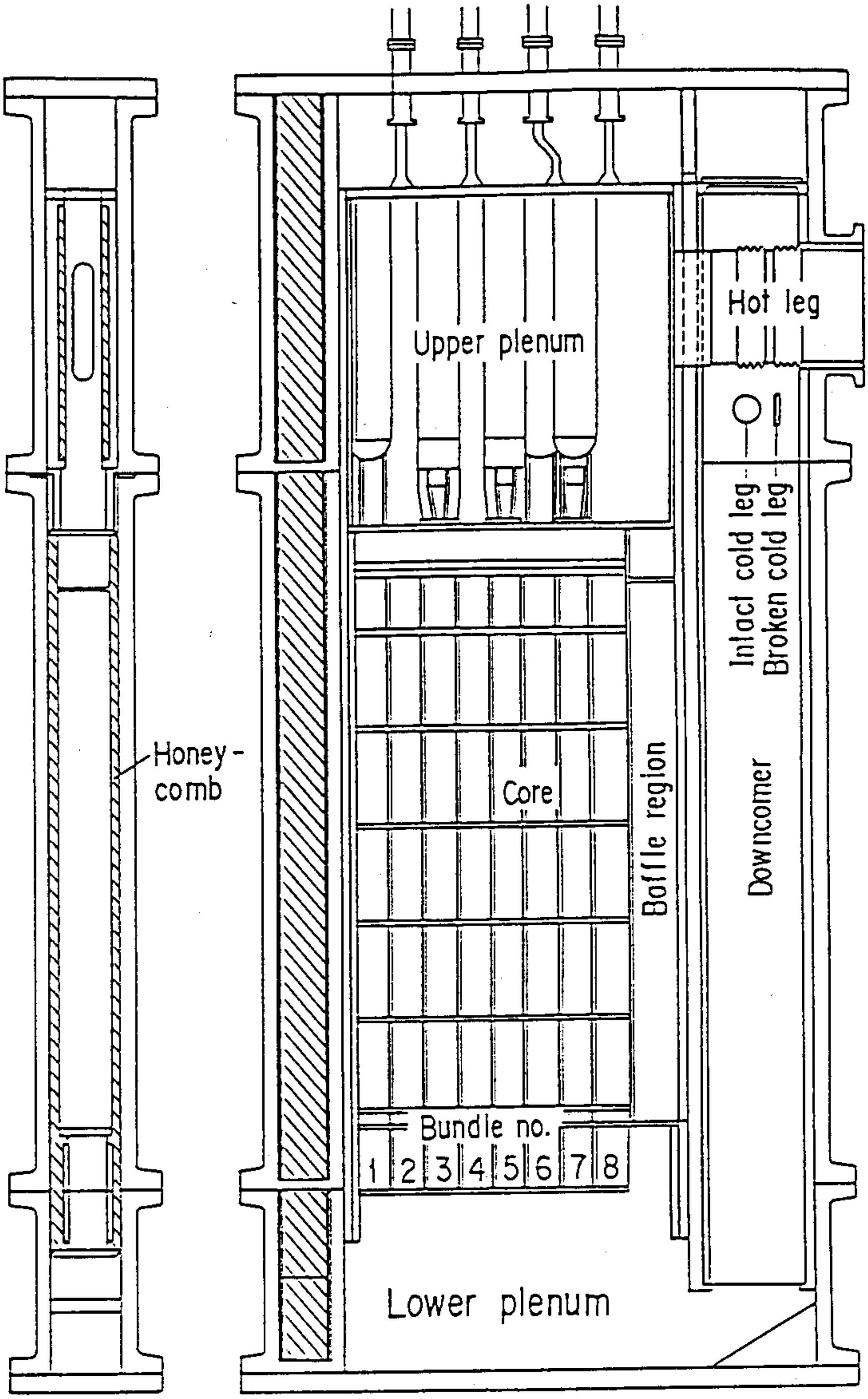

Fig. A-3 Vertical cross sections of pressure vessel

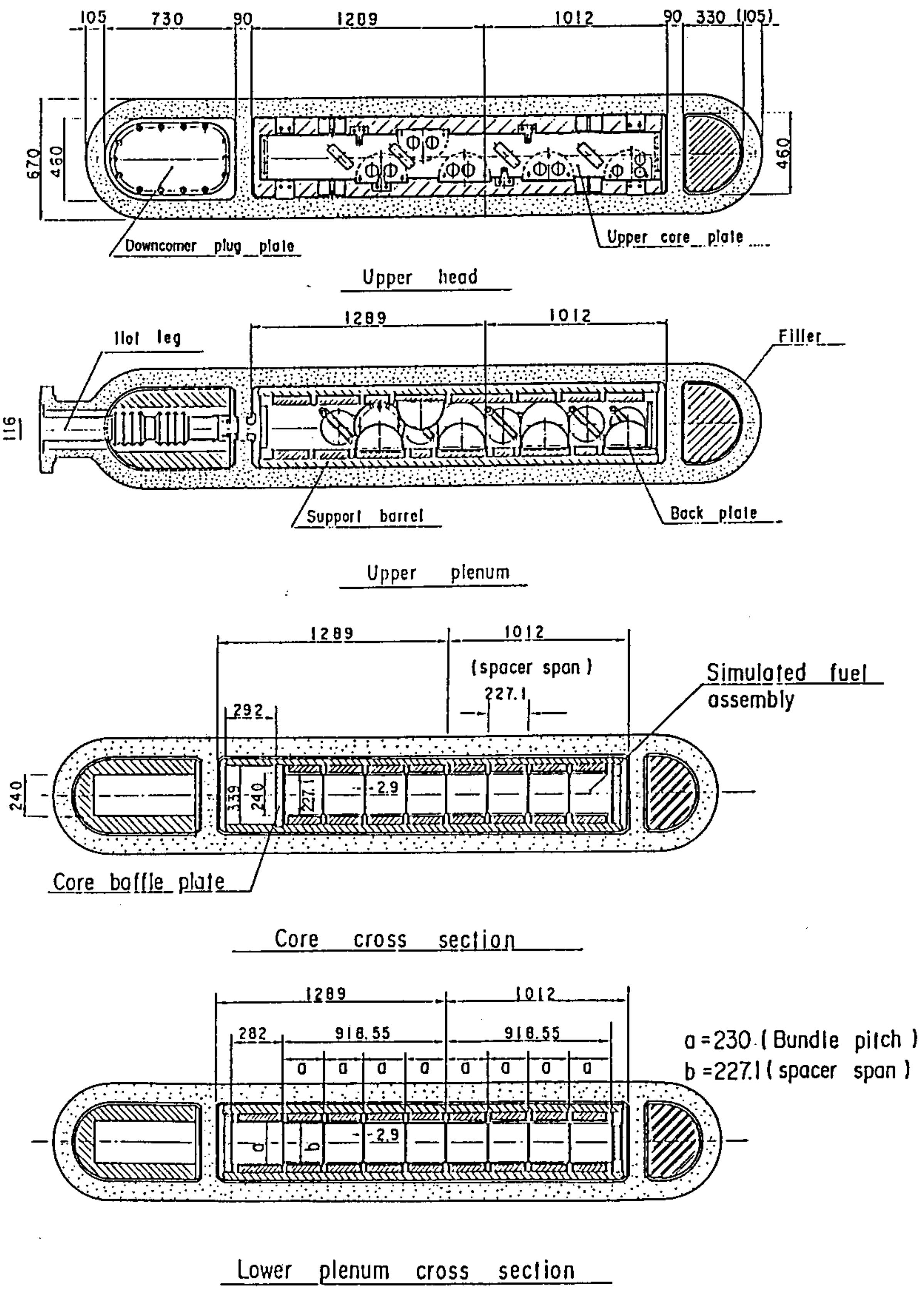

Fig. A-4 Horizontal cross sections of pressure vessel

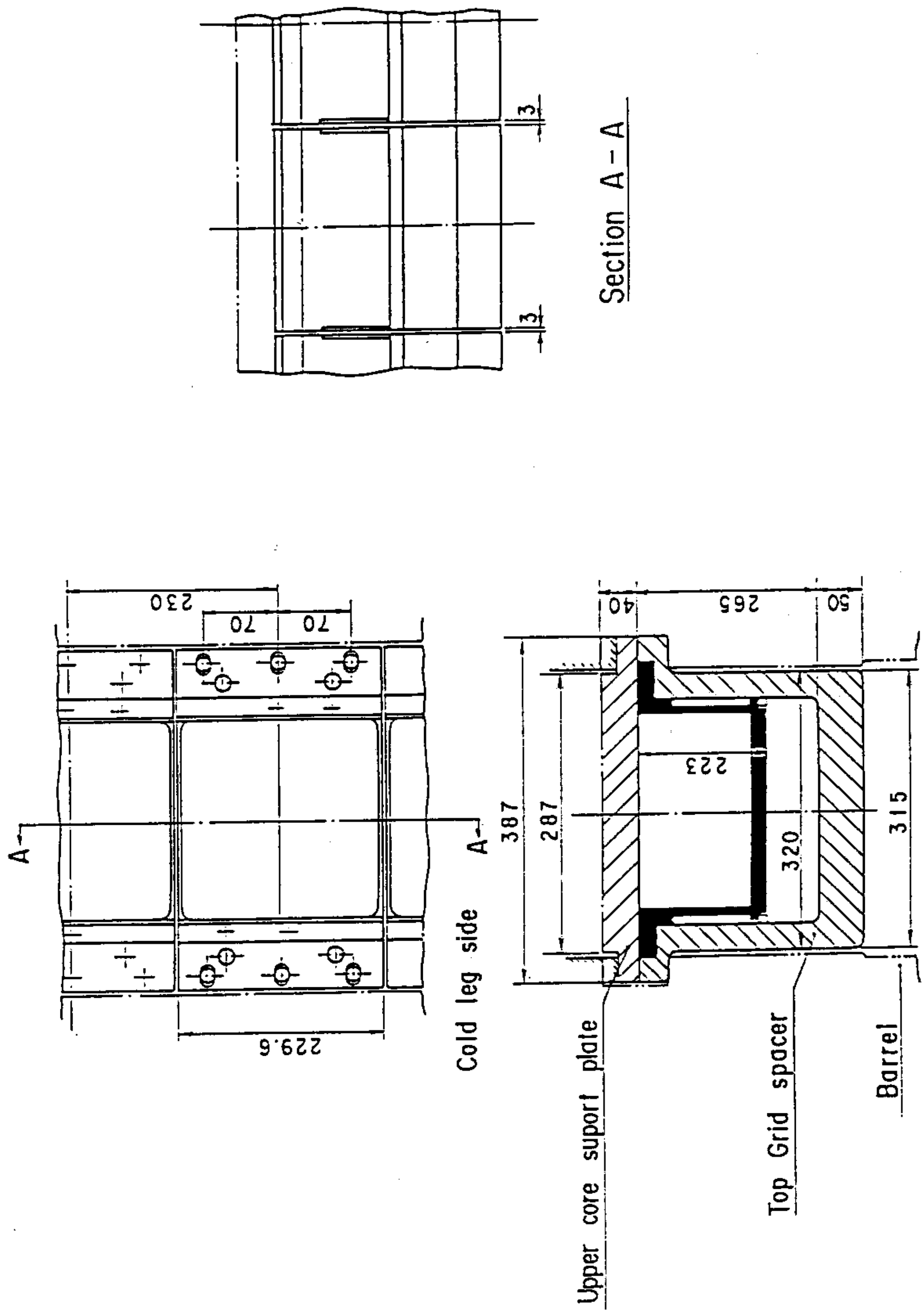

Fig. A-5 Arrangement and principal dimension of end boxes and top grid spacers

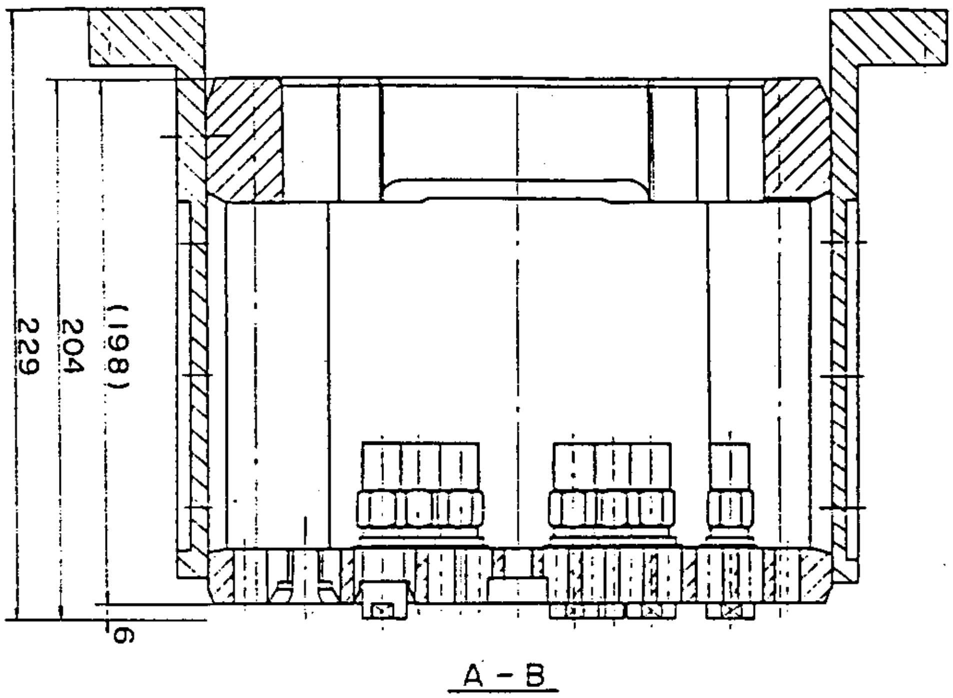

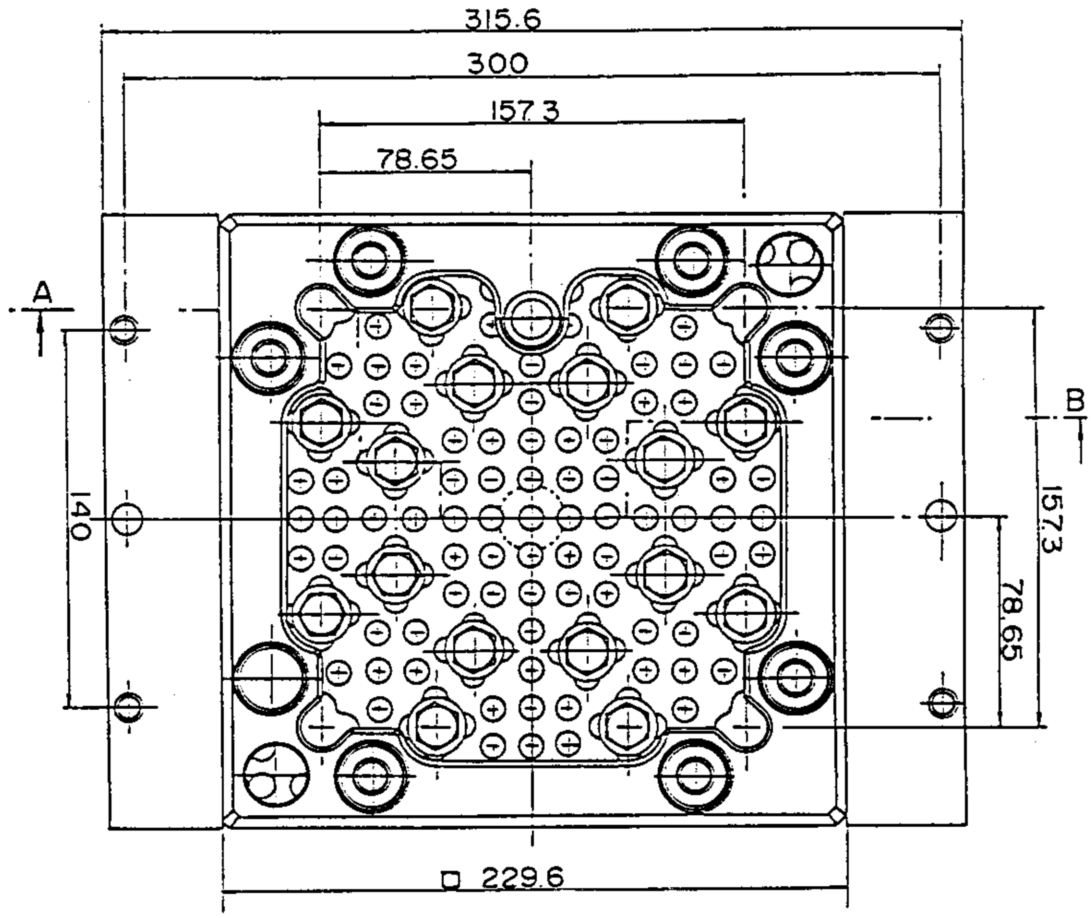

Fig. A-6 Configuration and dimension of end boxes

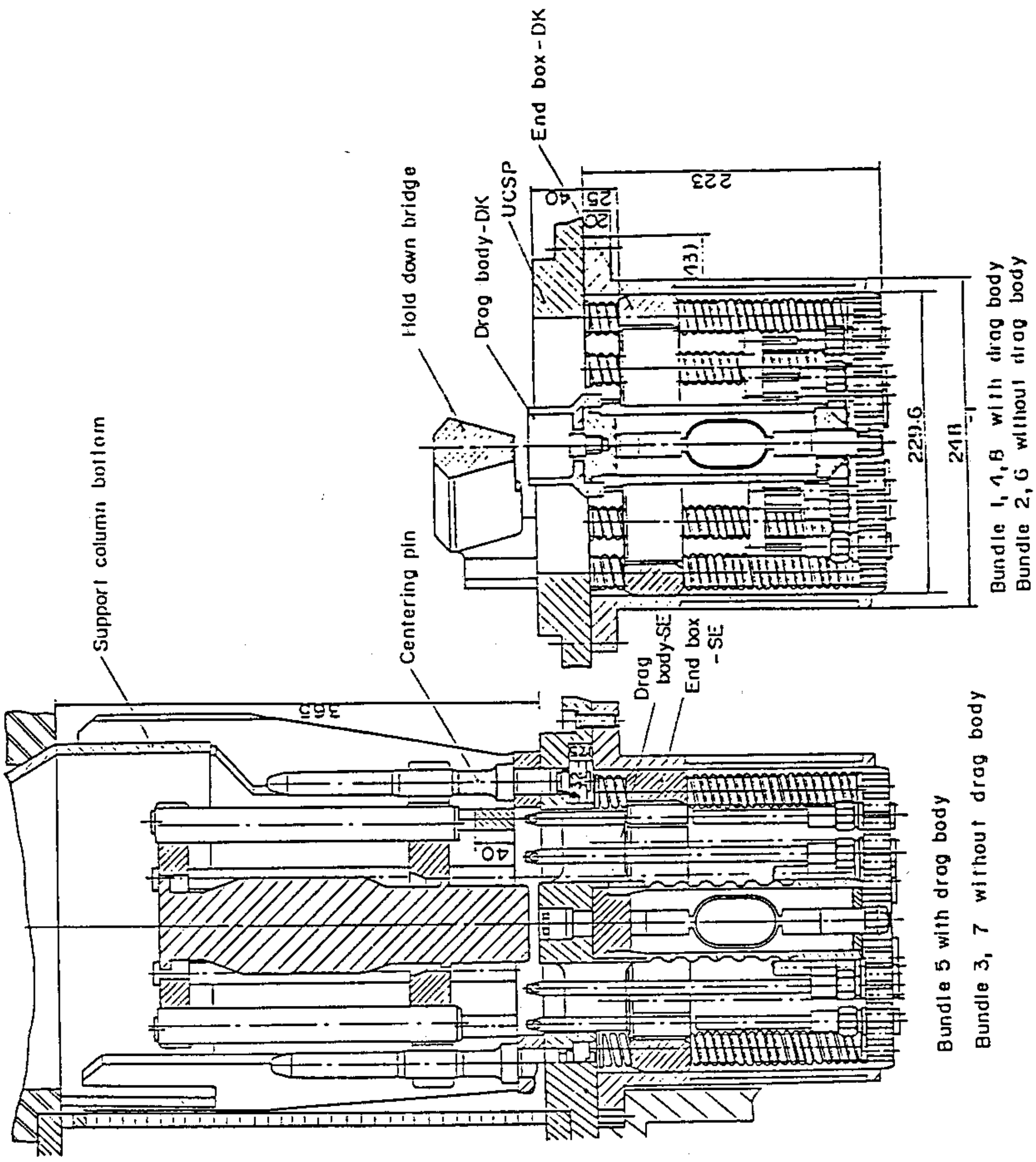

Fig. A-7 Detail of end boxes with drag bodies

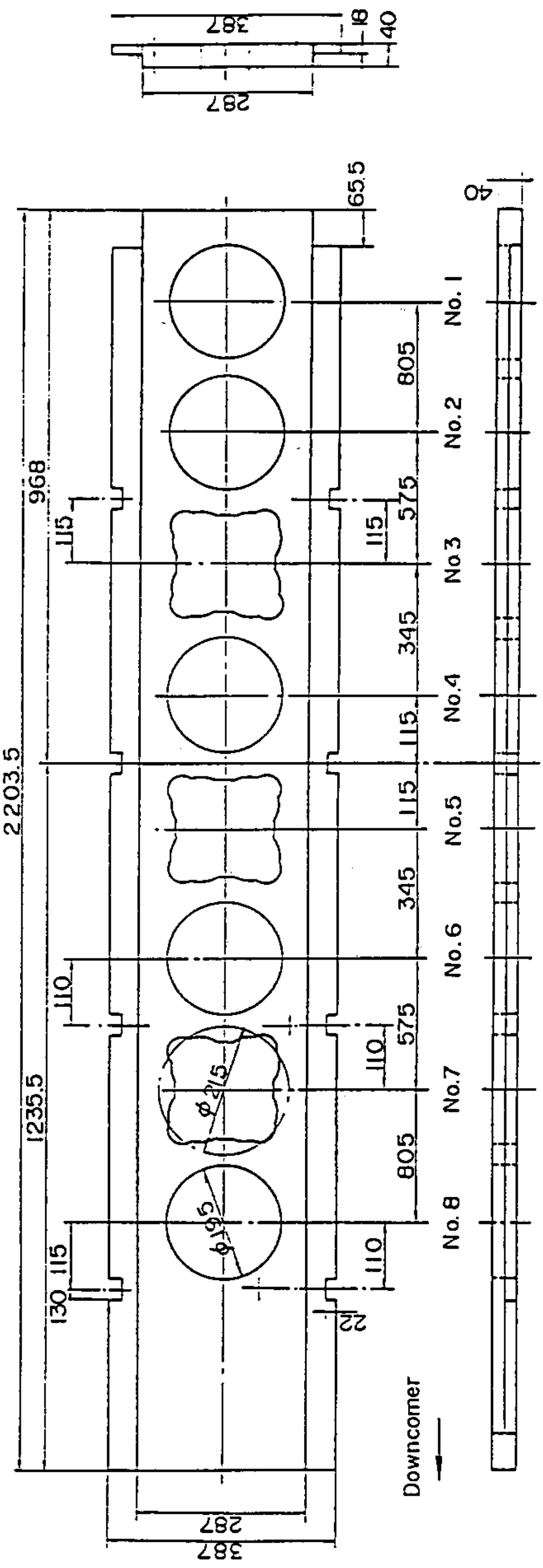

Fig. A-8 Dimension of upper core support plate

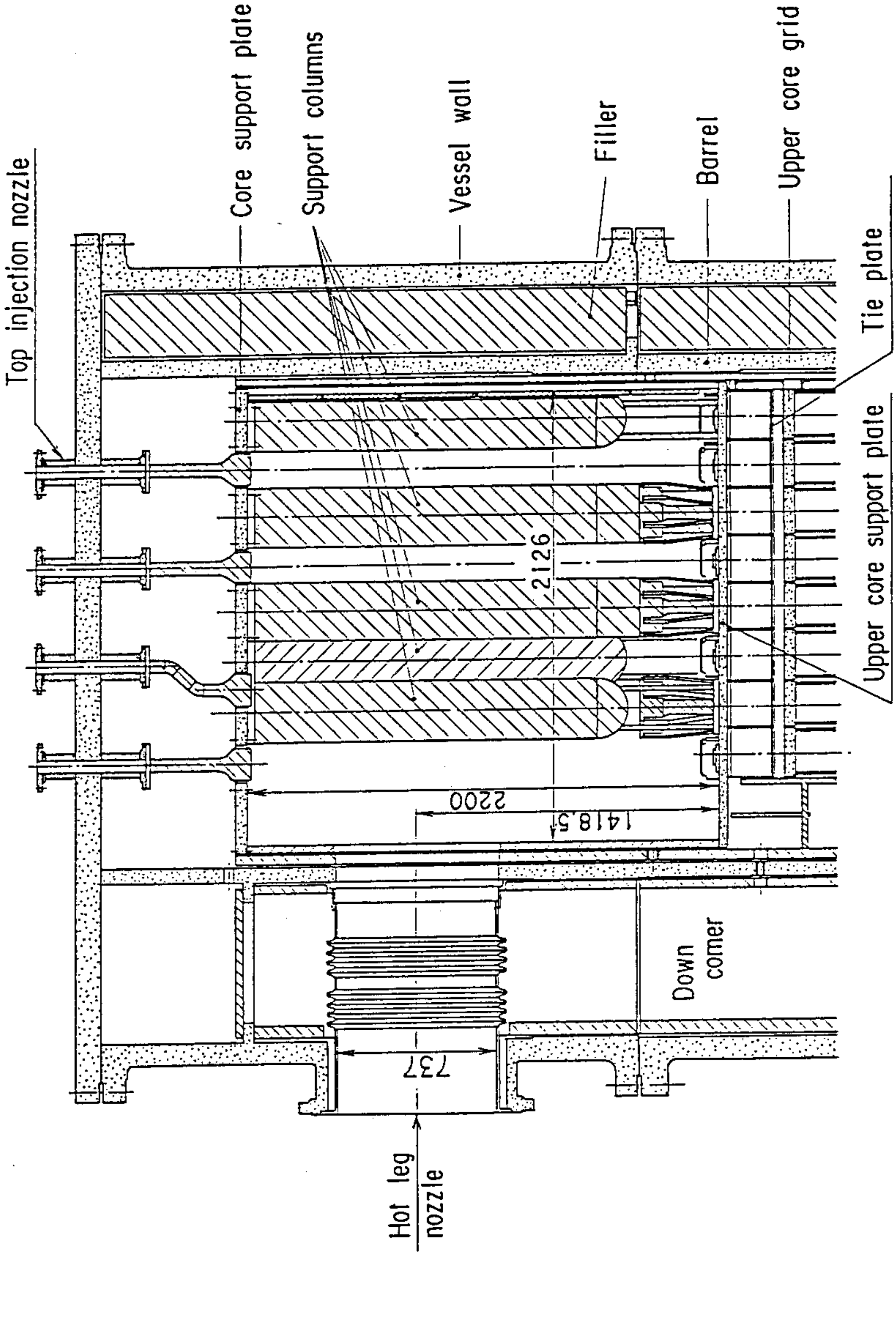

Fig. A-9 Vertical cross section of upper plenum internals

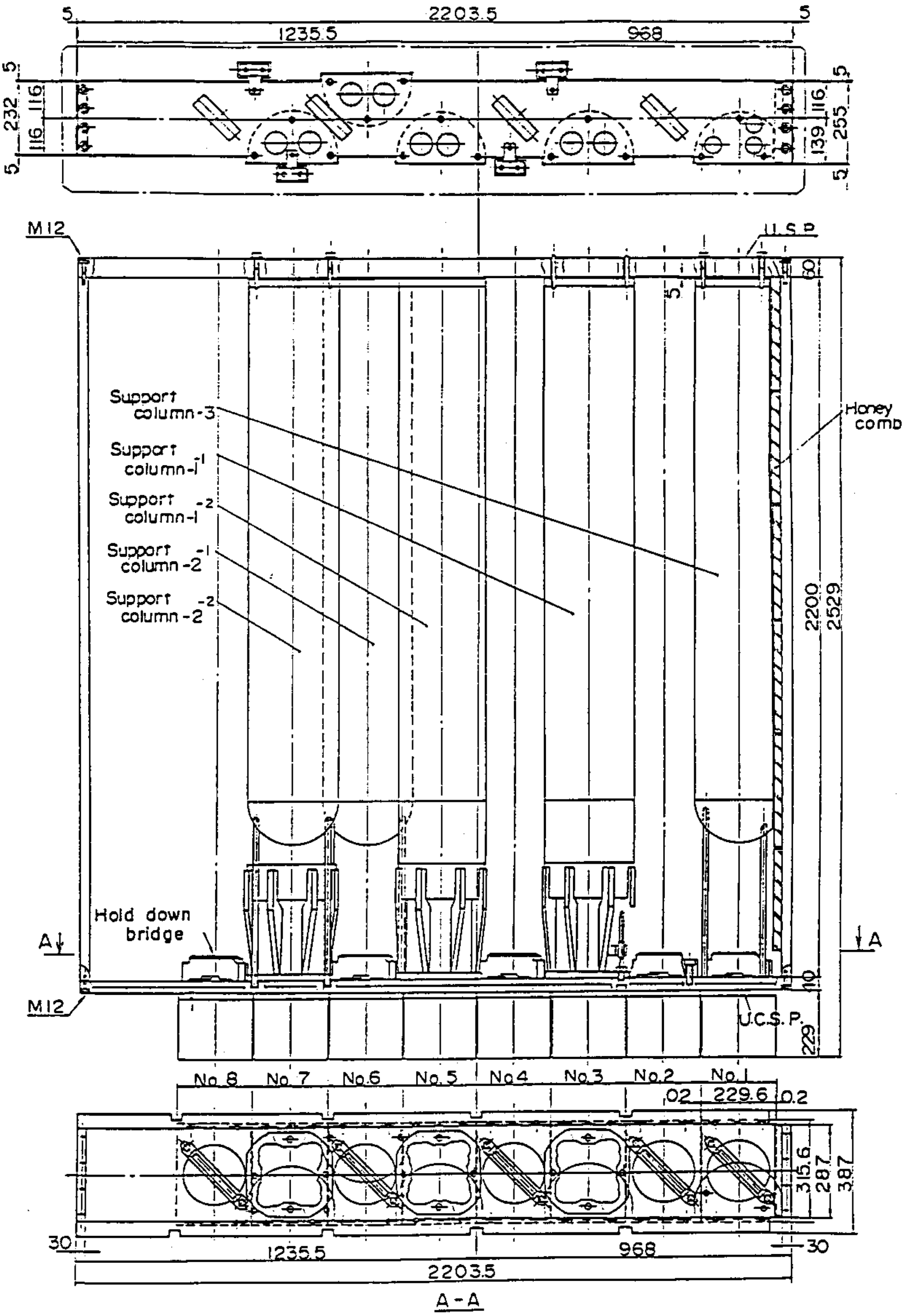

Fig. A-10 Three kinds of CRGA support column

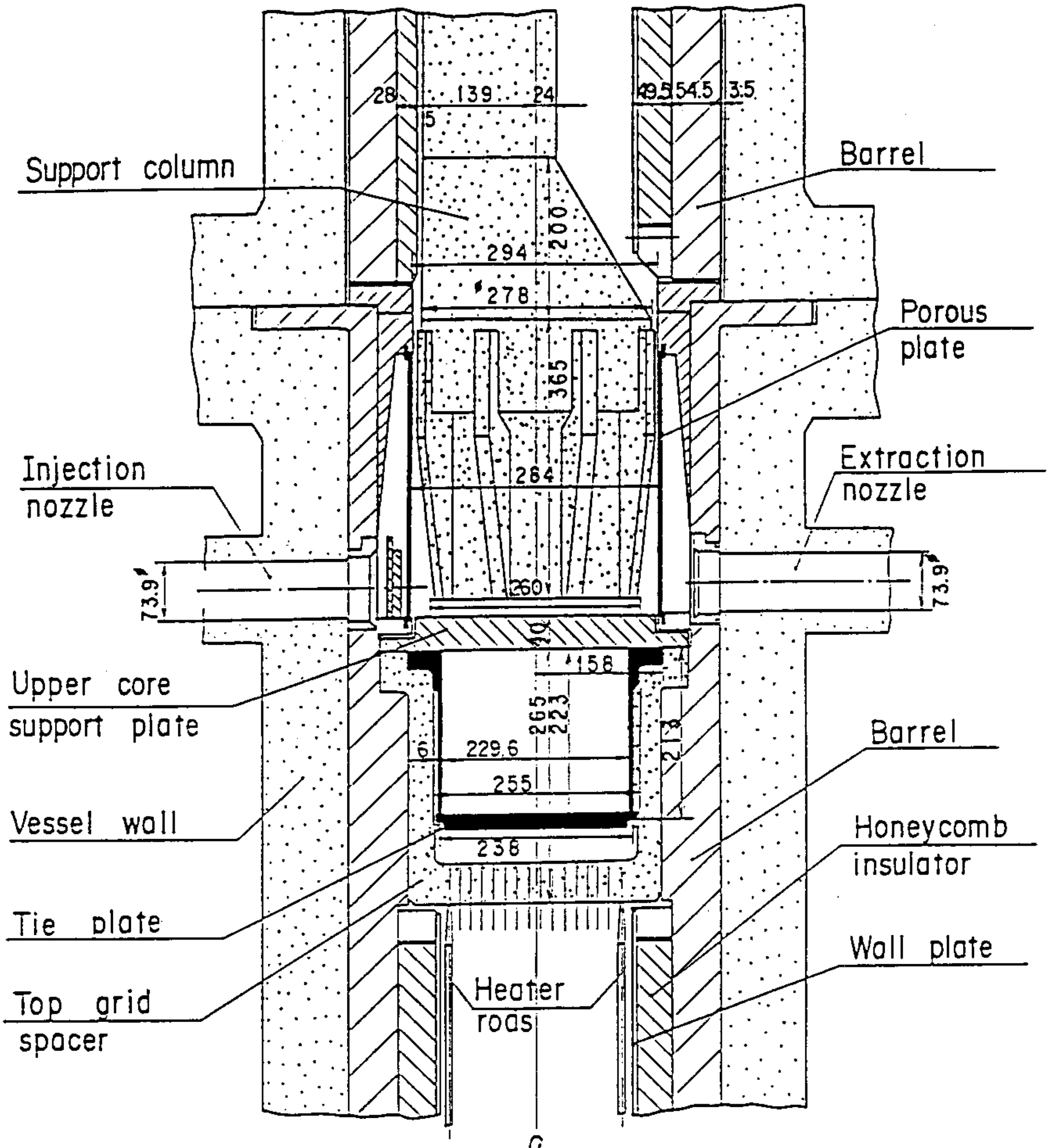

Fig. A-11 Vertical cross section of interface between core and upper plenum

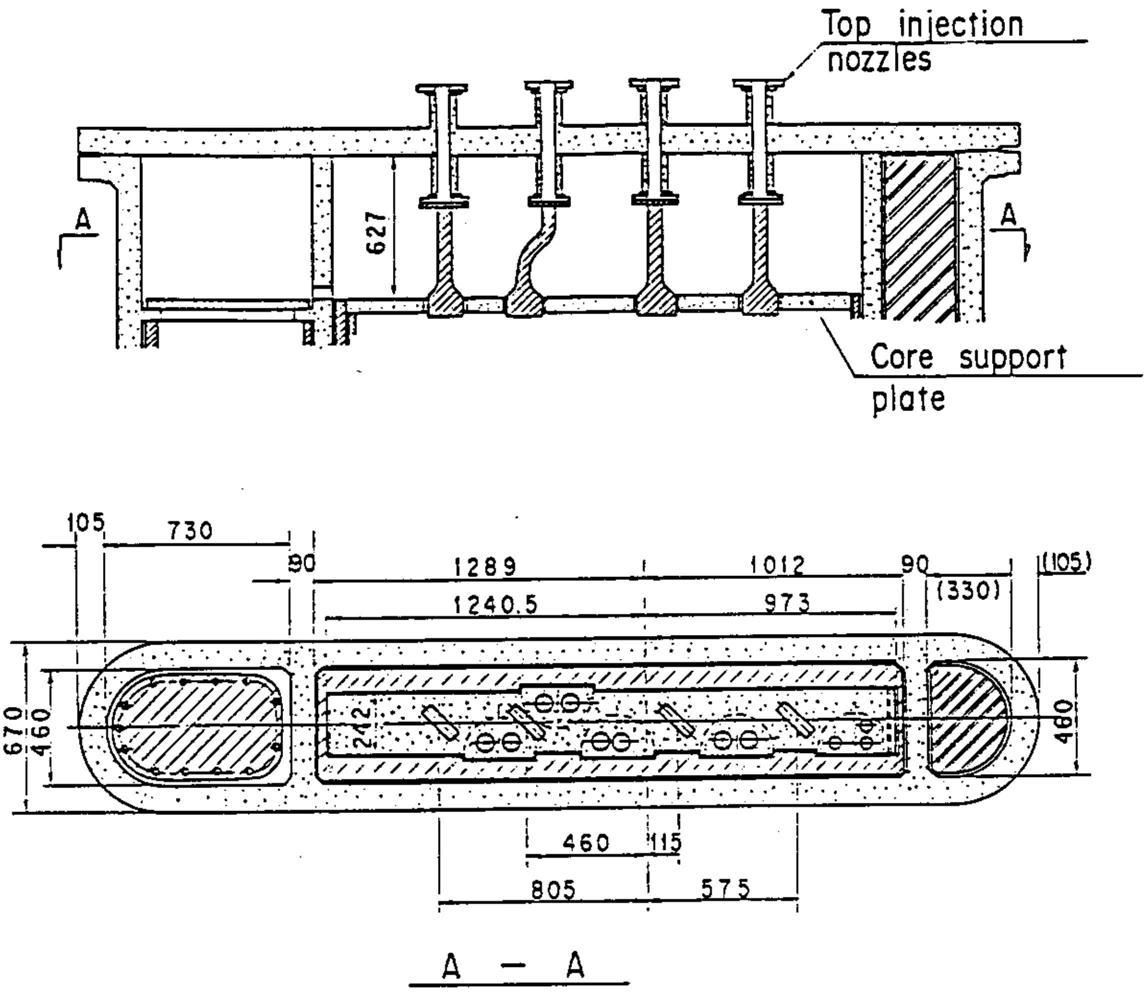

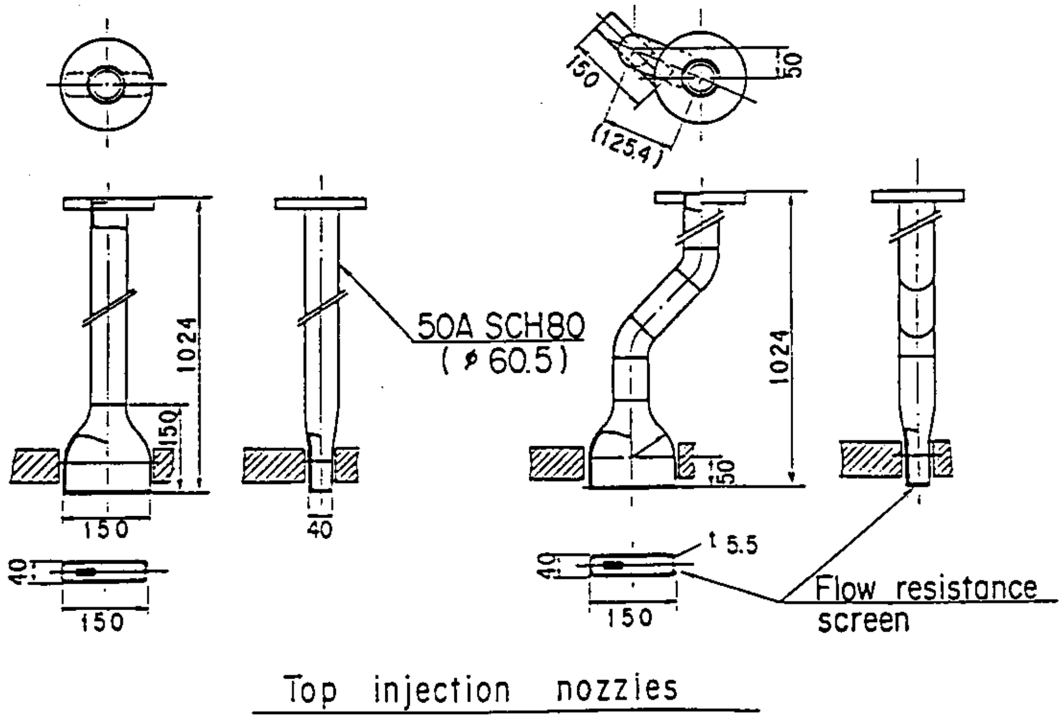

Fig. A-12 Schematic of upper head

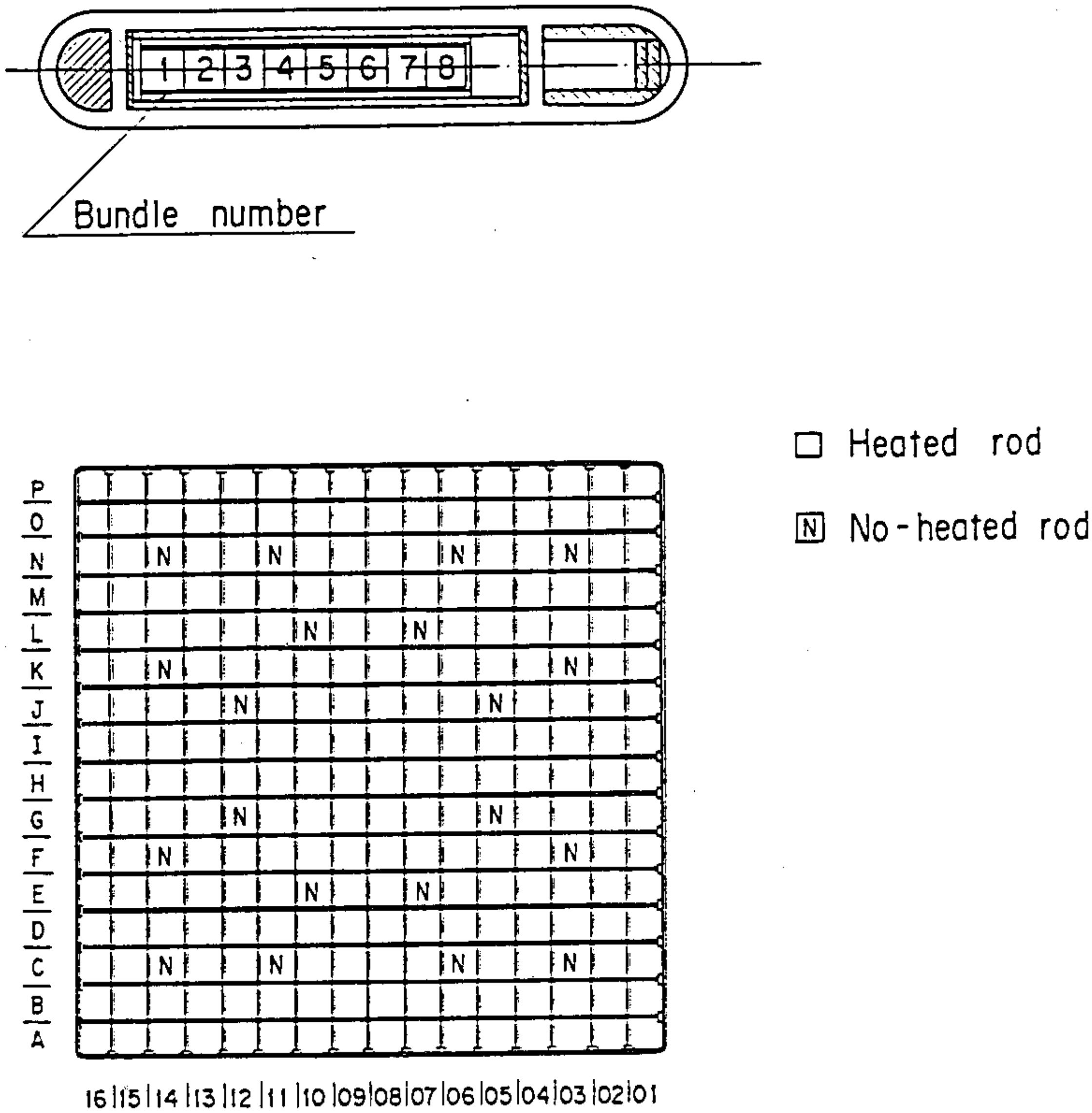

Fig. A-13 Arrangement of heater rod bundles

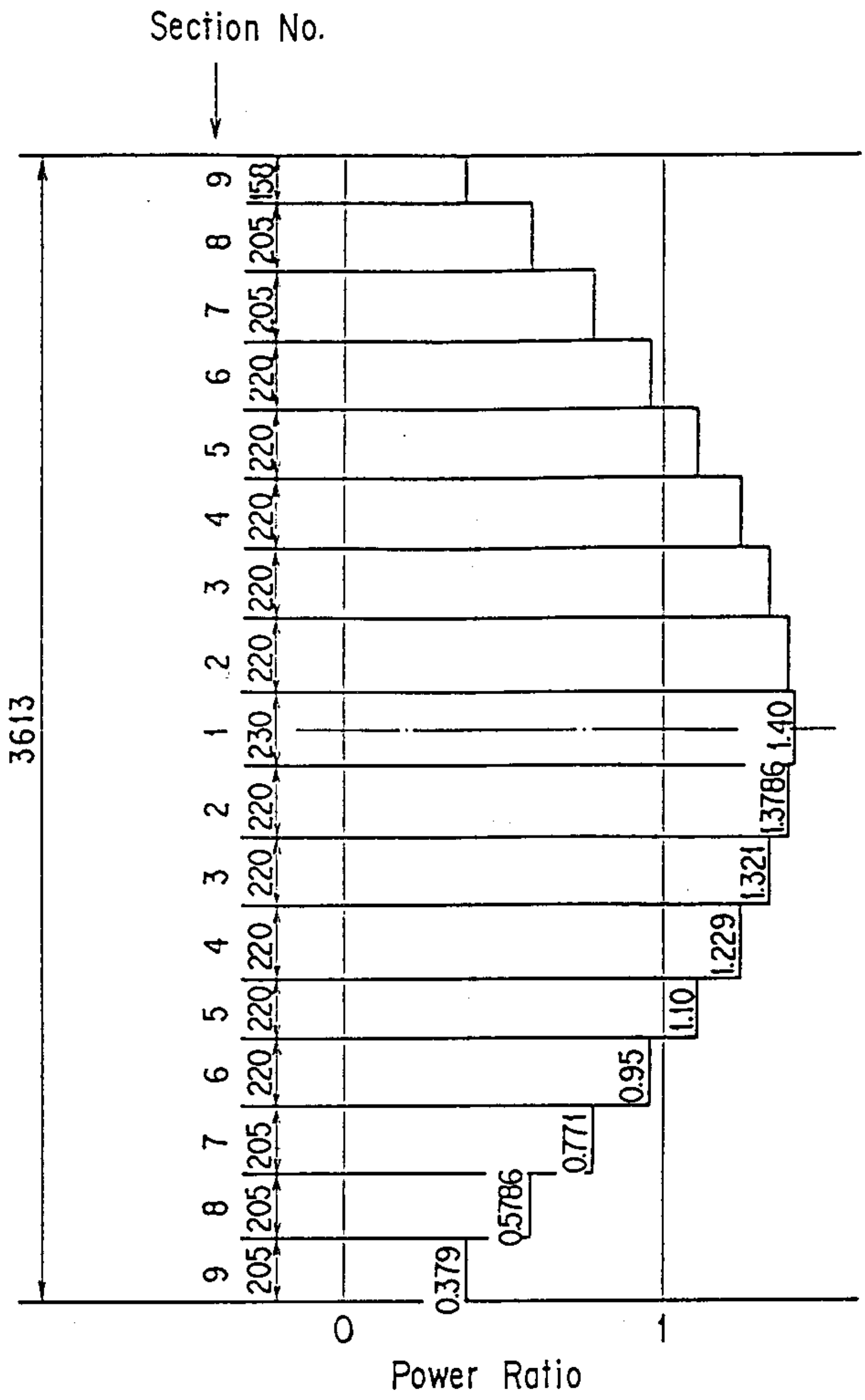

Fig. A-14 Axial power distribution of heater rods

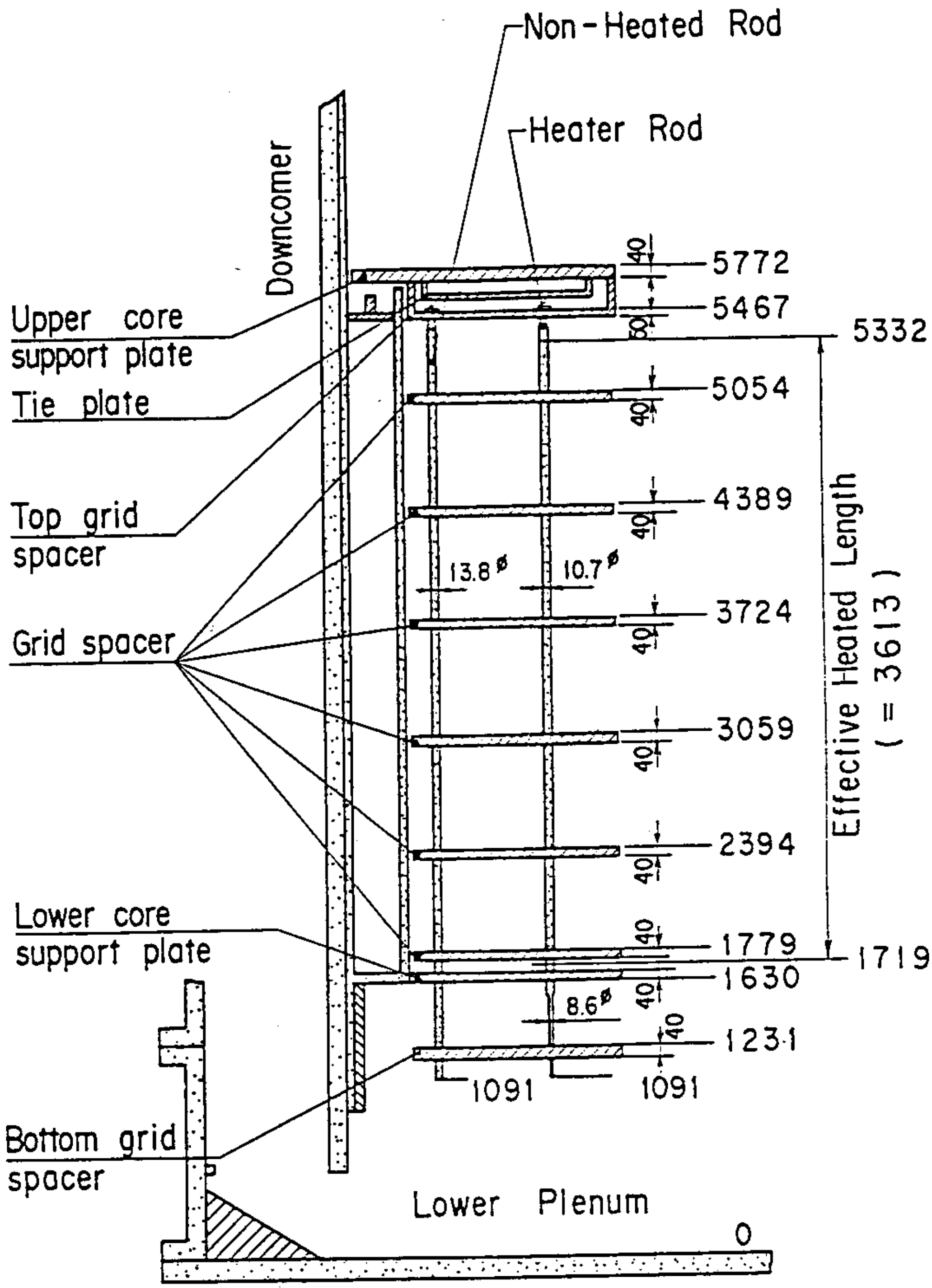

Fig. A-15 Relative Elevation and Dimension of core

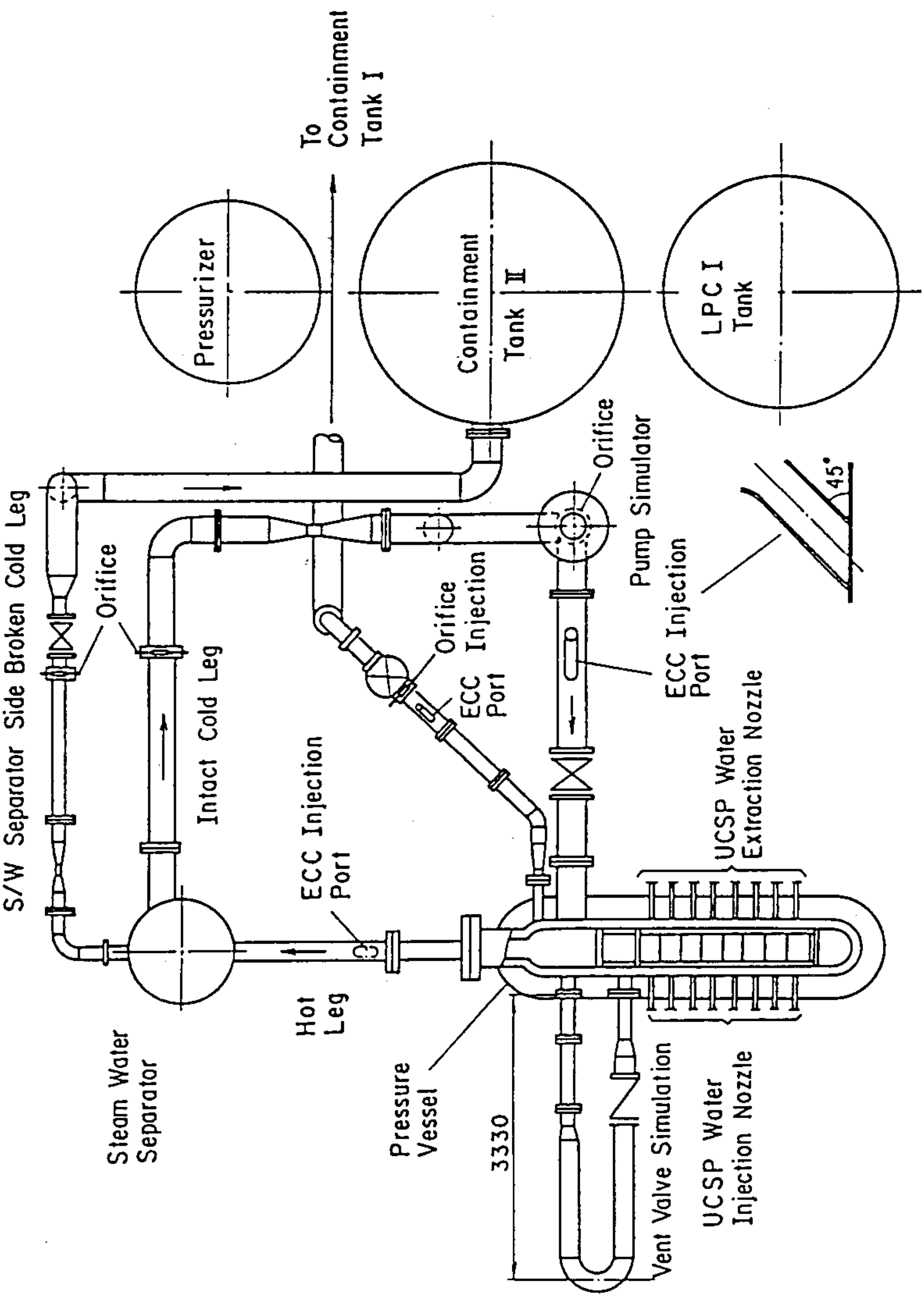

Fig. A-16 Overview of the arrangements of SCTF

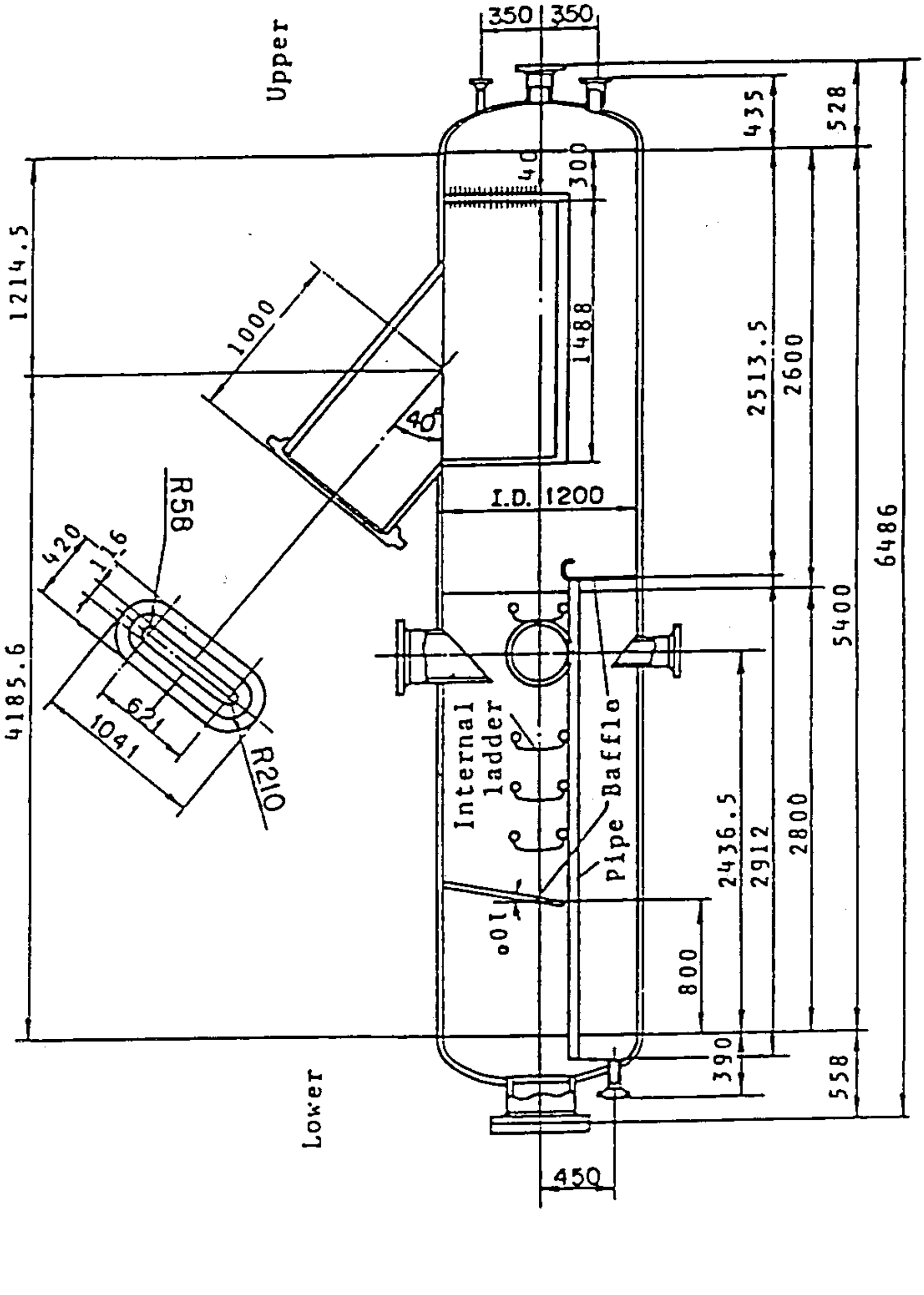

Fig. A-17 Steam/Water separator

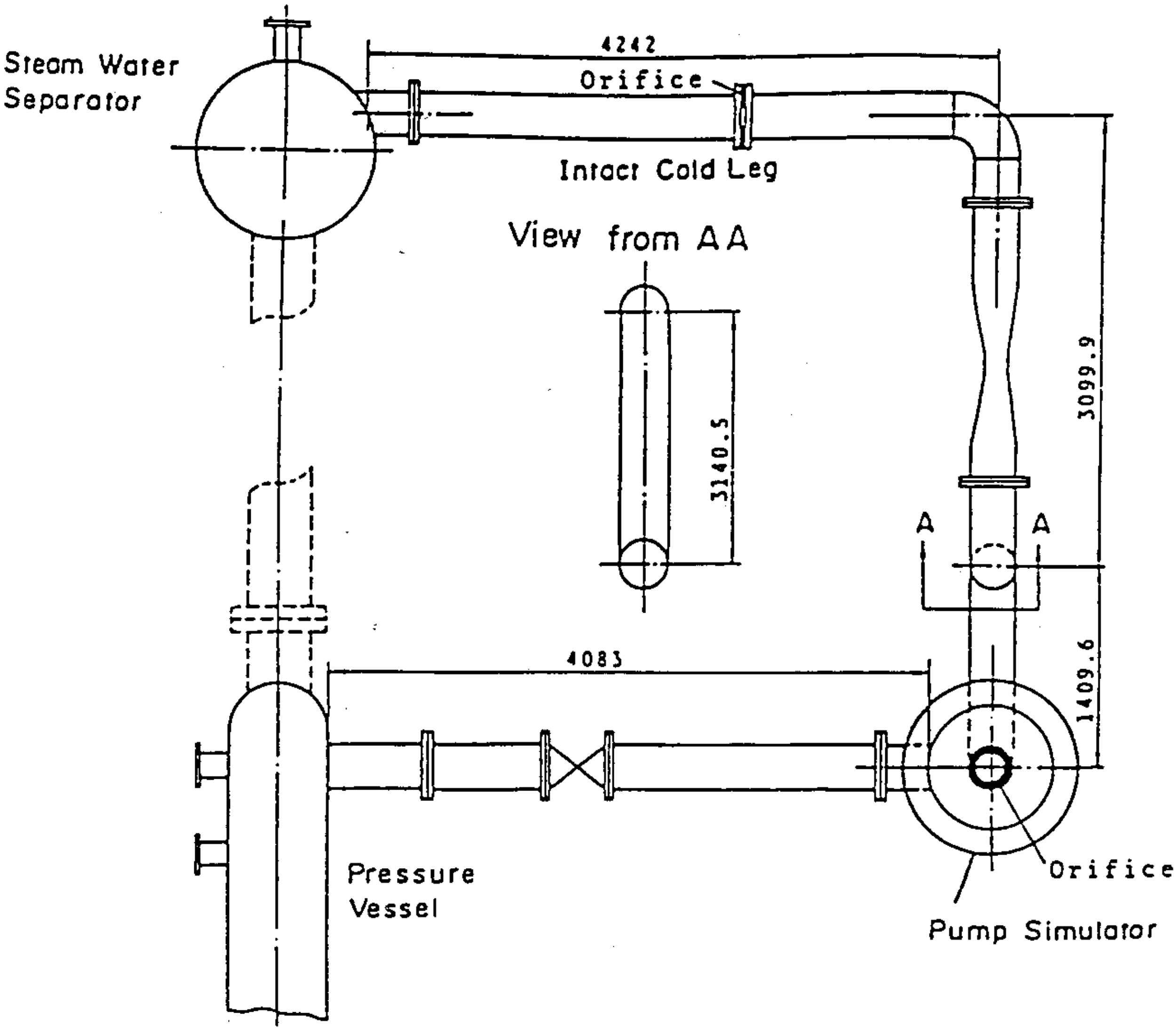

Fig. A-18 Arrangement of intact cold leg

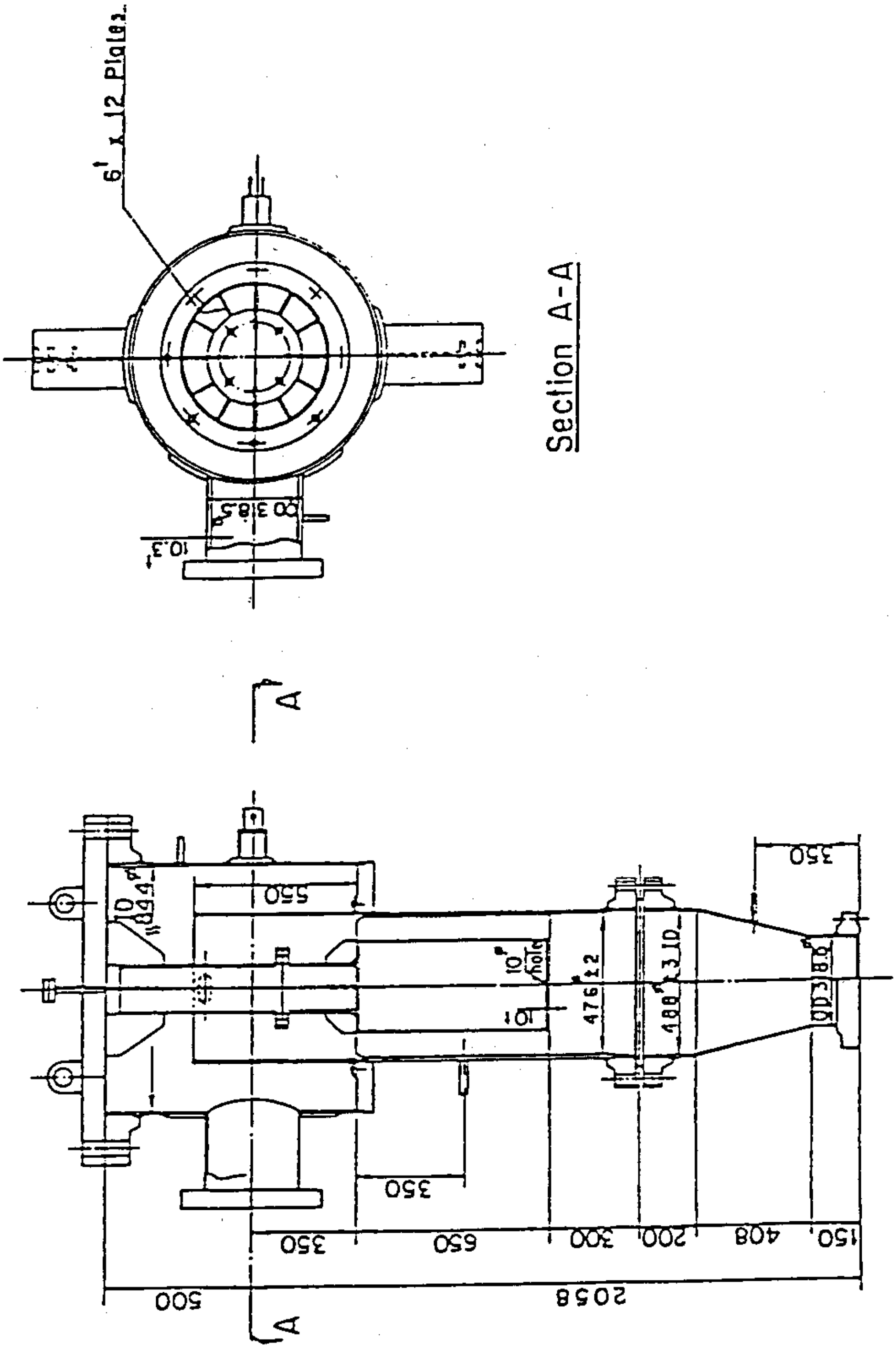

Fig. A-19　Configuration and dimension of pump simulator

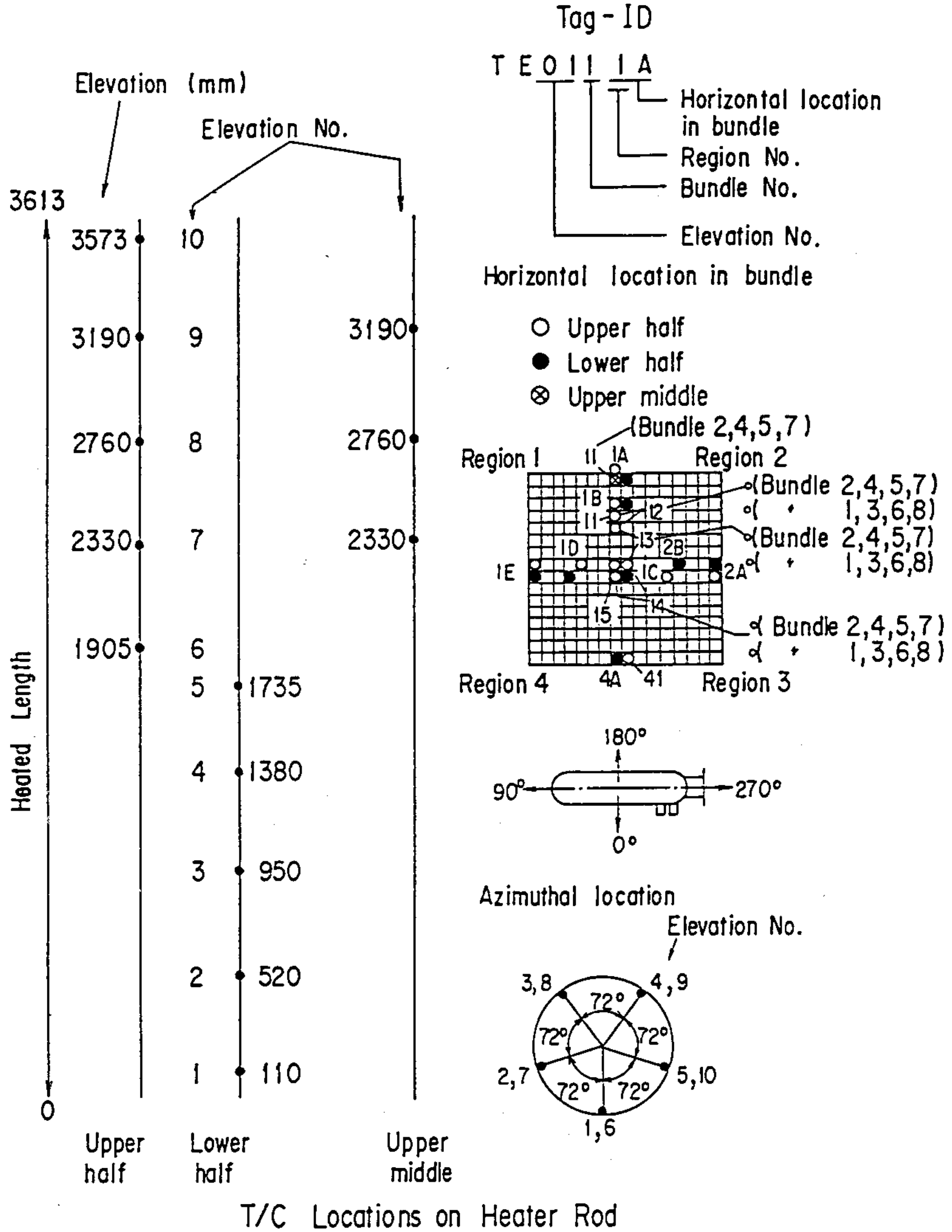

Fig. A-20 Thermocouple locations of heater rod surface temperature measurements

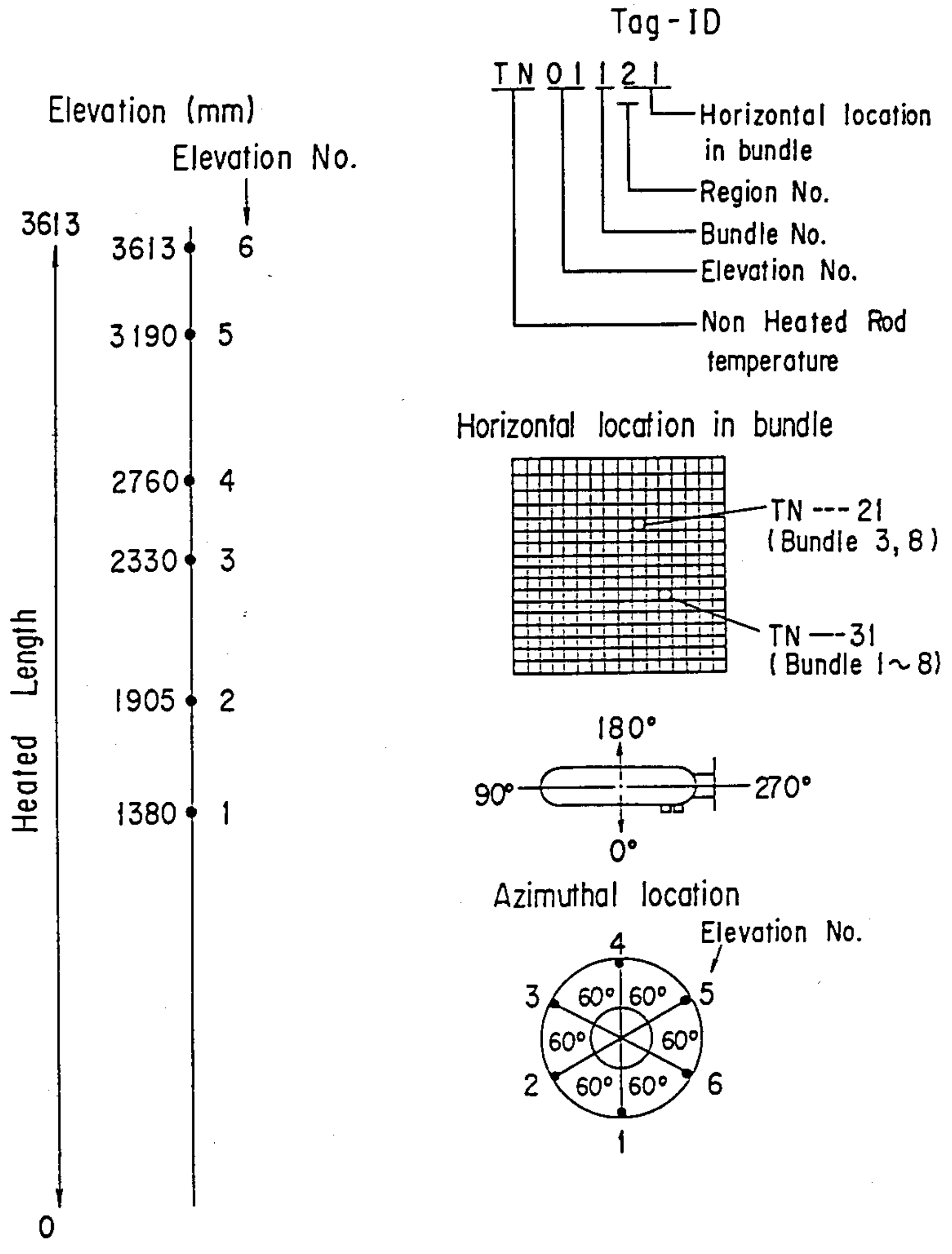

Fig. A-21 Thermocouple locations of Non-Heated rod surface temperature measurements

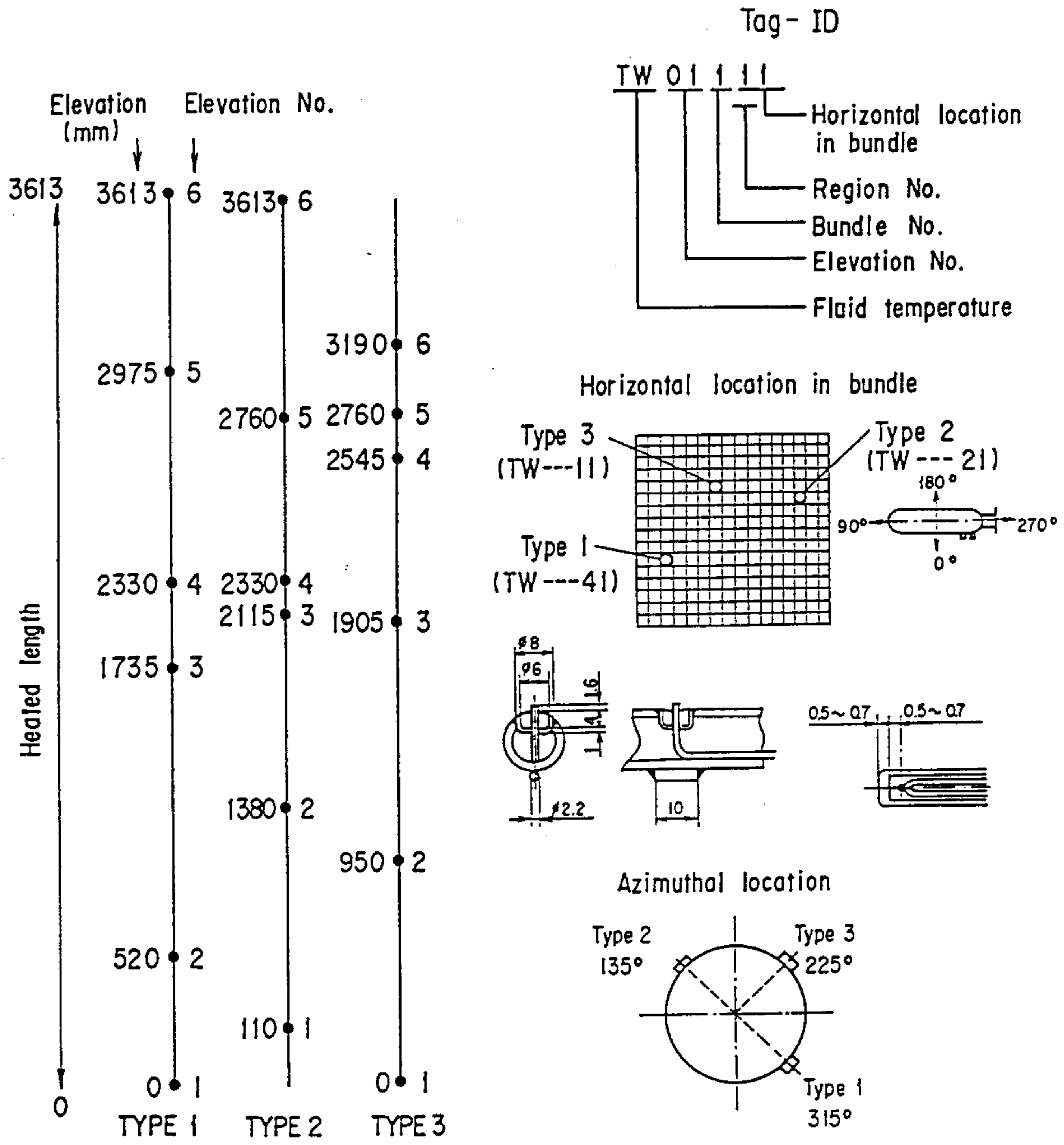

Fig. A-22 Thermocouple locations of fluid temperature measurements in core

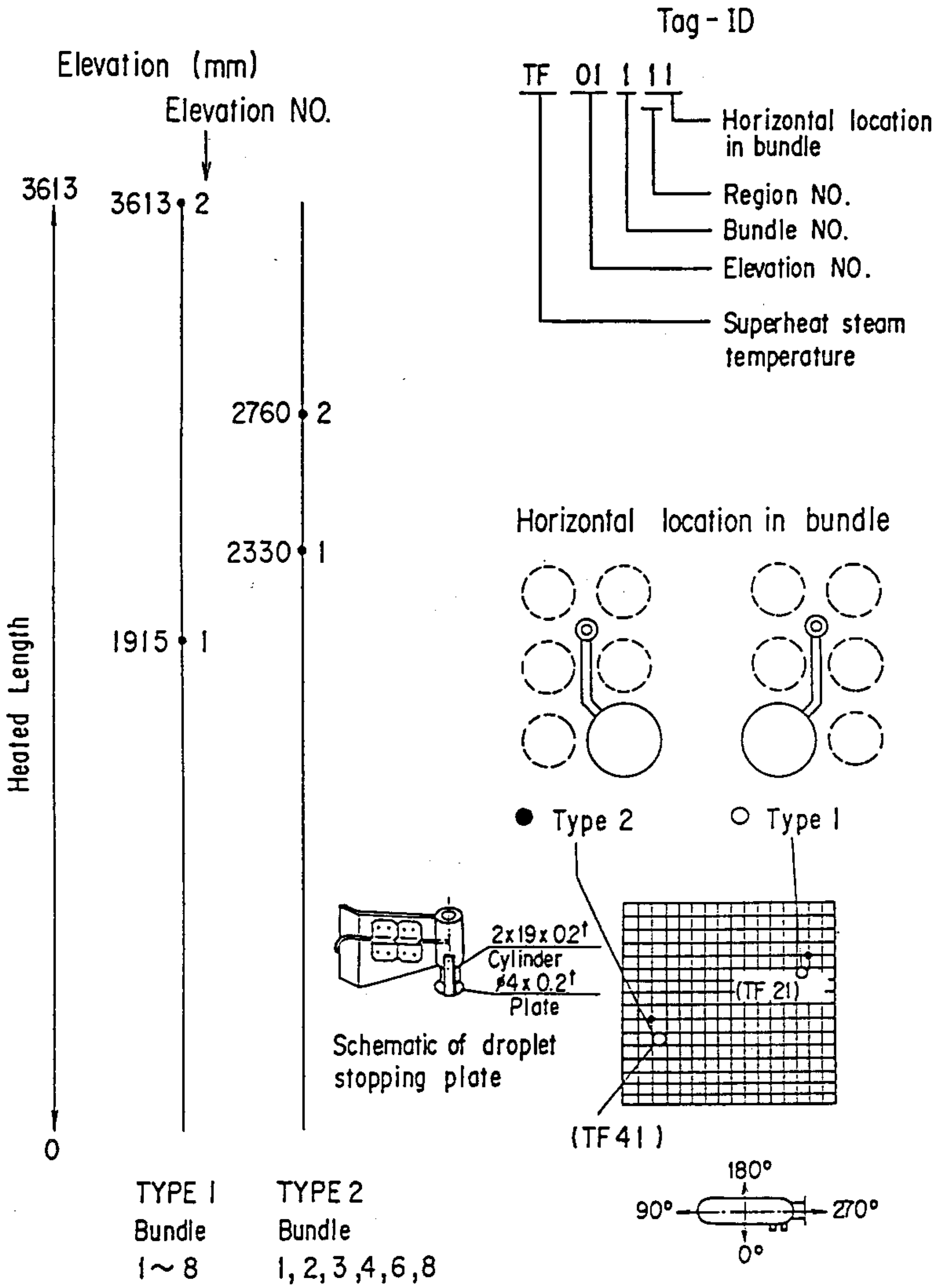

Fig. A-23 Thermocouple locations of steam temperature measurements in core

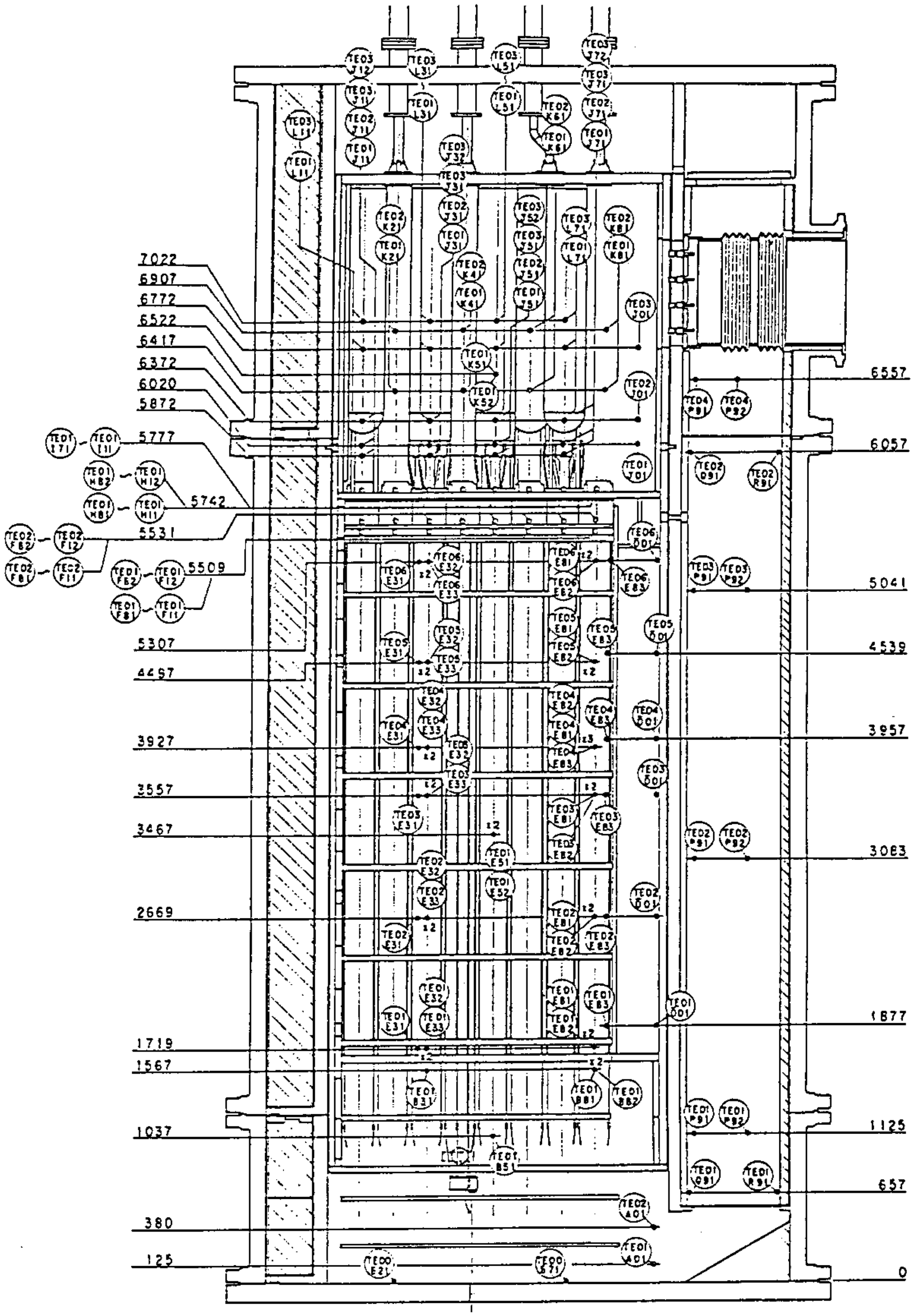

Fig. A-24 Thermocouple locations of temperature measurements in pressure vessel except core region (Vertical view)

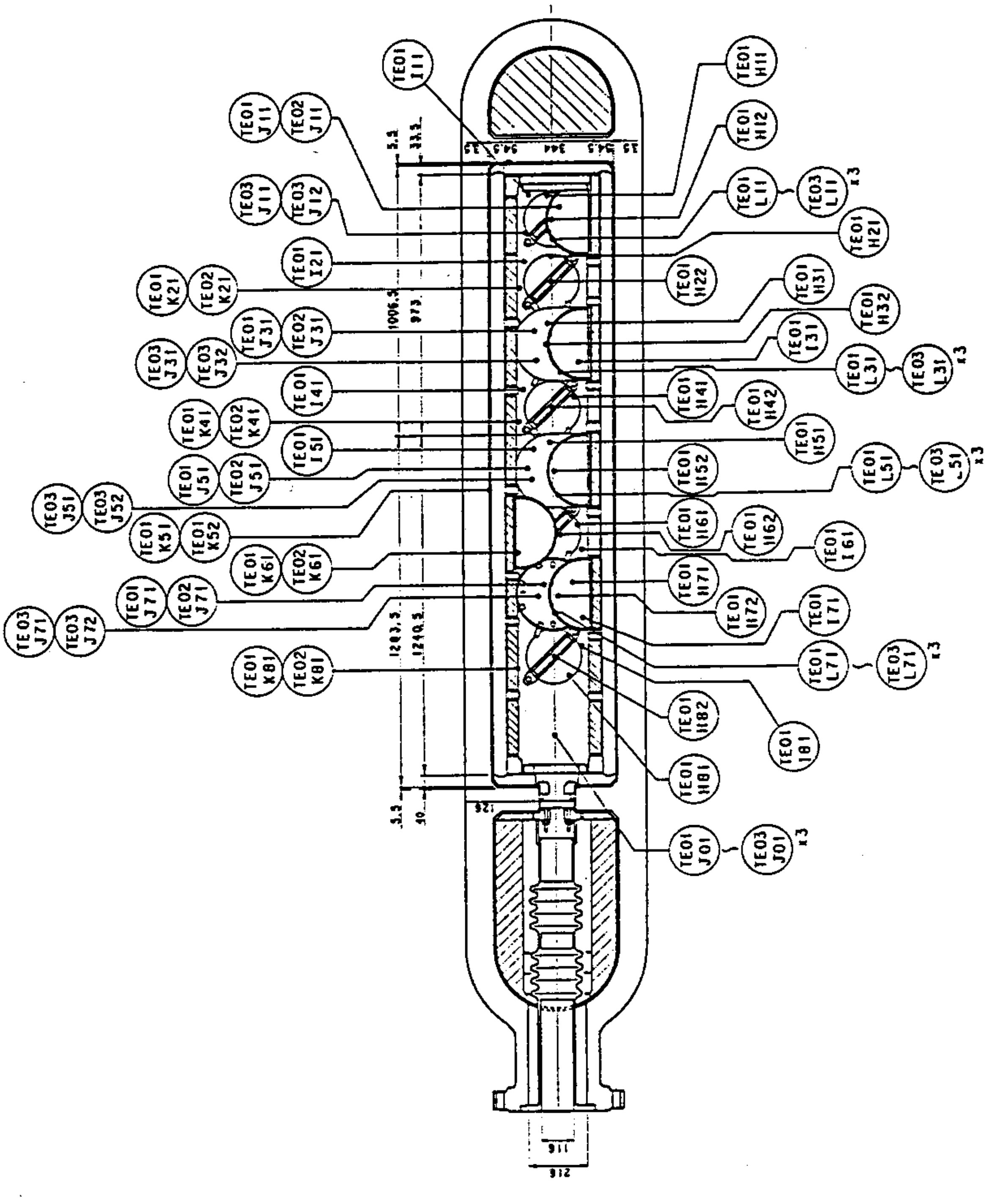

Fig. A-25 Thermocouple locations of temperature measurements in upper plenum (Horizontal view)

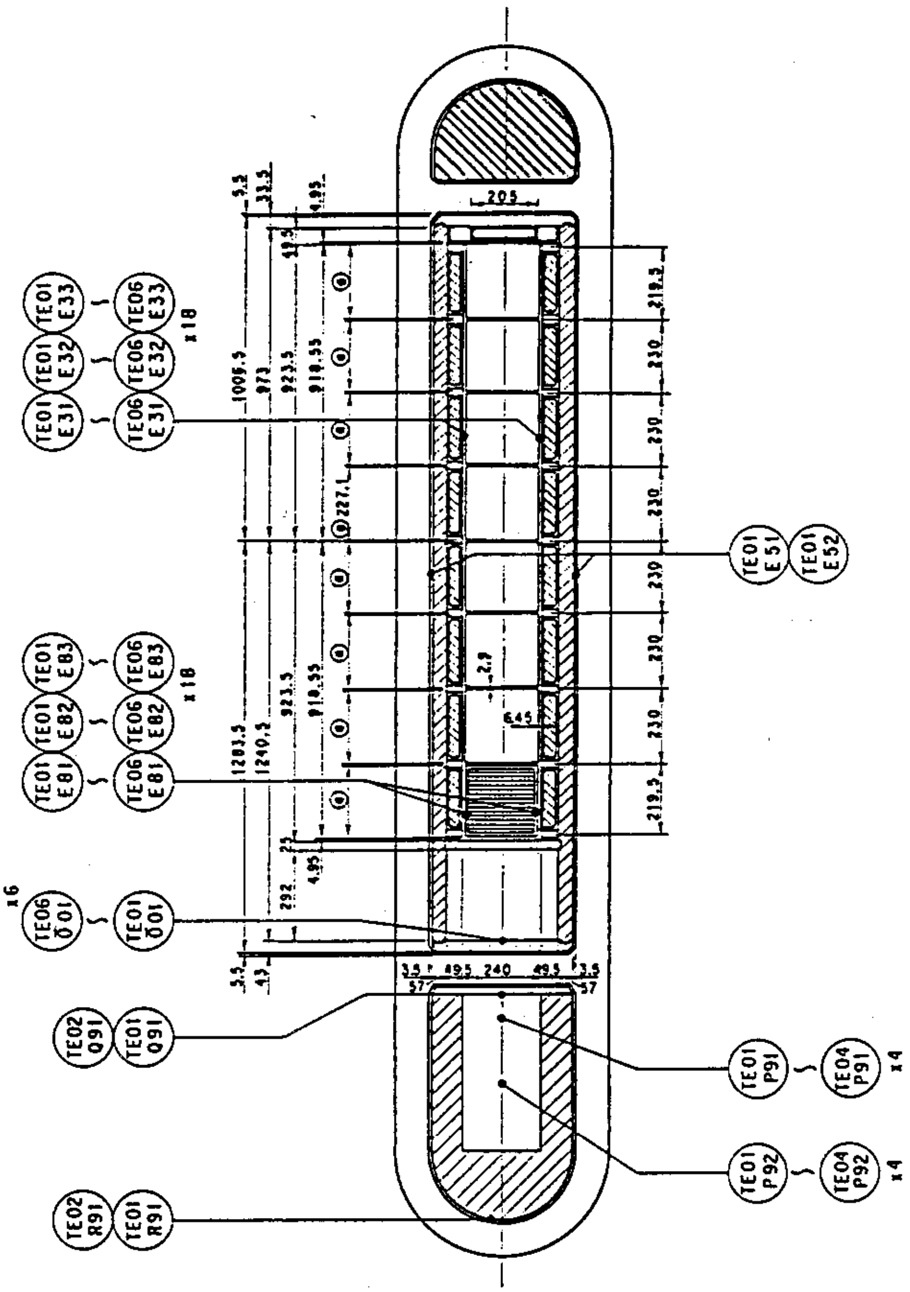

Fig. A-26 Thermocouple locations of temperature measurements in pressure vessel except upper plenum (Horizontal view)

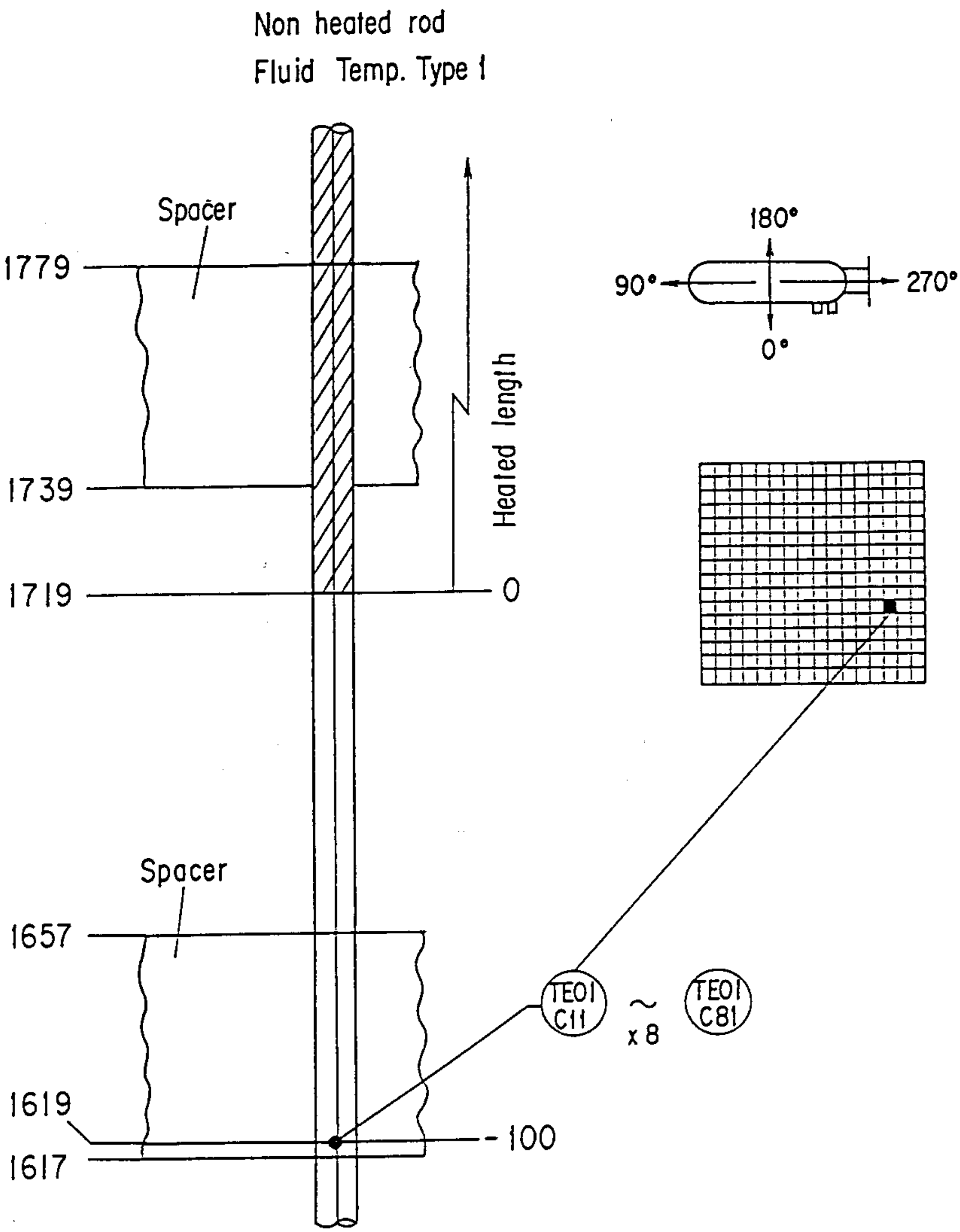

Fig. A-27 Thermocouple locations of fluid temperature measurements at core inlet

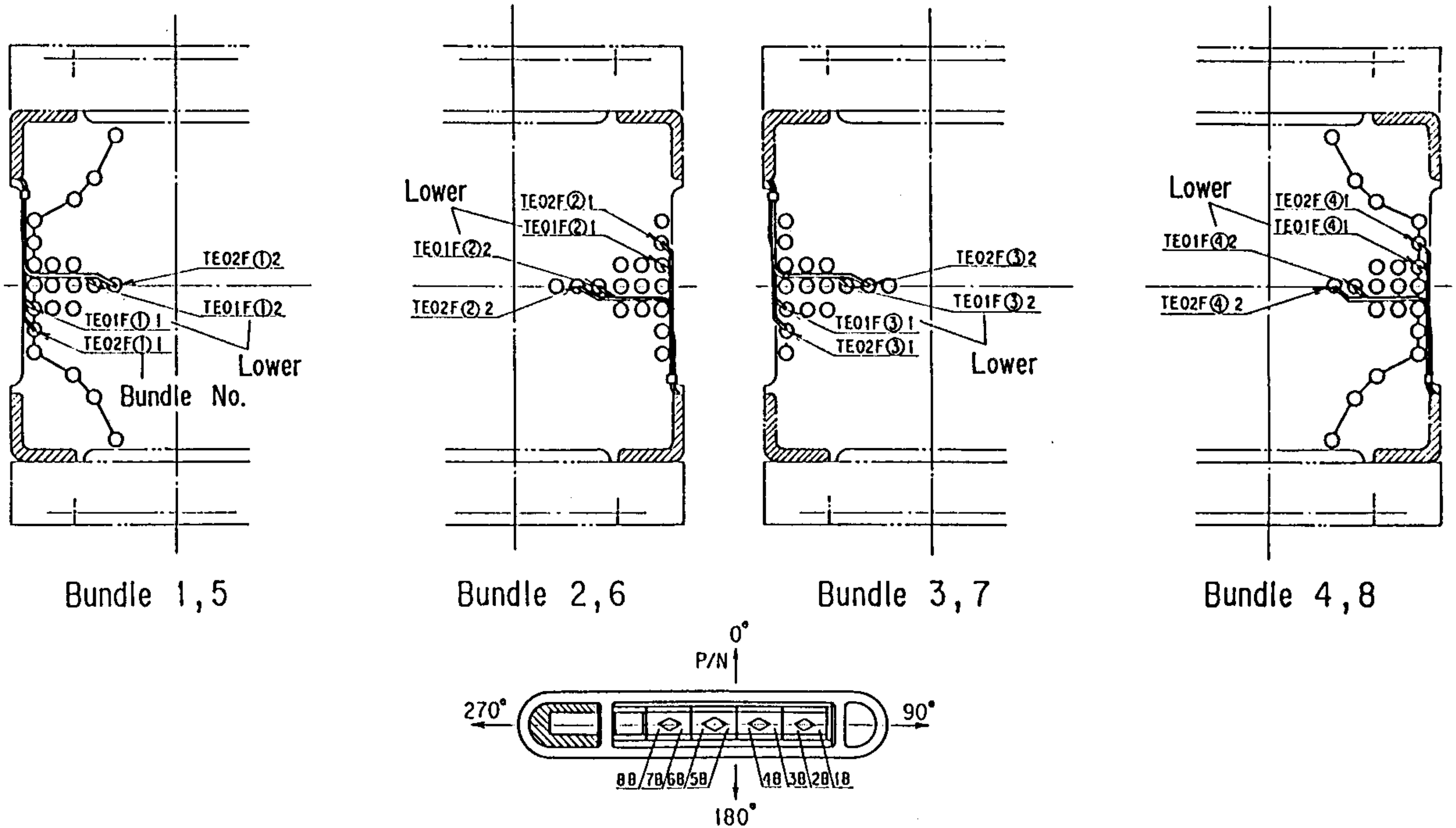

Fig. A-28　Thermocouple locations of fluid temperature measurements just above and below end box tie plates

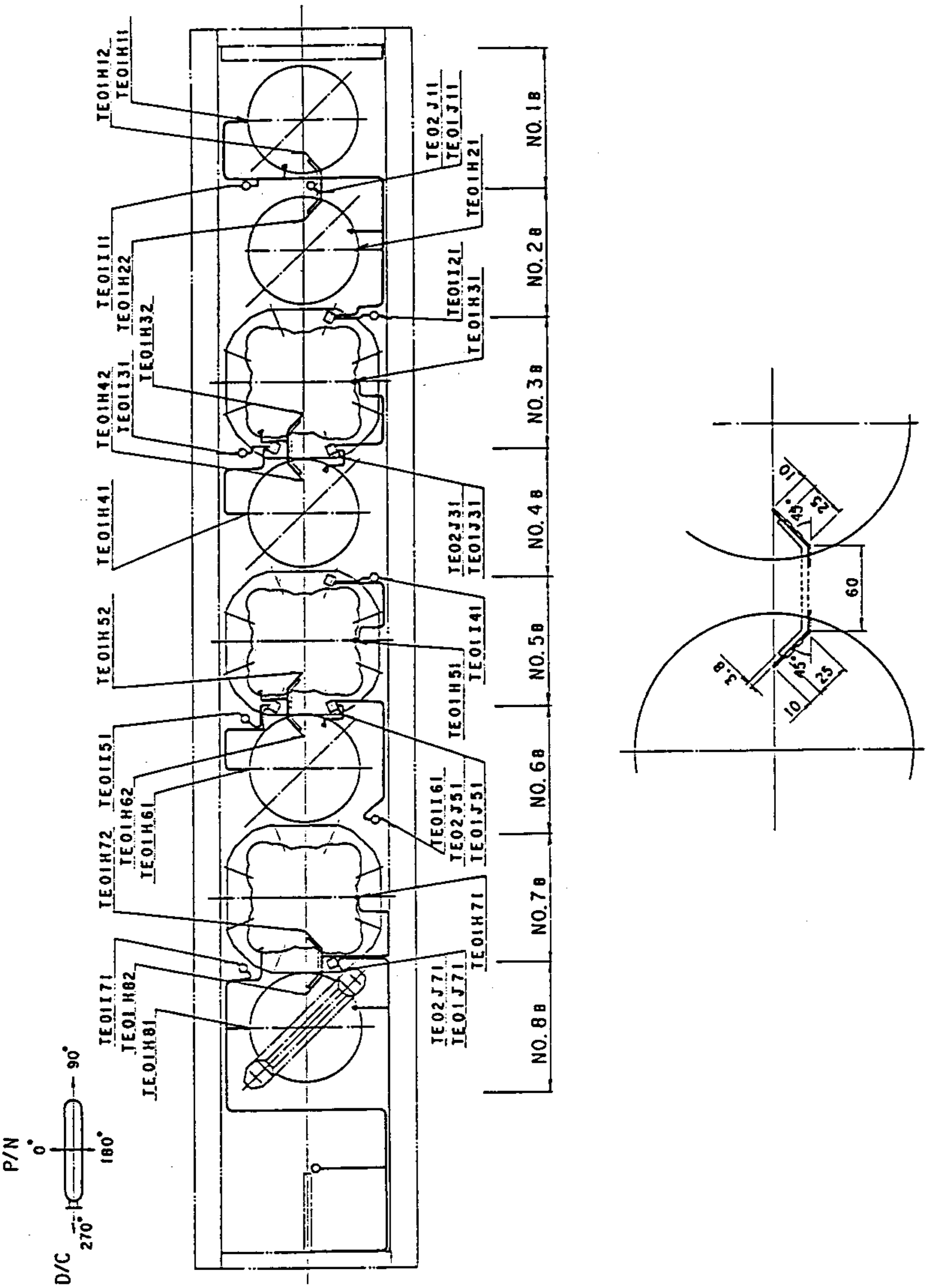

Fig. A-29 Thermocouple locations of fluid temperature measurements on UCSP and at inside and periphery of UCSP holes

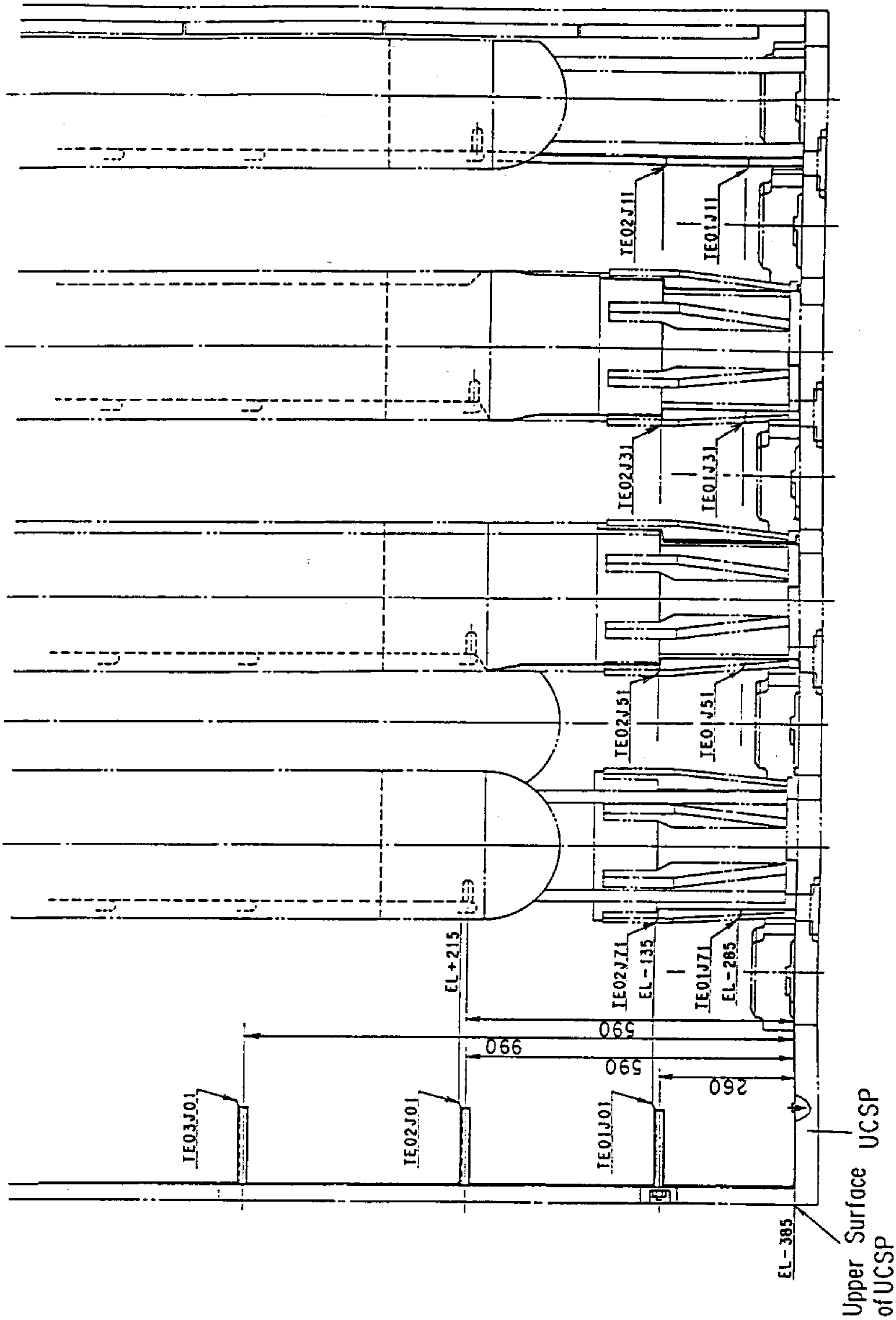

Fig. A-30 Thermocouple locations of fluid temperature measurements on and above UCSP

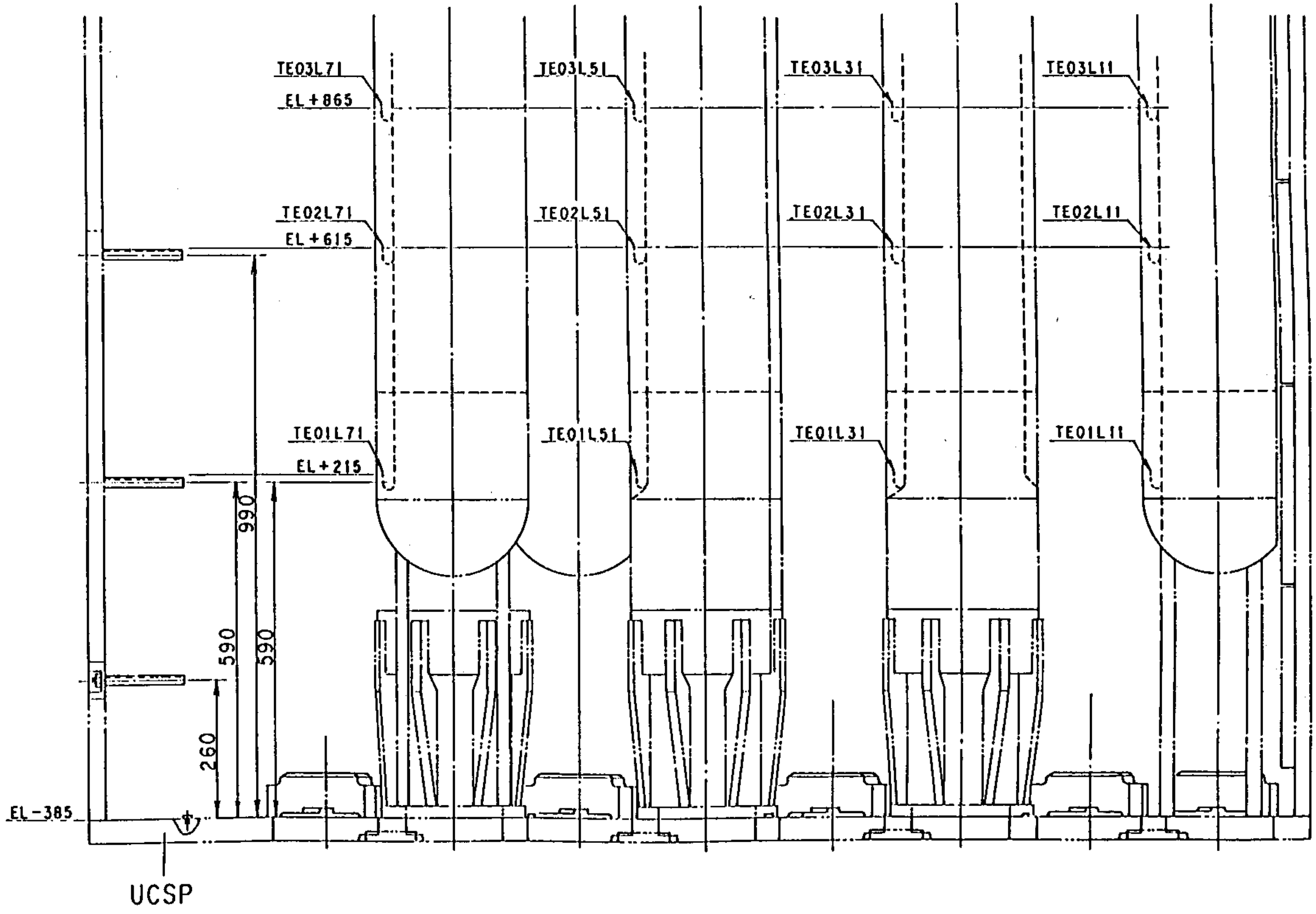

Fig. A-31 Thermocouple locations of surface temperature measurements of upper plenum structures

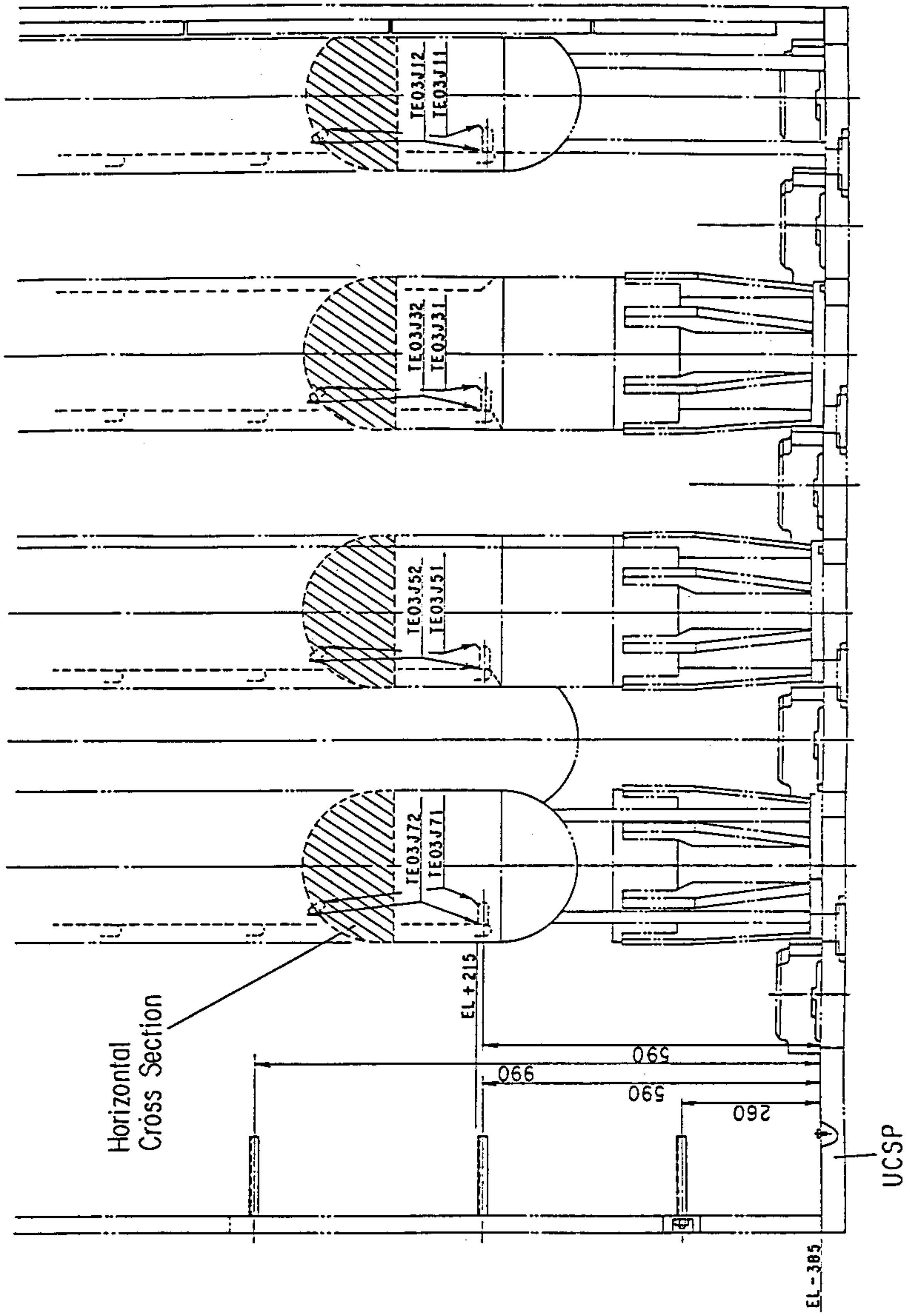

Fig. A-32 Thermocouple locations of steam temperature measurements above UCSP holes

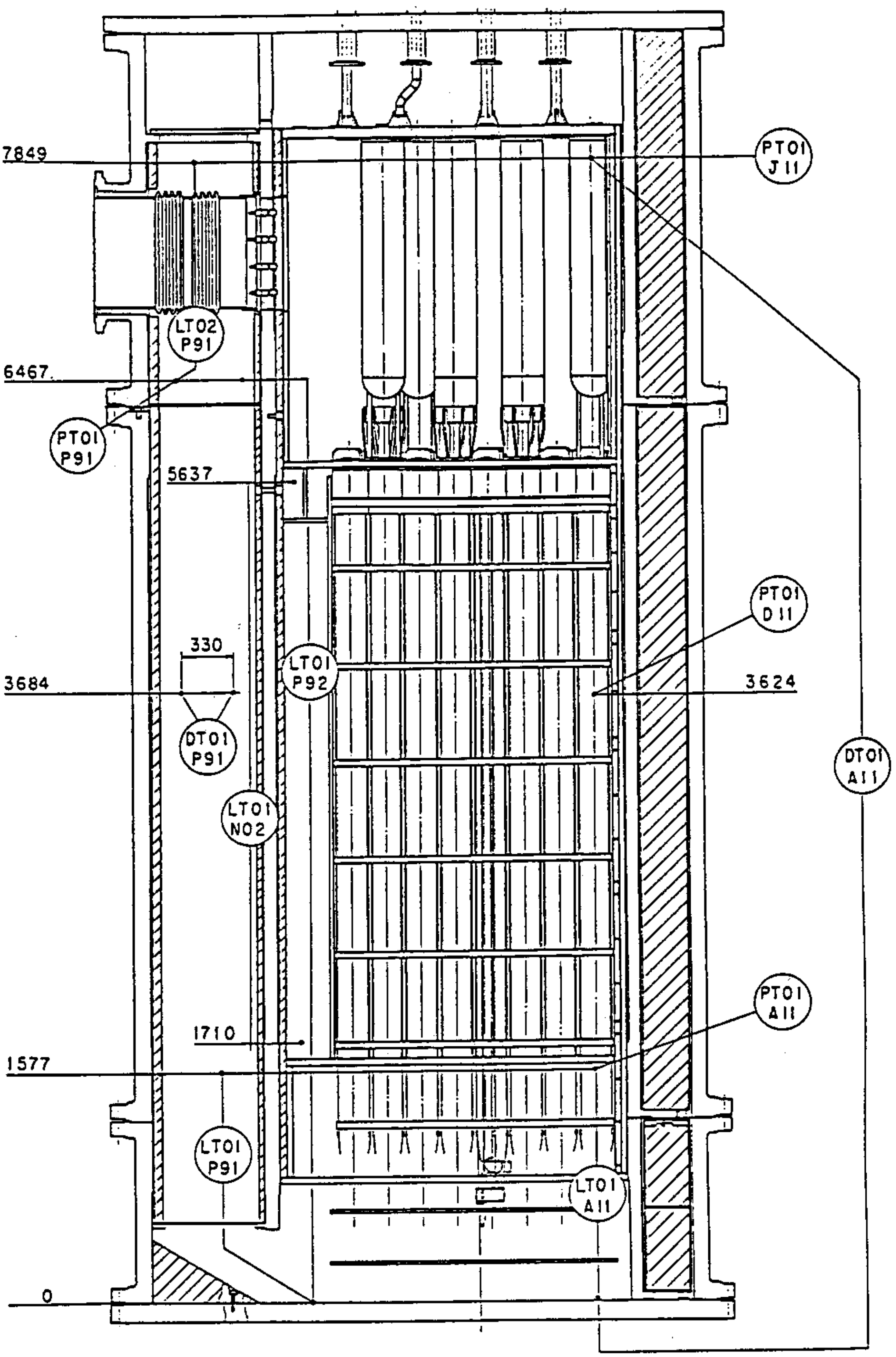

Fig. A-33 Locations of pressure measurements in pressure vessel, differential pressure measurements between upper and lower plenums and liquid level measurements in downcomer and lower plenum

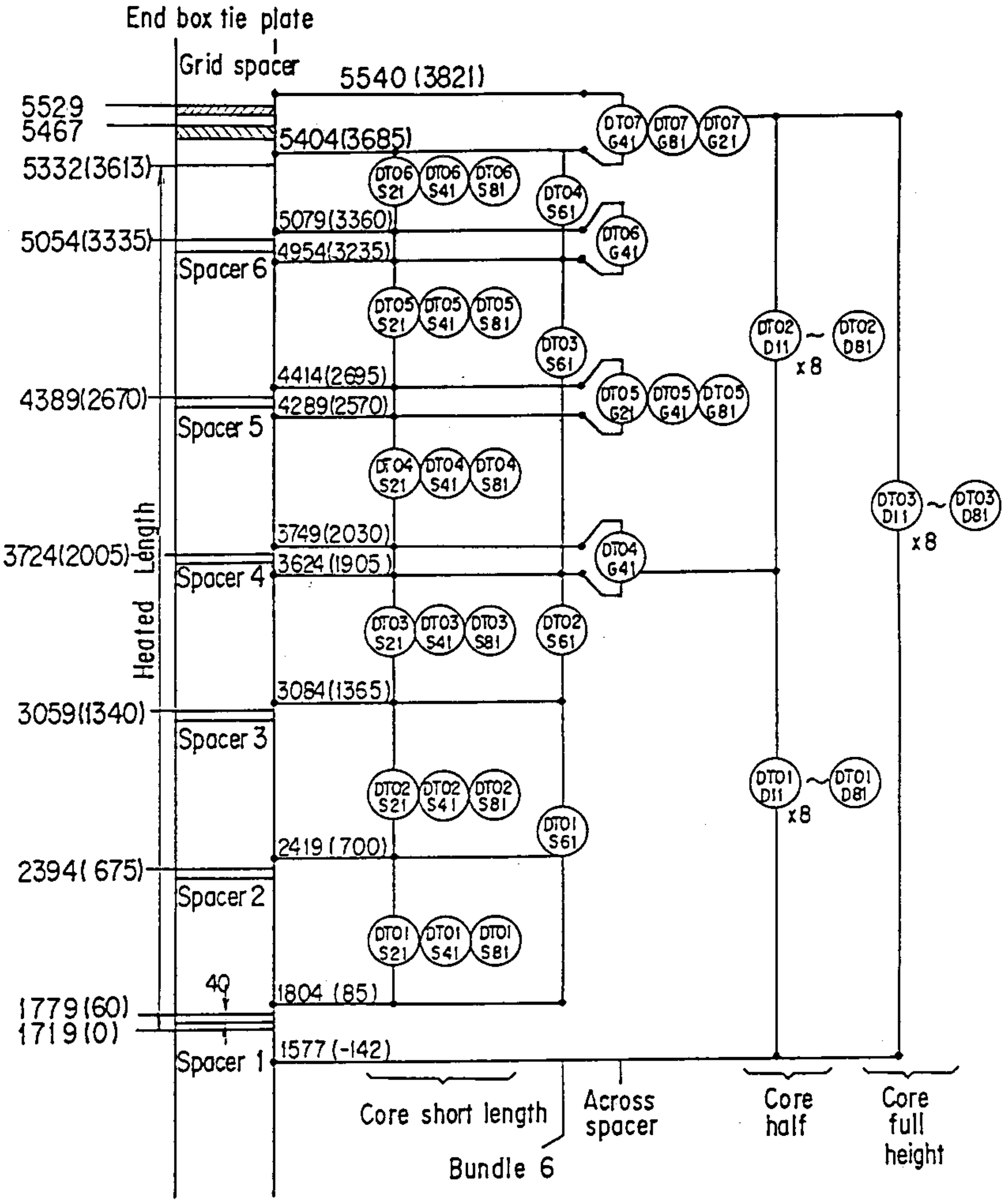

Fig. A-34 Locations of vertical differential pressure measurements in core

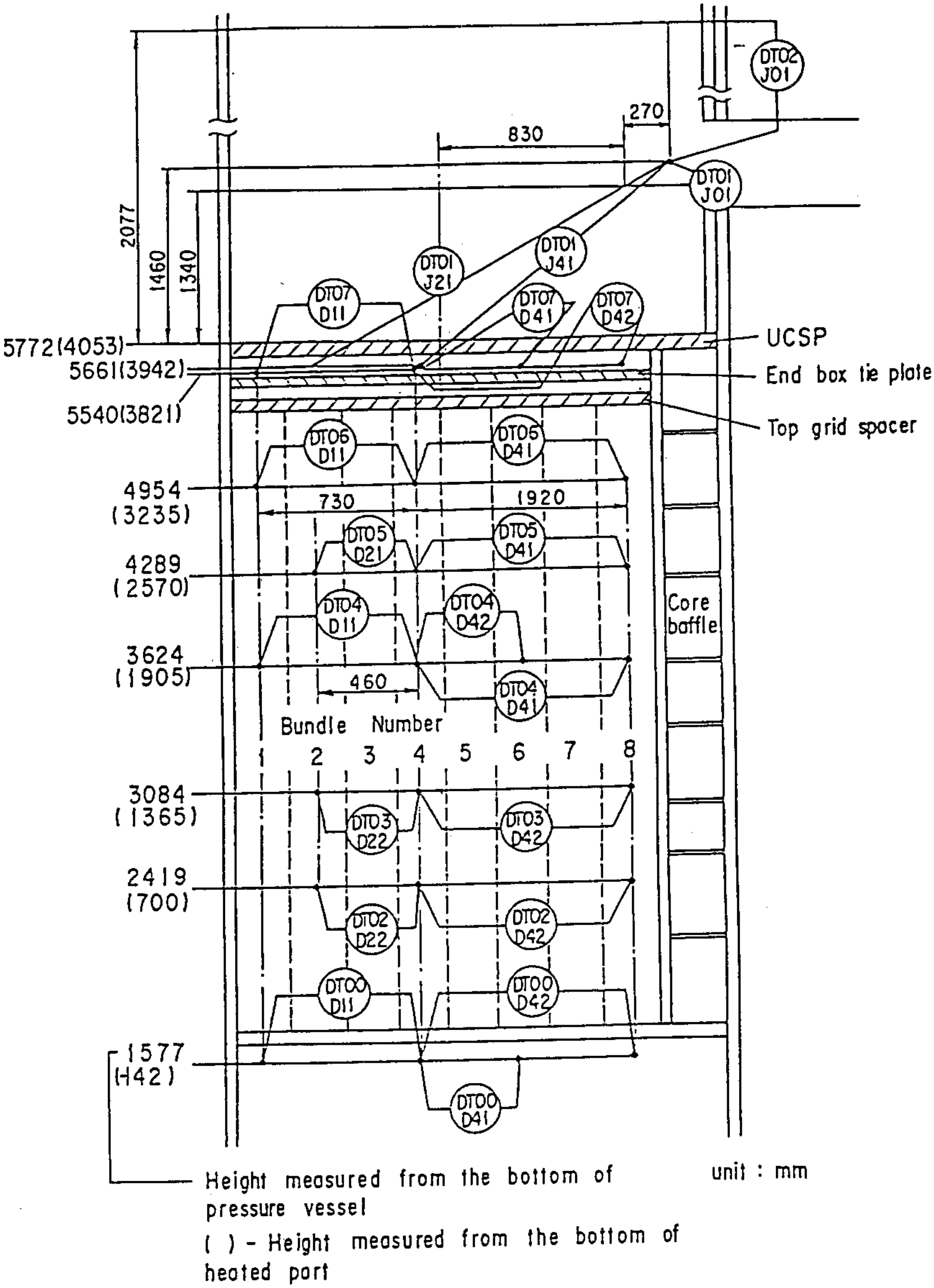

Fig. A-35 Locations of horizontal differential pressure measurements in core and differential pressure measurements between end boxes and inlet of hot leg

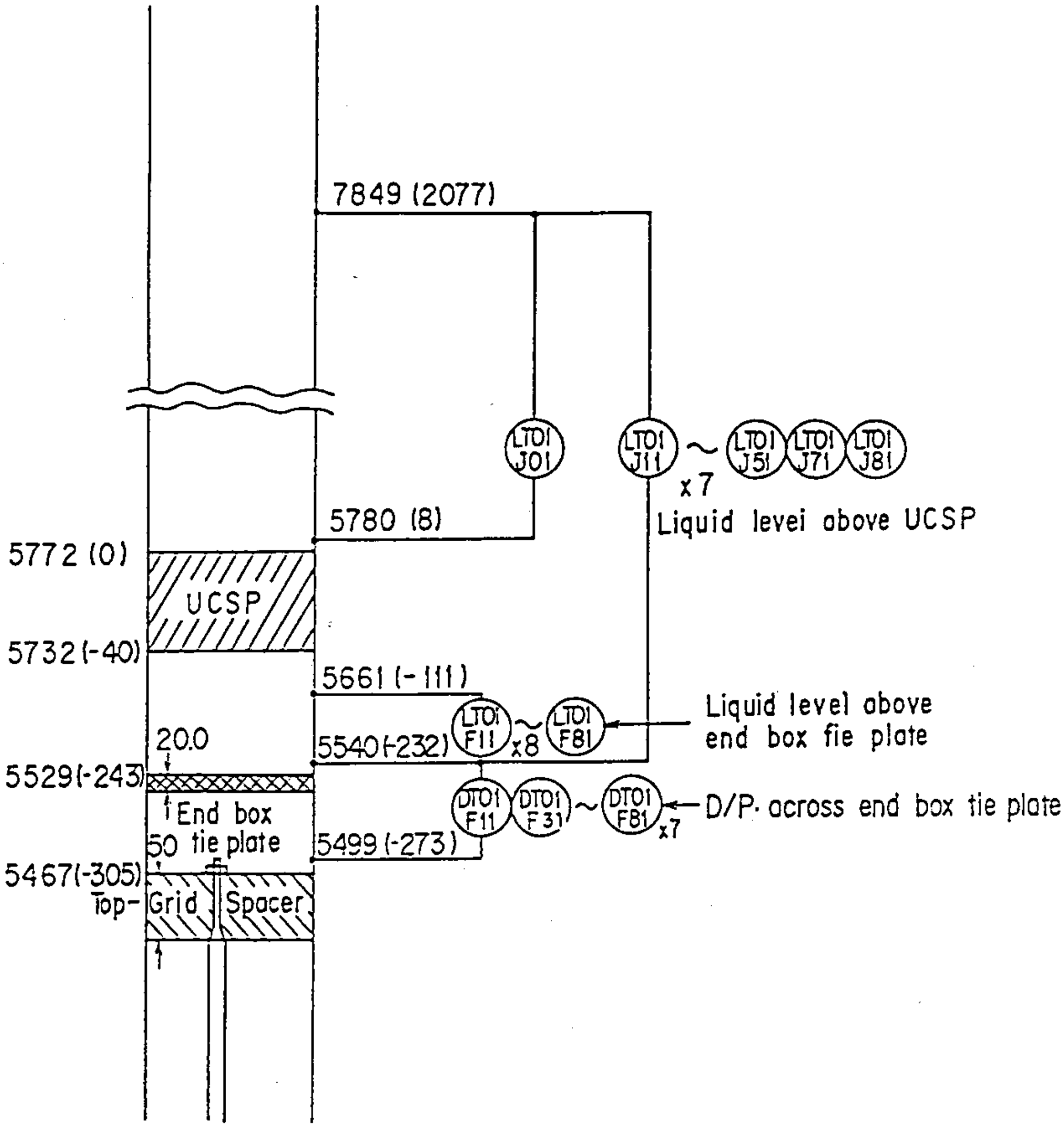

Fig. A-36 Locations of differential pressure measurements across end box tie plate

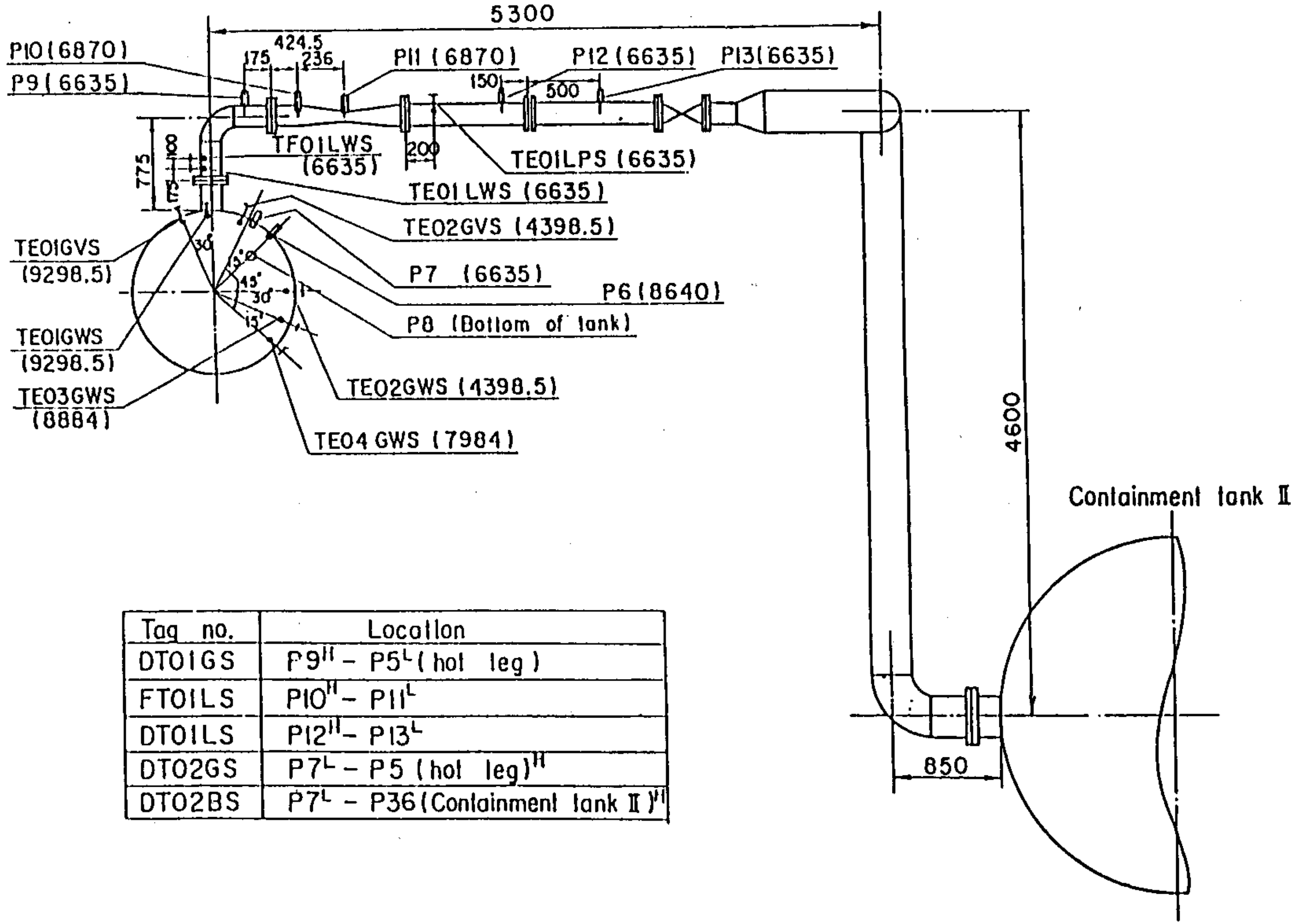

Tag no.	Location
DT01GS	$P9^{H}$ - $P5^{L}$ (hot leg)
FT01LS	$P10^{H}$ - $P11^{L}$
DT01LS	$P12^{H}$ - $P13^{L}$
DT02GS	$P7^{L}$ - P5 (hot leg)^{H}
DT02BS	$P7^{L}$ - P36 (Containment tank II)^{H}

Fig. A-37 Locations of broken cold leg instruments
(Steam-Water separator side)

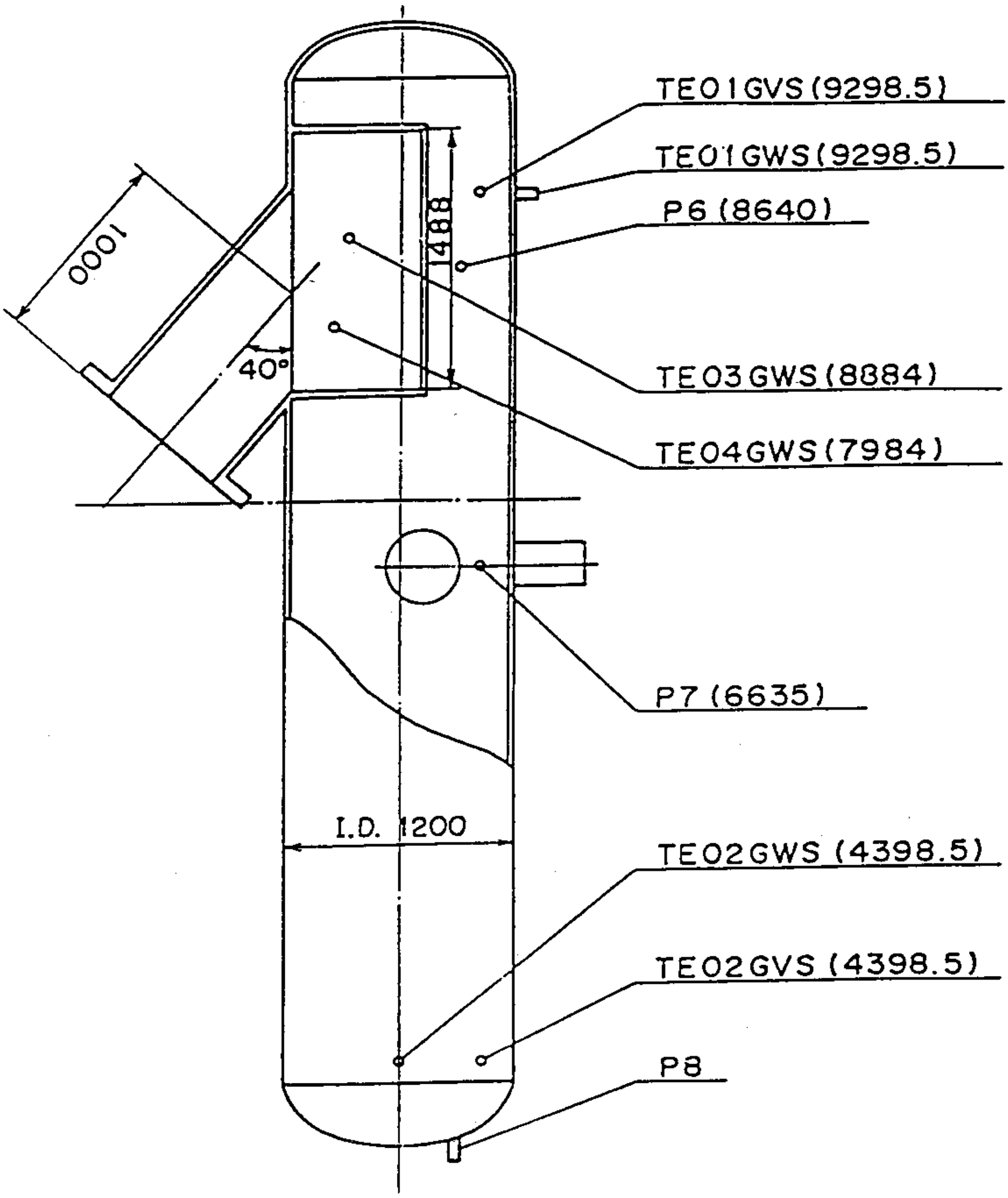

Fig. A-38 Locations of Steam-Water separator instruments

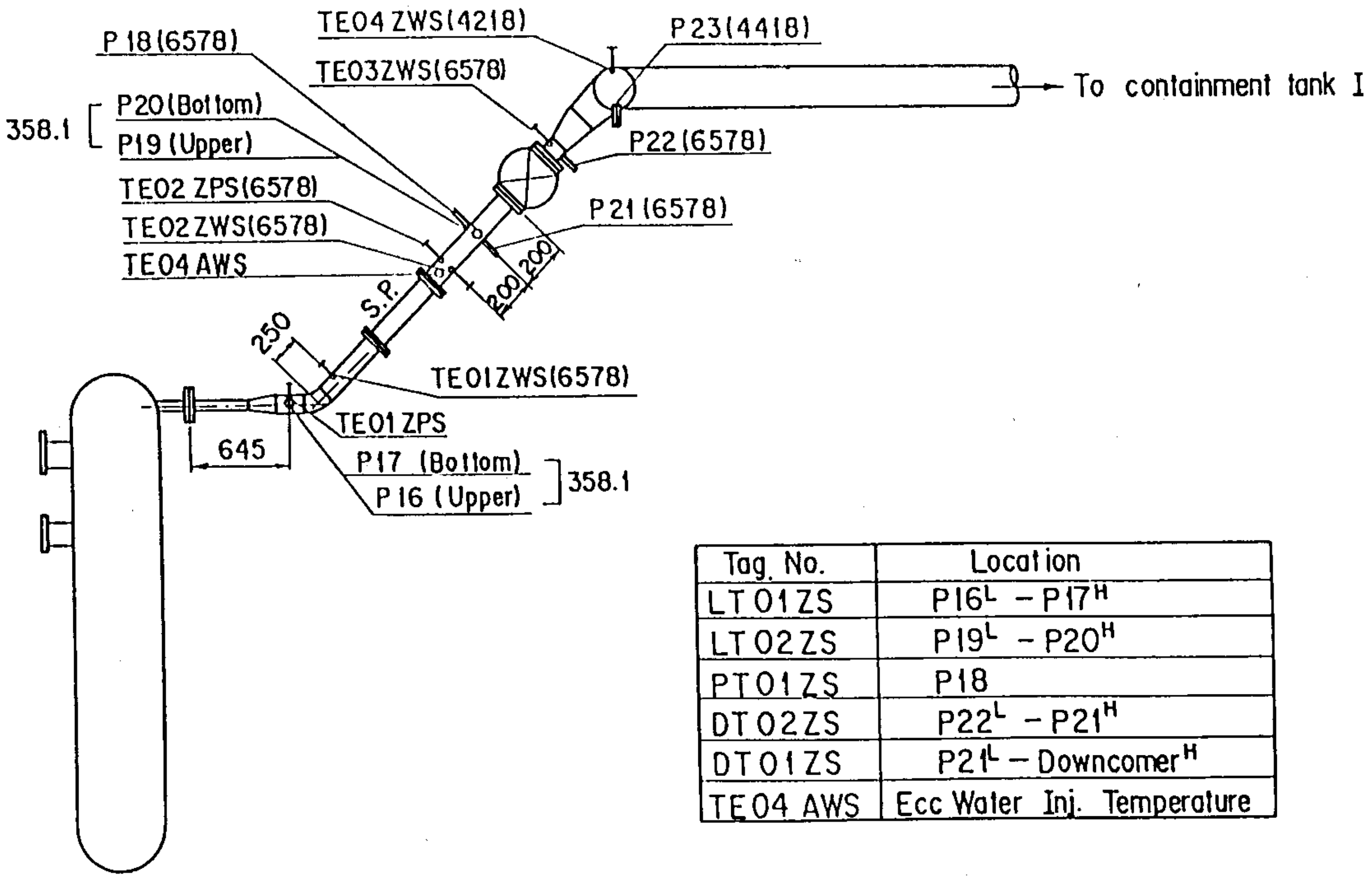

Tag. No.	Location
LT01ZS	$P16^L - P17^H$
LT02ZS	$P19^L - P20^H$
PT01ZS	P18
DT02ZS	$P22^L - P21^H$
DT01ZS	$P21^L$ – Downcomer^H
TE04 AWS	Ecc Water Inj. Temperature

Fig. A-39 Locations of broken cold leg instruments
(Pressure vessel side)

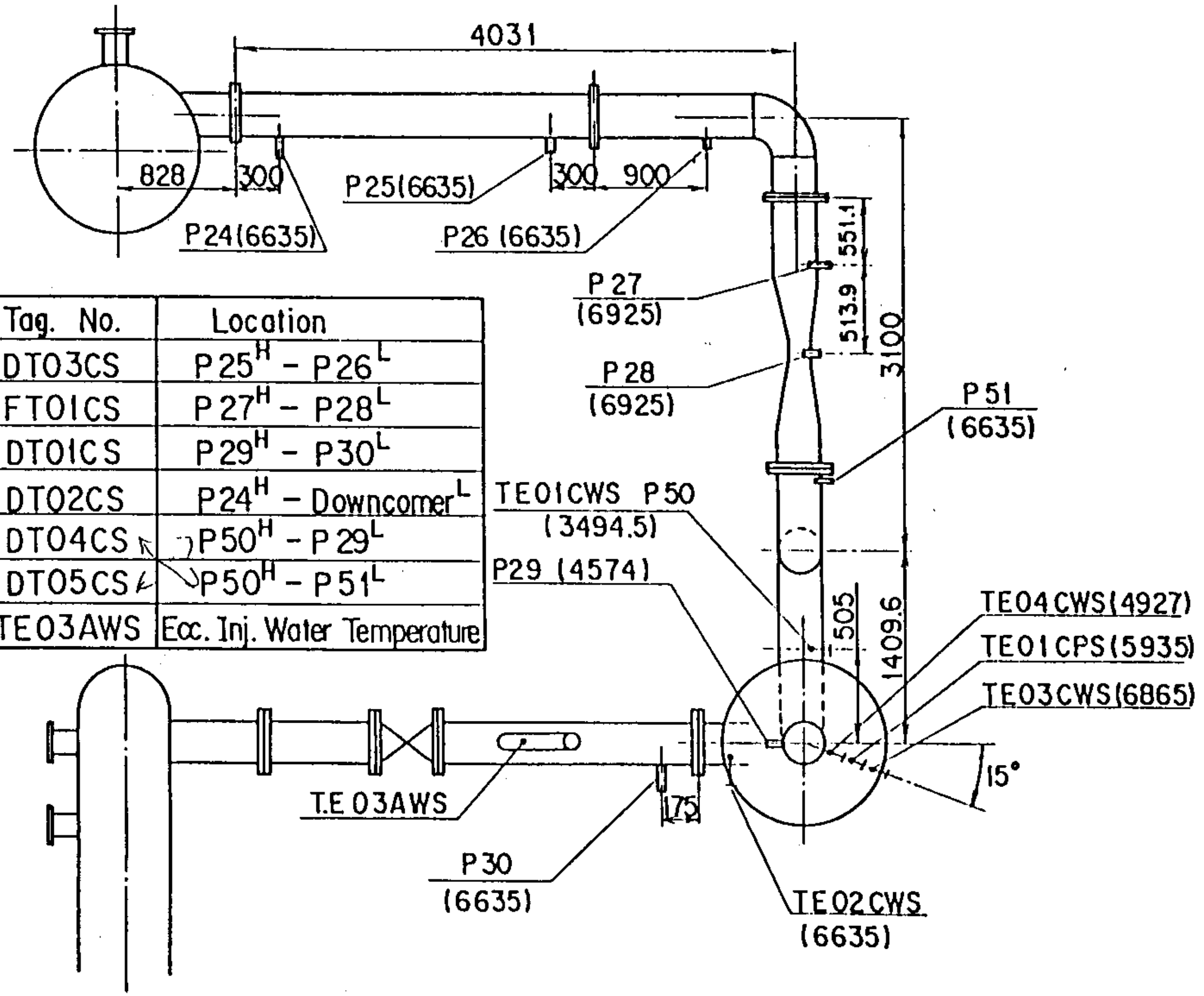

Tag. No.	Location
DT03CS	$P25^{H} - P26^{L}$
FT01CS	$P27^{H} - P28^{L}$
DT01CS	$P29^{H} - P30^{L}$
DT02CS	$P24^{H}$ − Downcomer^{L}
DT04CS	$P50^{H} - P29^{L}$
DT05CS	$P50^{H} - P51^{L}$
TE03AWS	Ecc. Inj. Water Temperature

Fig. A-40 Locations of intact cold leg instruments

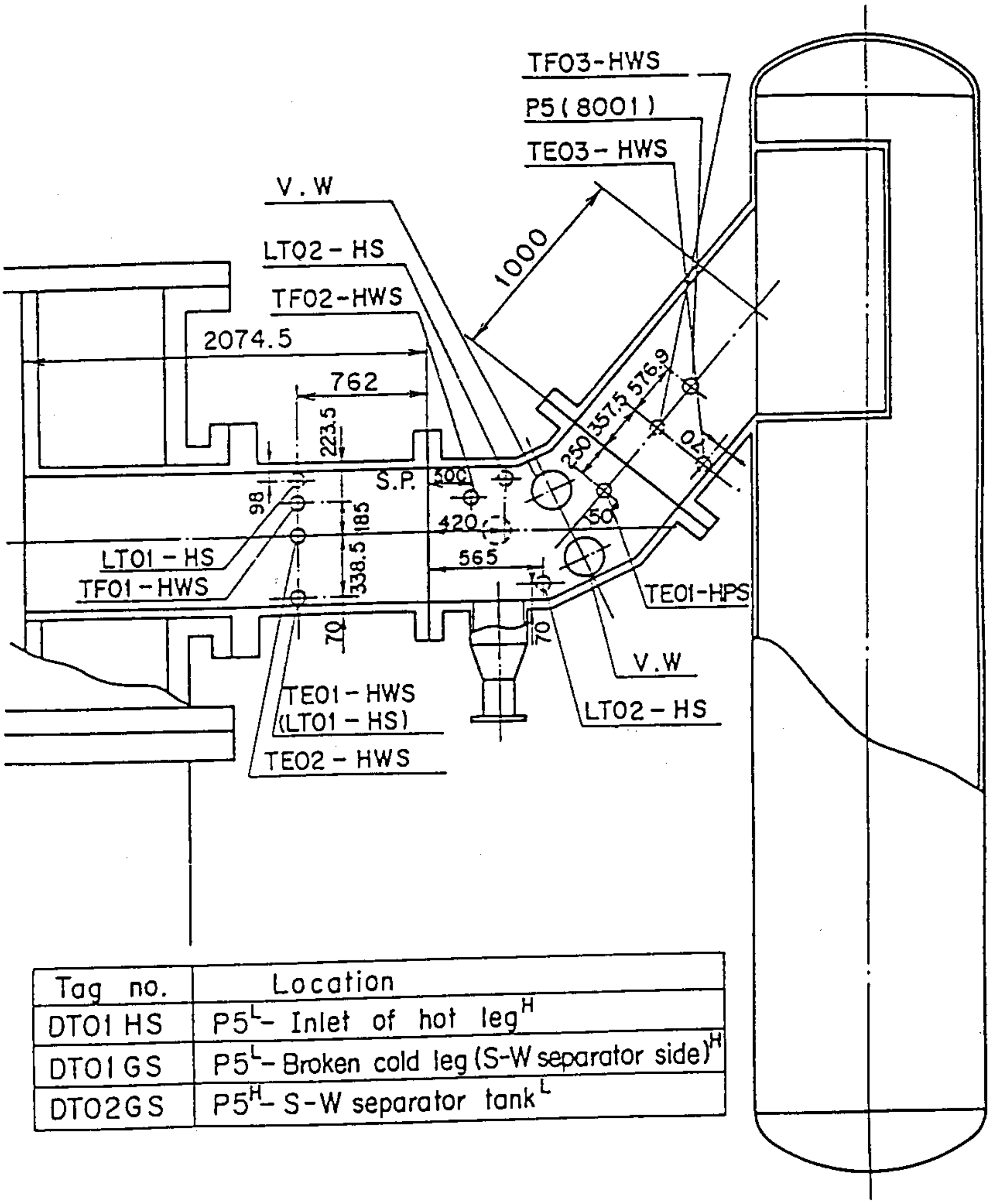

Tag no.	Location
DT01 HS	P5^{L}– Inlet of hot leg^{H}
DT01 GS	P5^{L}– Broken cold leg (S-W separator side)^{H}
DT02GS	P5^{H}– S-W separator tank^{L}

Fig. A-41 Locations of hot leg instruments

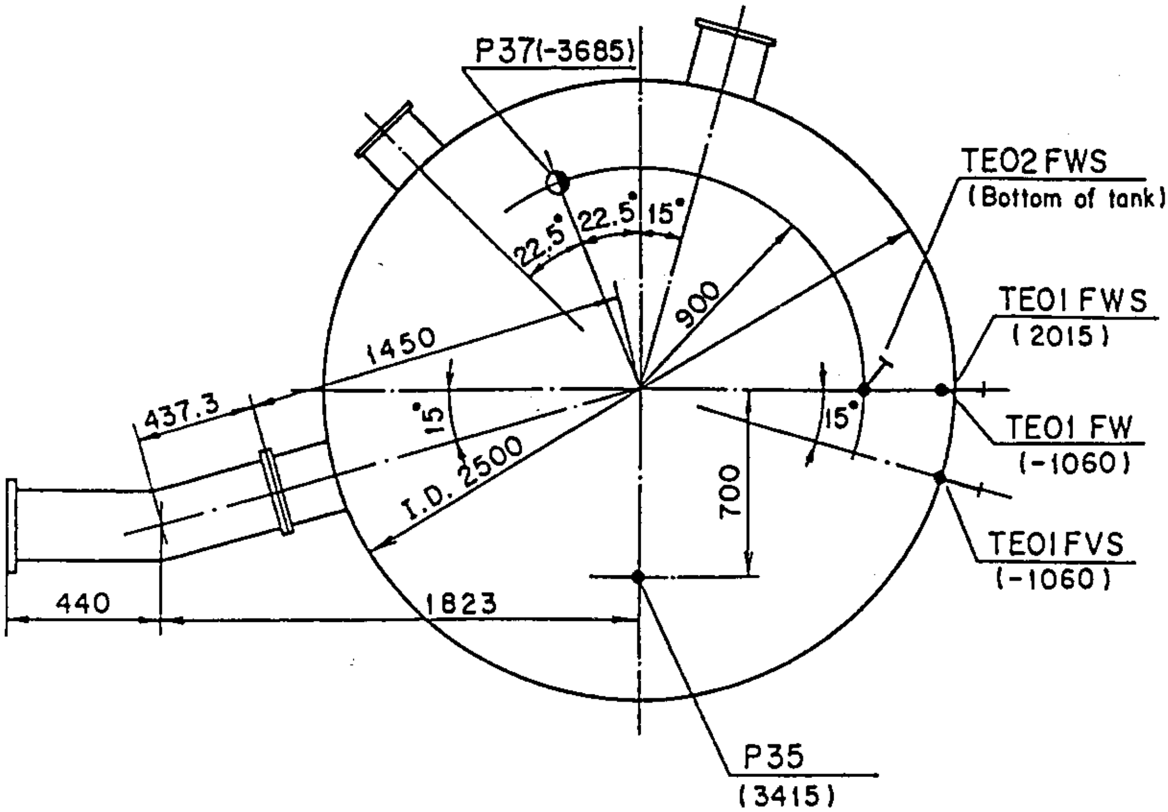

Tag. no.	Location
LT01 FS	P35^L– P37^H
DT01 FS	P35^H– Downcomer^L
DT01 E	P35^L– P36 (C.T. II)^H
PT01 F	P35

Fig. A-42 Locations of containment Tank-I instruments

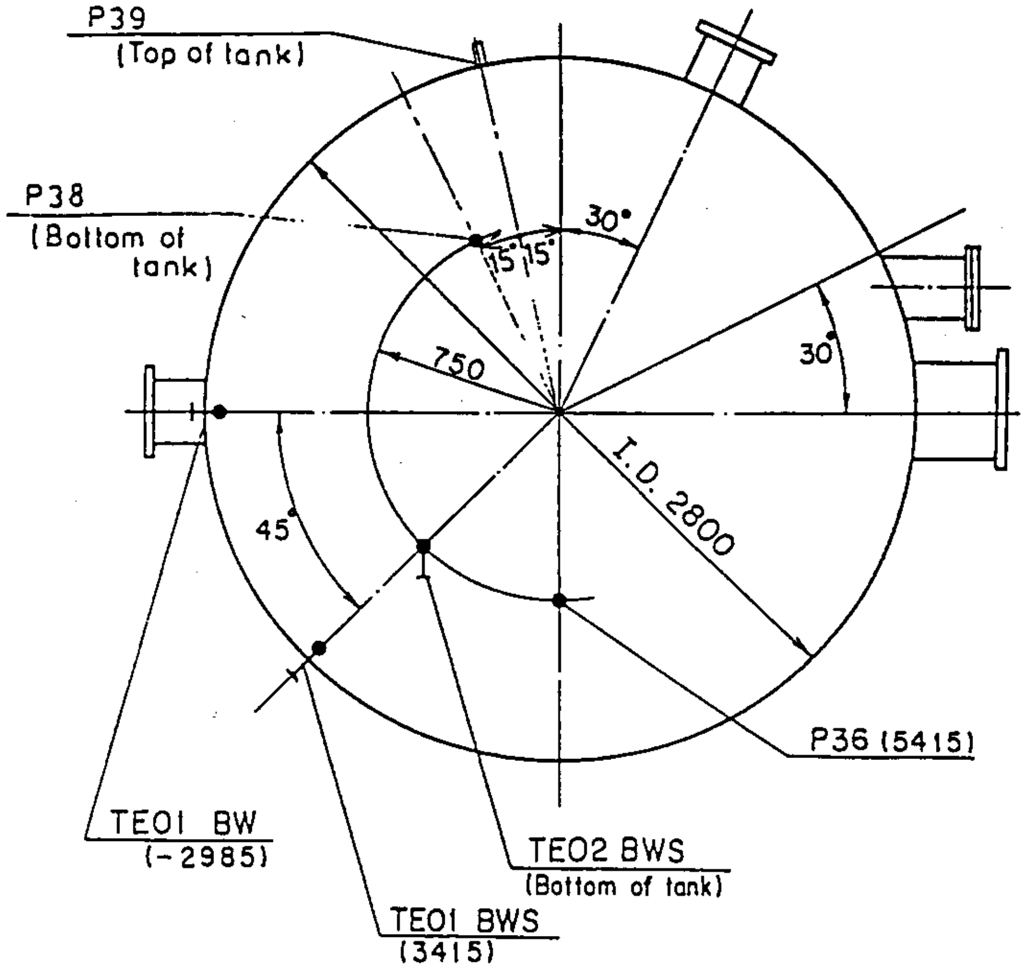

Tag no.	Location
DT01 BS	P36^H – Upper plenum^L
DT02 BS	P36^H – S-W Separator^L
DT01 E	P36^H – P35 (C.T.I)^L
PT01 B	P36
LT01 1B	P38^H – P39^L

Fig. A-43 Locations of containment Tank-II instruments

Appendix B Selected Data from Test S3-22

Figs. B- 1 ~ B- 8	Heater rod temperatures
Figs. B- 9 ~ B-12	Non-heated rod temperatures
Figs. B-13 ~ B-16	Steam temperatures in core
Figs. B-17 ~ B-18	Fluid temperatures just above end box tie plate
Figs. B-19 ~ B-20	Fluid temperatures above UCSP
Figs. B-21 ~ B-22	Liquid levels above end box tie plate
Figs. B-23 ~ B-24	Liquid levels above UCSP
Fig. B-25	Liquid level in steam/water separator
Figs. B-26	Liquid levels in hot leg
Figs. B-27 ~ B-28	Differential pressures across core full height
Figs. B-29 ~ B-30	Differential pressures across end box tie plate
Figs. B-31 ~ B-33	Horizontal differential pressures in core
Figs. B-34 ~ B-38	Differential pressures in primary loops
Figs. B-39 ~ B-40	Pressures in pressure vessel and containment tanks
Figs. B-41 ~ B-42	Bundle powers
Figs. B-43 ~ B-46	ECC flow rates
Figs. B-47 ~ B-49	ECC fluid temperatures

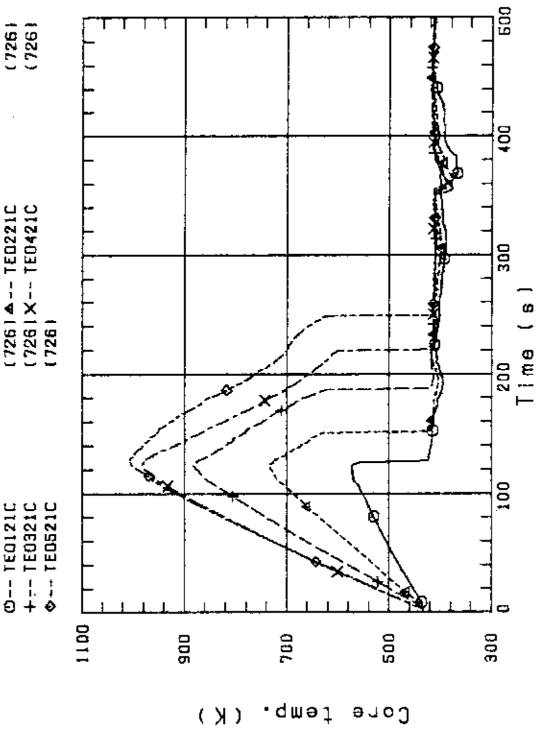

FIG. B-01 HEATER ROD TEMPERATURE (BUNDLE 2-1C, LOWER HALF)

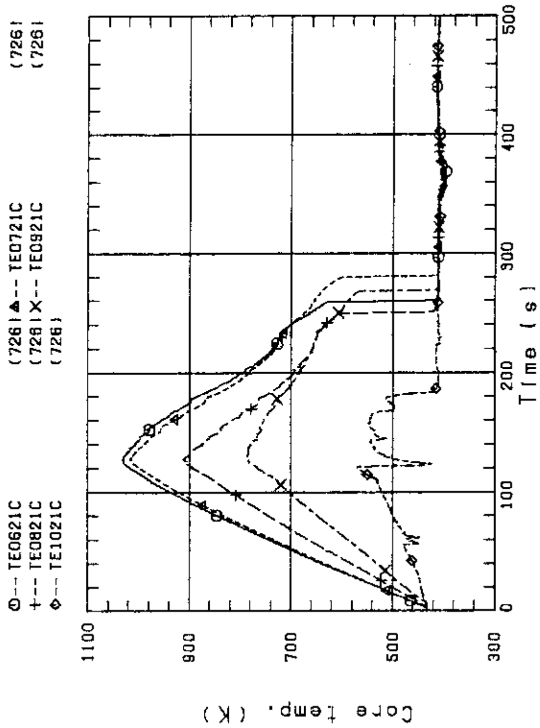

FIG. B-02 HEATER ROD TEMPERATURE (BUNDLE 2-1C, UPPER HALF)

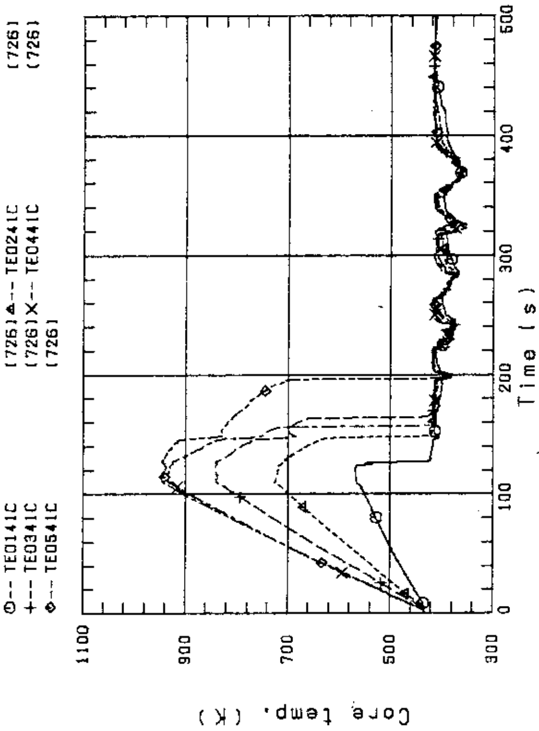

FIG. B-03 HEATER ROD TEMPERATURE (BUNDLE 4-1C, LOWER HALF)

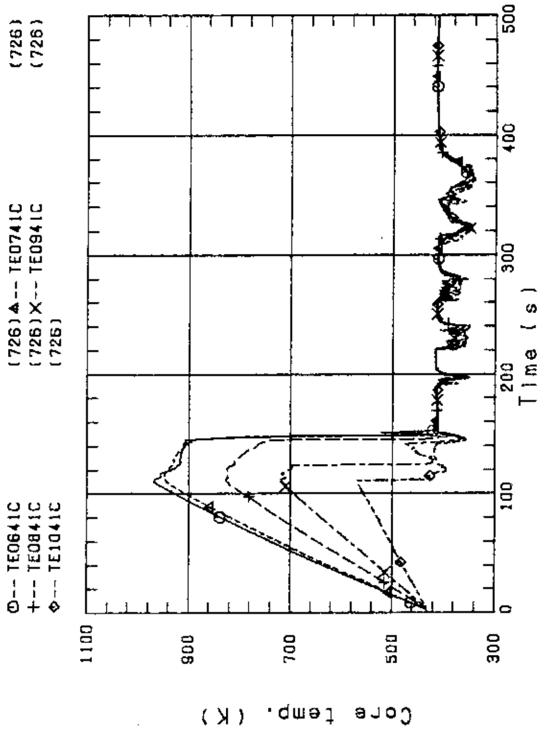

FIG. B-04 HEATER ROD TEMPERATURE (BUNDLE 4-1C, UPPER HALF)

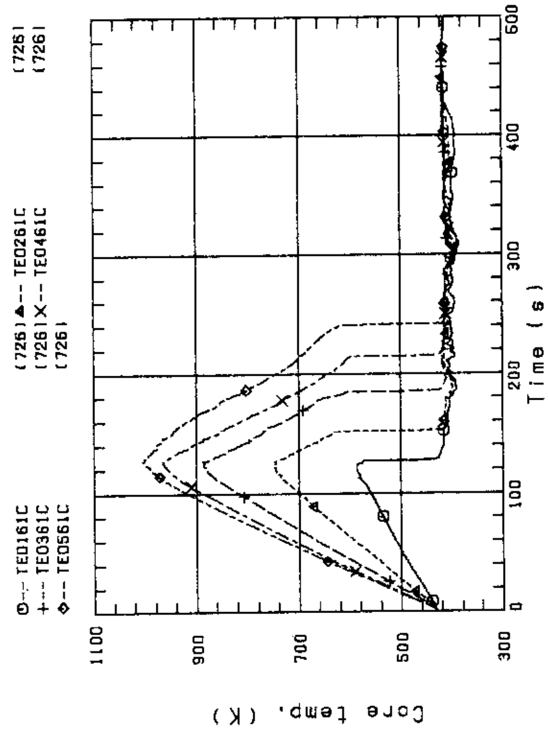

FIG. B-05 HEATER ROD TEMPERATURE (BUNDLE 6-1C, LOWER HALF)

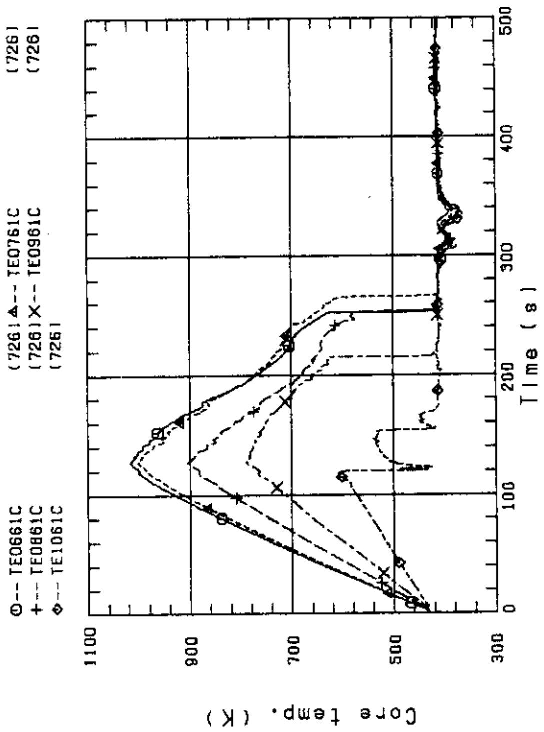

FIG. B-06 HEATER ROD TEMPERATURE (BUNDLE 6-1C, UPPER HALF)

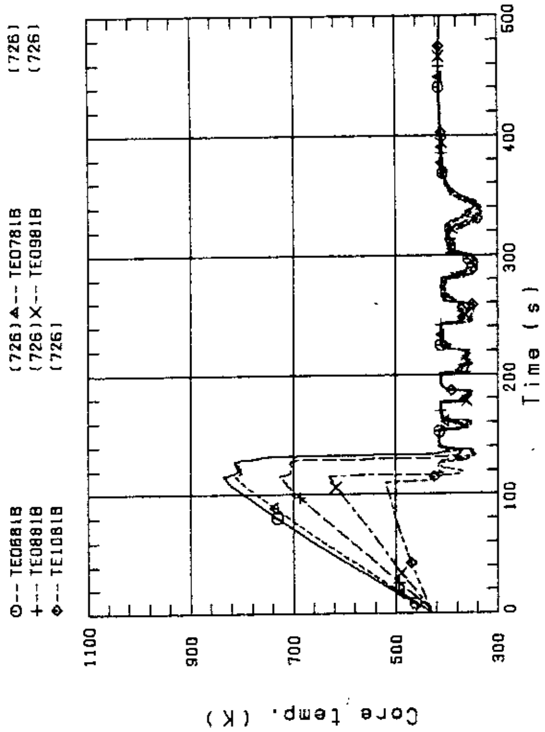

FIG. B-07 HEATER ROD TEMPERATURE (BUNDLE 8-1B, UPPER HALF)

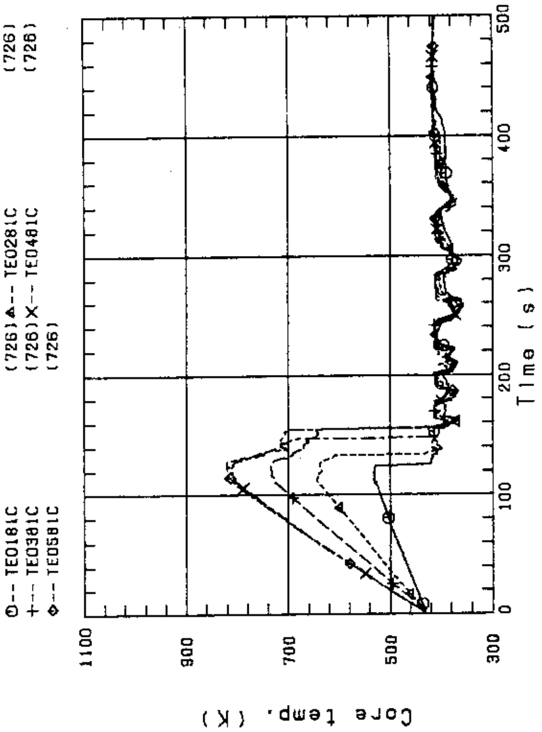

FIG. B-08 HEATER ROD TEMPERATURE (BUNDLE 8-1C, LOWER HALF)

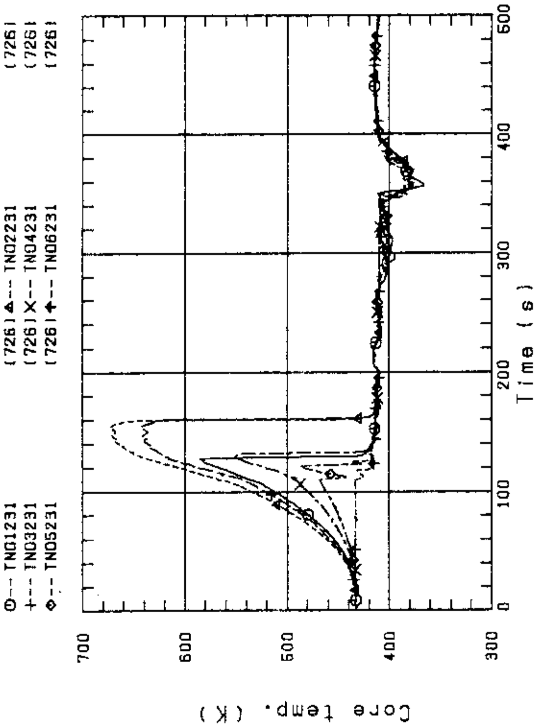

FIG. B-09 NON-HEATED ROD TEMPERATURE (BUNDLE 2-31)

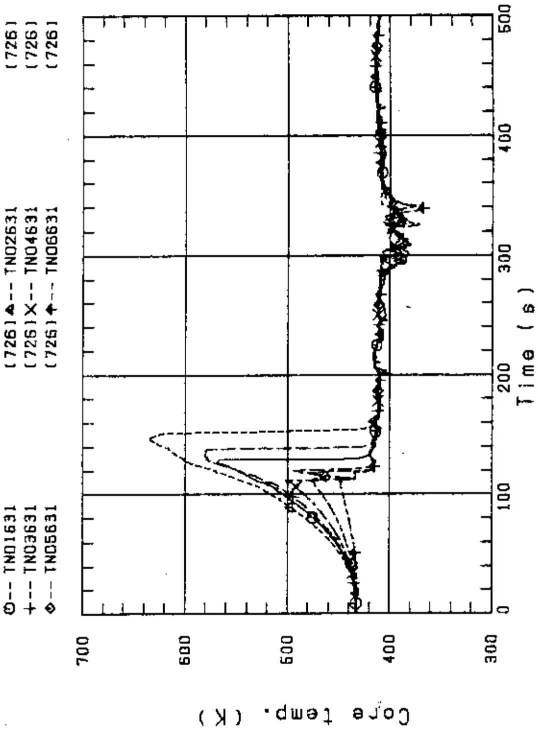

FIG. B-11 NON-HEATED ROD TEMPERATURE (BUNDLE 6-31)

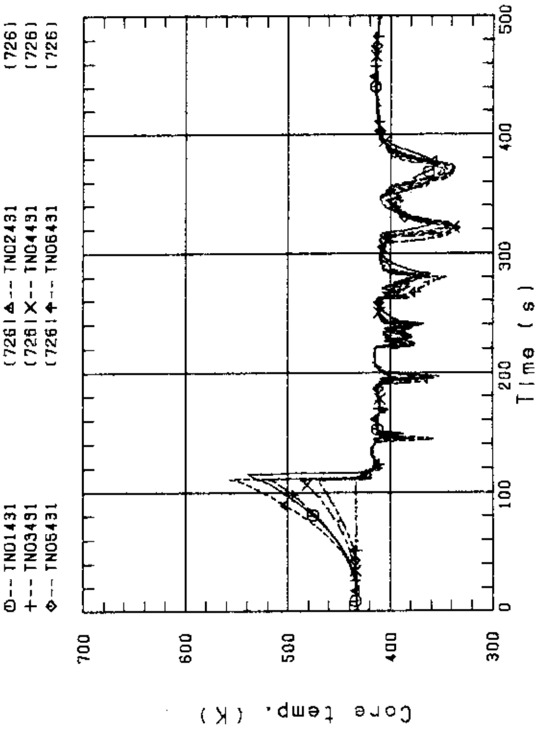

FIG. B-10 NON-HEATED ROD TEMPERATURE (BUNDLE 4-31)

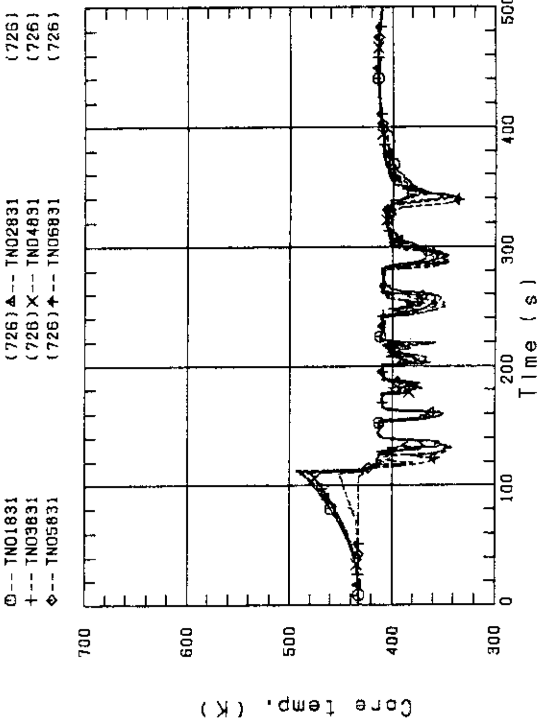

FIG. B-12 NON-HEATED ROD TEMPERATURE (BUNDLE 6-31)

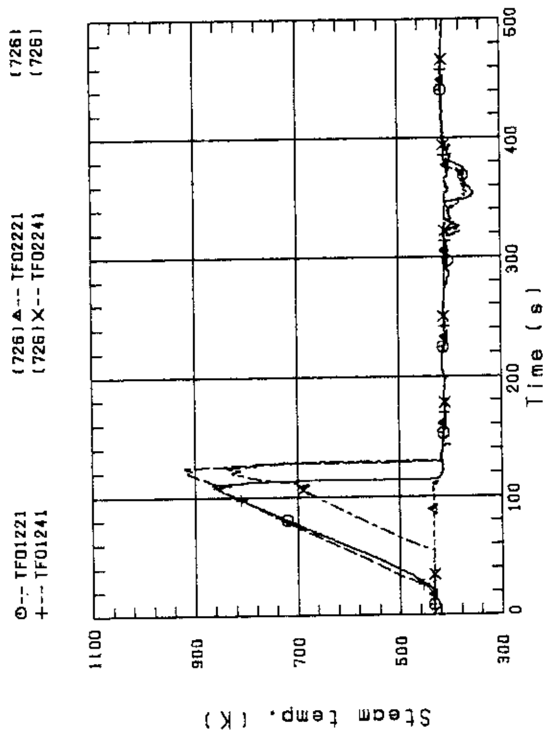

FIG. B-13 STEAM TEMPERATURE IN CORE, BUNDLE 2

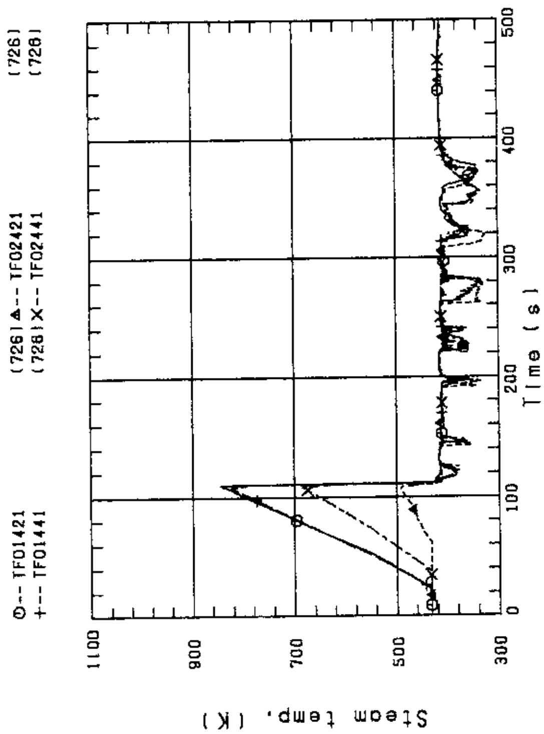

FIG. B-14 STEAM TEMPERATURE IN CORE, BUNDLE 4

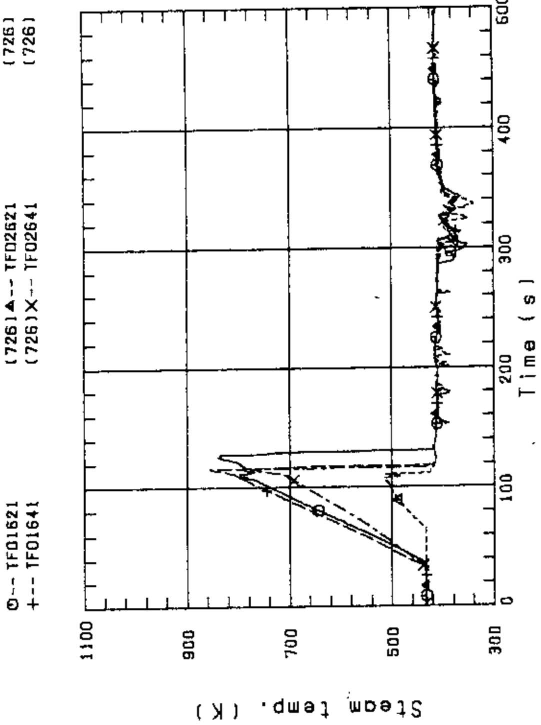

FIG. B-15 STEAM TEMPERATURE IN CORE, BUNDLE 6

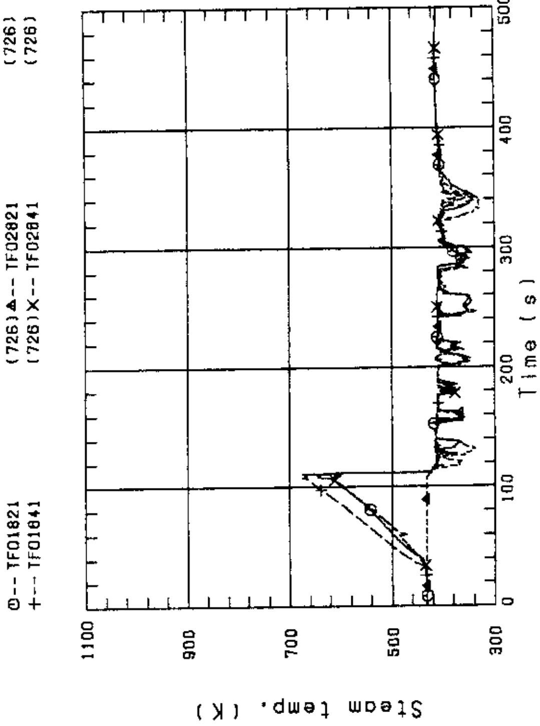

FIG. B-16 STEAM TEMPERATURE IN CORE, BUNDLE 8

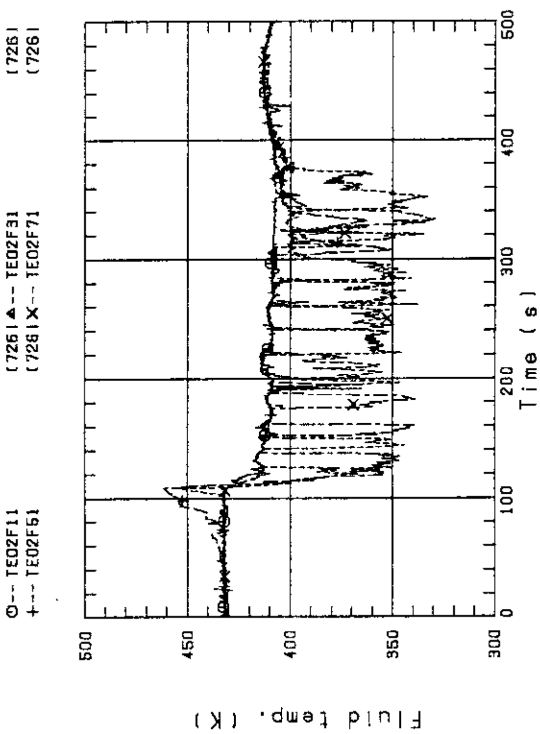

FIG. B-17 FLUID TEMPERATURE JUST ABOVE END BOX TIE PLATE
(BUNDLE 1,3,5,7 OPPOSITE SIDE OF COLD LEG, OUTER)

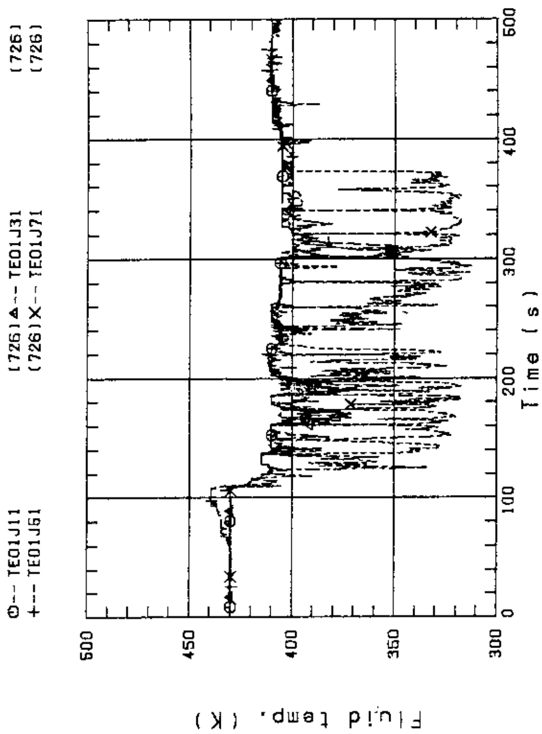

FIG. B-19 FLUID TEMPERATURE ABOVE UCSP
(BUNDLE 1,3,5,7 100MM ABOVE UCSP)

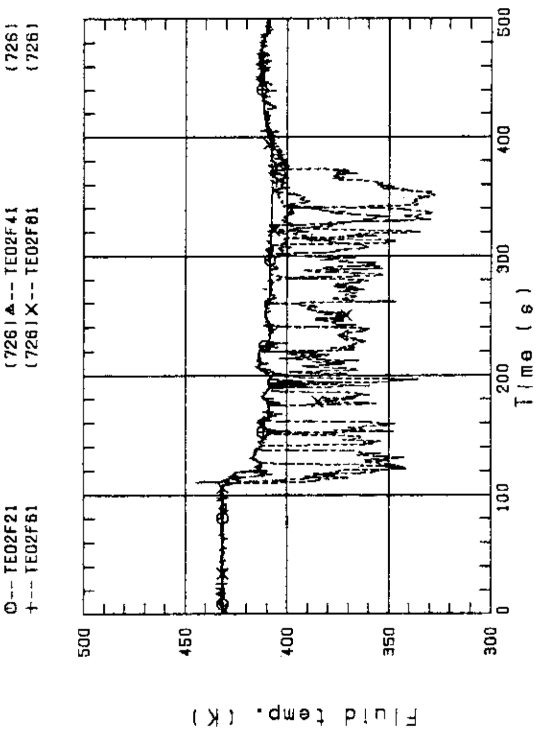

FIG. B-18 FLUID TEMPERATURE JUST ABOVE END BOX TIE PLATE
(BUNDLE 2,4,6,8 OPPOSITE SIDE OF COLD LEG, OUTER)

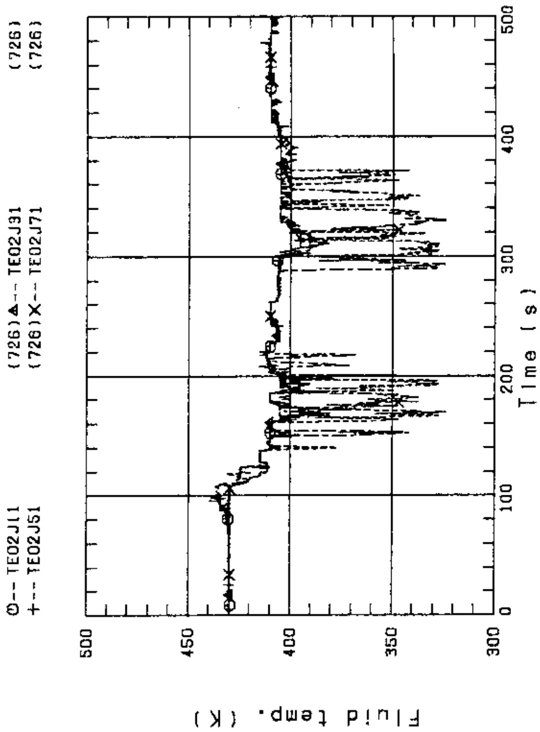

FIG. B-20 FLUID TEMPERATURE ABOVE UCSP
(BUNDLE 1,3,5,7 250MM ABOVE UCSP)

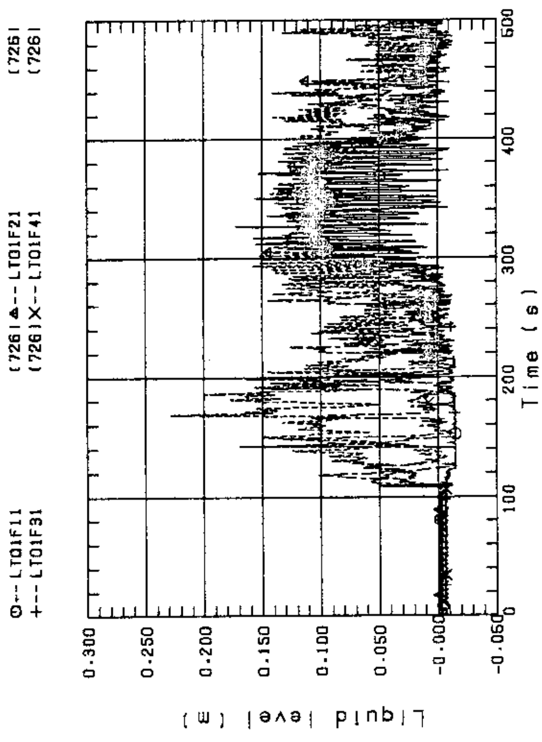

FIG. B-21 LIQUID LEVEL ABOVE END BOX TIE PLATE (BUNDLE 1,2,3,4)

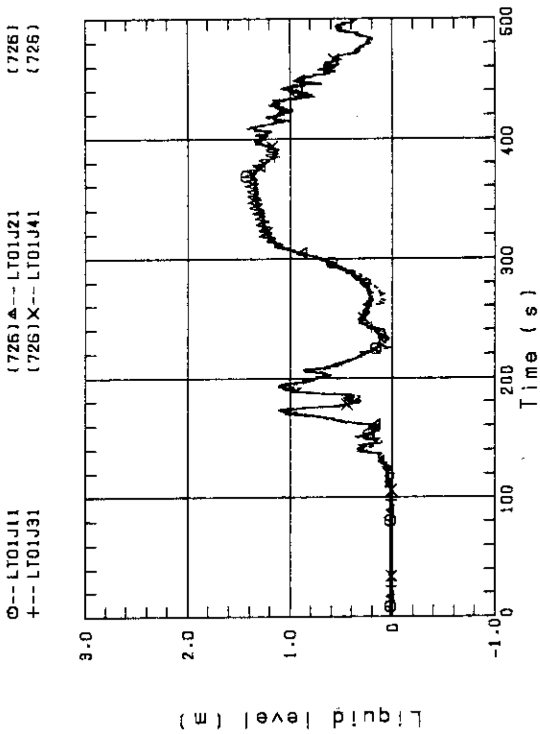

FIG. B-23 LIQUID LEVEL ABOVE UCSP (BUNDLE 1,2,3,4)

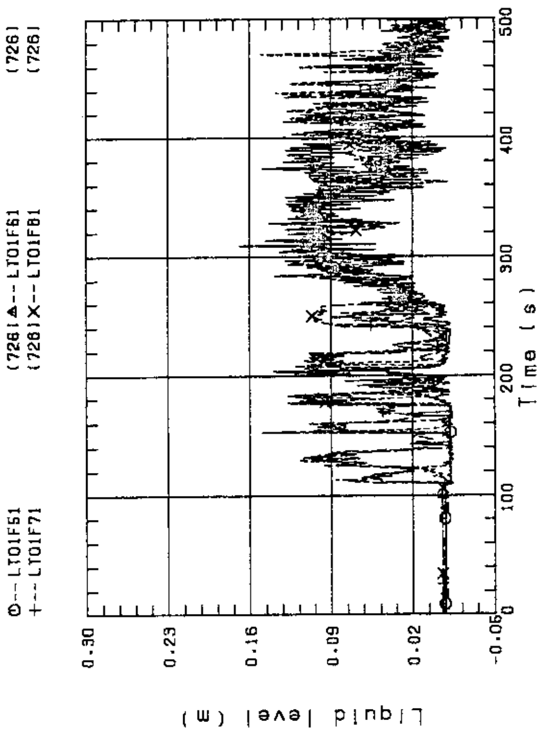

FIG. B-22 LIQUID LEVEL ABOVE END BOX TIE PLATE (BUNDLE 5,6,7,8)

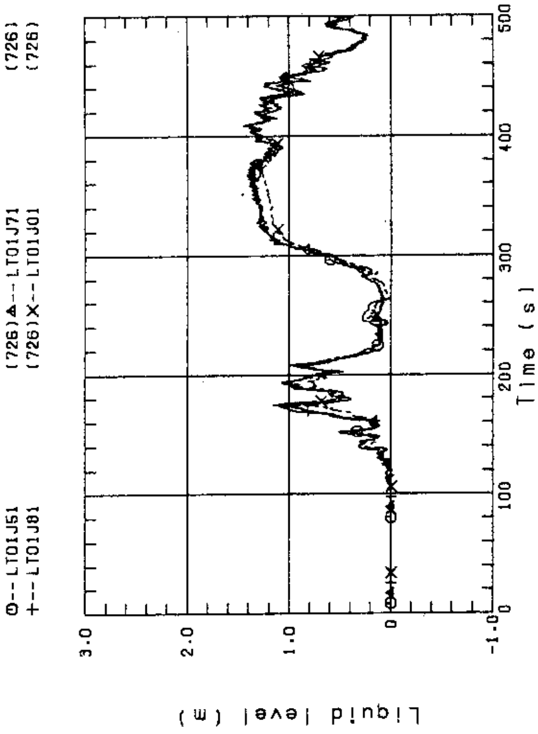

FIG. B-24 LIQUID LEVEL ABOVE UCSP (BUNDLE 5,6,7,8 AND CORE BUFFLE)

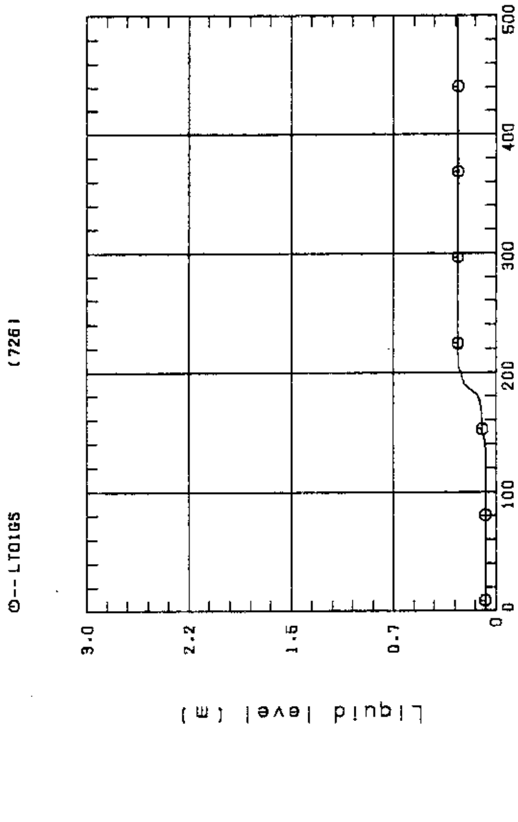

FIG. B-25 LIQUID LEVEL IN STEAM/WATER SEPARATOR

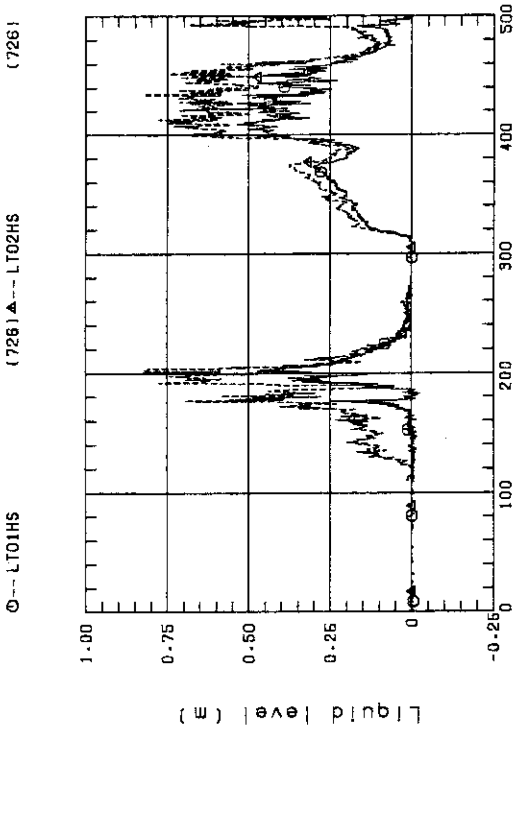

FIG. B-26 LIQUID LEVEL IN HOT LEG
(01HS - PV SIDE, 02HS - STEAM/WATER SEPARATOR SIDE)

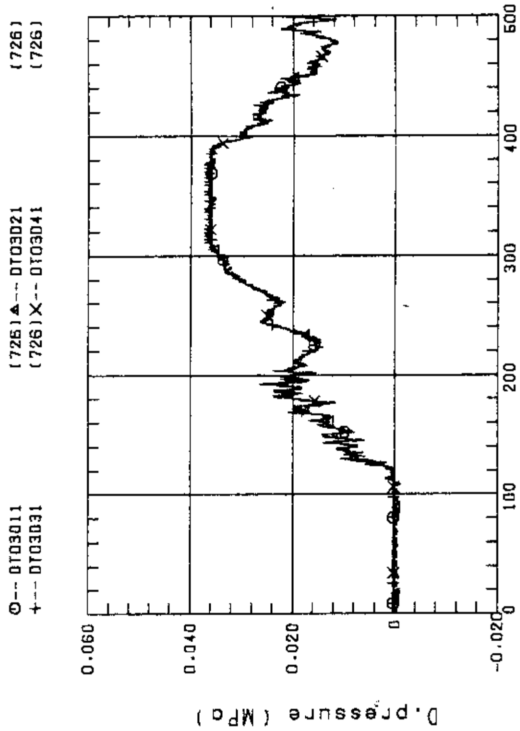

FIG. B-27 DIFFERENTIAL PRESSURE OF CORE FULL HIGHT
(BUNDLE 1,2,3,4)

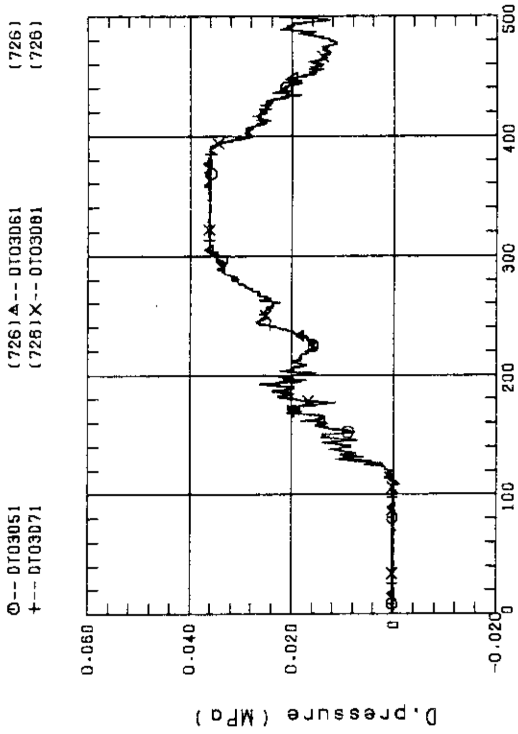

FIG. B-28 DIFFERENTIAL PRESSURE OF CORE FULL HIGHT
(BUNDLE 5,6,7,8)

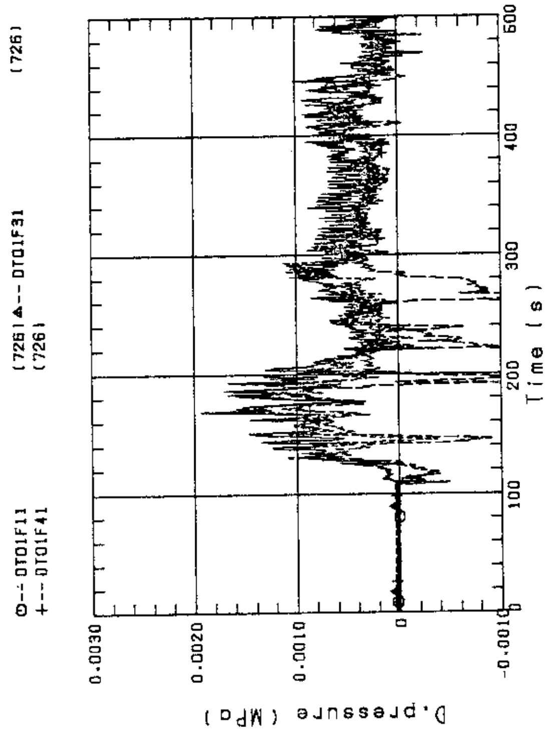

FIG. B-29 DIFFERENTIAL PRESSURE ACROSS END BOX TIE PLATE (BUNDLE 1,3,4)

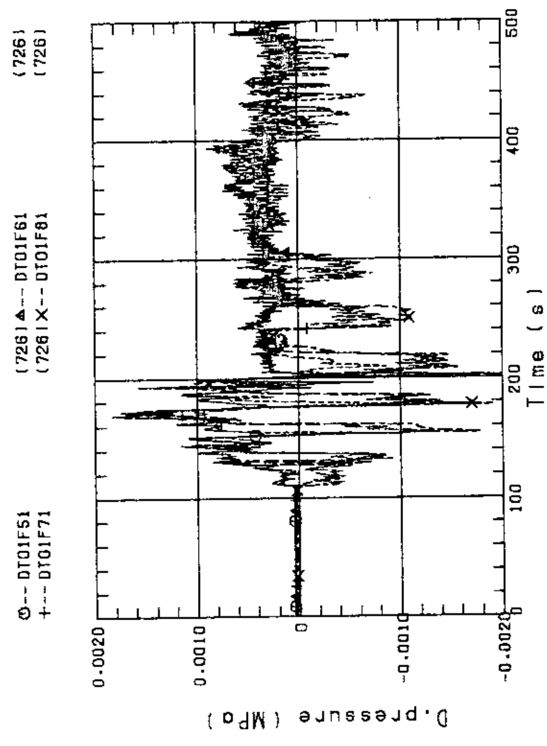

FIG. B-30 DIFFERENTIAL PRESSURE ACROSS END BOX TIE PLATE (BUNDLE 5,6,7,8)

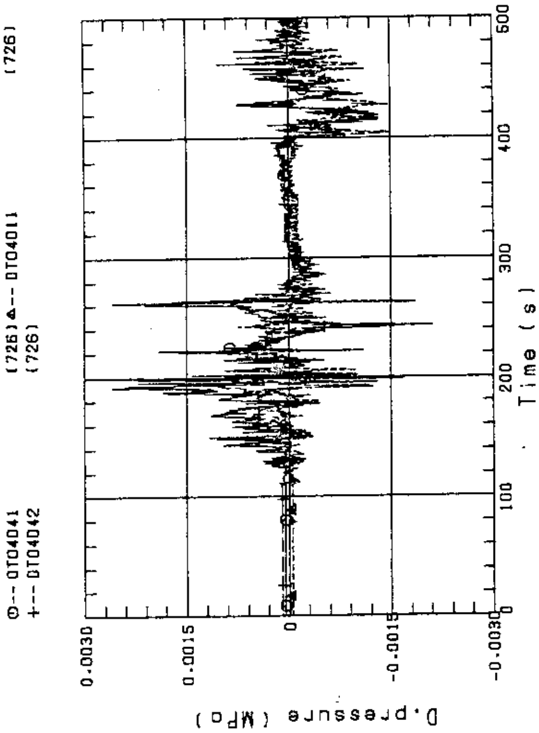

FIG. B-31 DIFFERENTIAL PRESSURE , HORIZONTAL AT 1905 MM (11-BUNDLE 1-4, 41-BUNDLE 4-8, 42-BUNDLE 4-6)

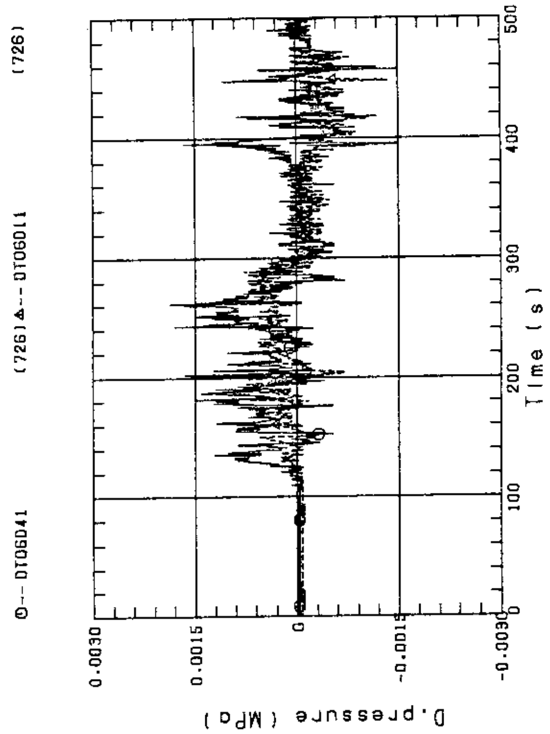

FIG. B-32 DIFFERENTIAL PRESSURE , HORIZONTAL AT 3235 MM (11-BUNDLE 1-4, 41-BUNDLE 4-8)

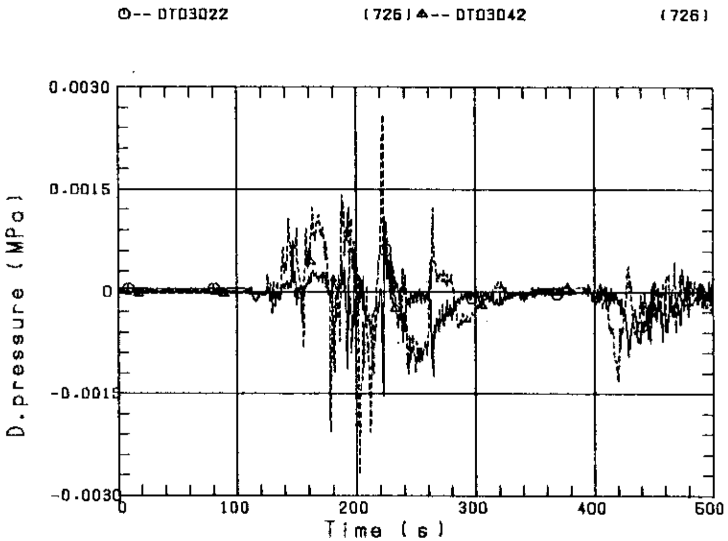

FIG. B-33 DIFFERENTIAL PRESSURE, HORIZONTAL AT 1365 MM (22-BUNDLE 2-4, 42-BUNDLE 4-8)

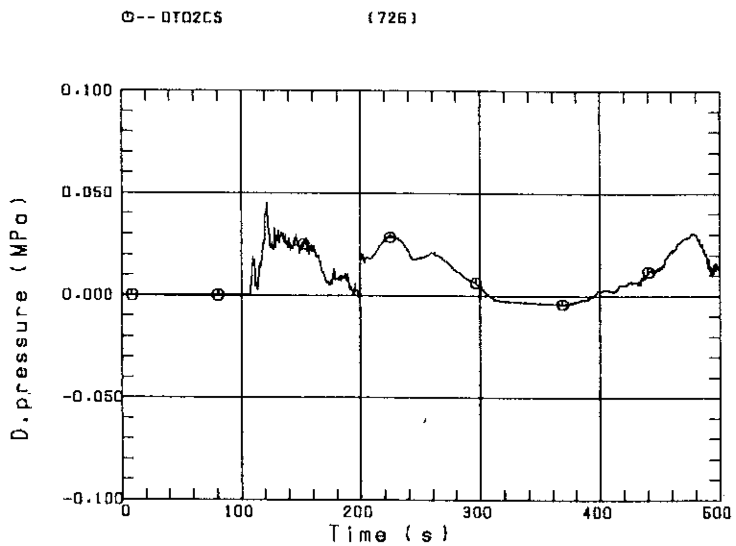

FIG. B-35 DIFFERENTIAL PRESSURE OF INTACT COLD LEG

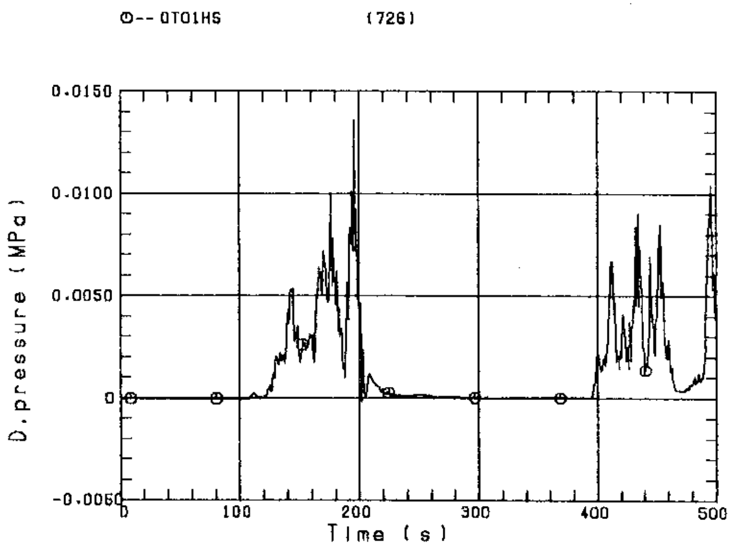

FIG. B-34 DIFFERENTIAL PRESSURE OF HOT LEG HOT LEG INLET - STEAM/WATER SEPARATOR INLET

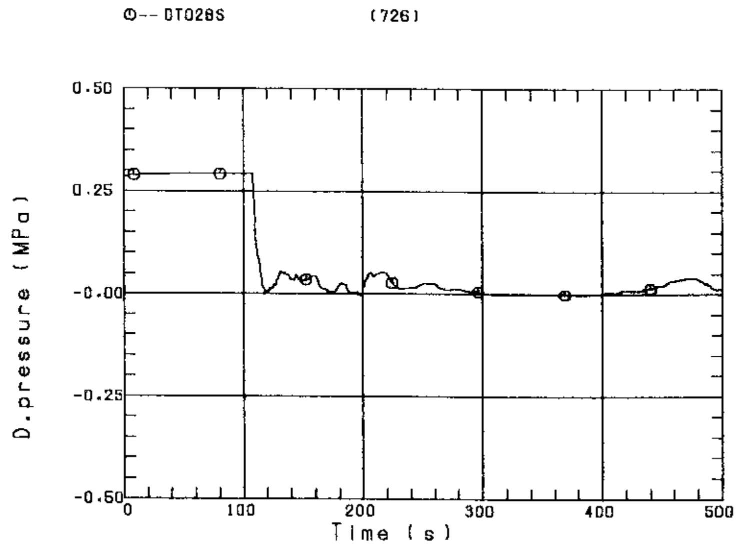

FIG. B-36 DIFFERENTIAL PRESSURE, STEAM/WATER SEPARATOR - CONTAINMENT TANK-II

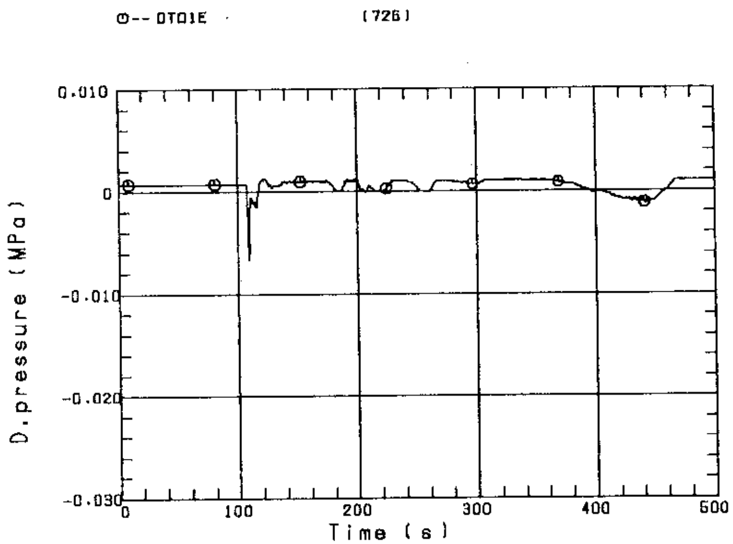

FIG. B-37 DIFFERENTIAL PRESSURE, CONTAINMENT TANK-II - CONTAINMENT TANK-I

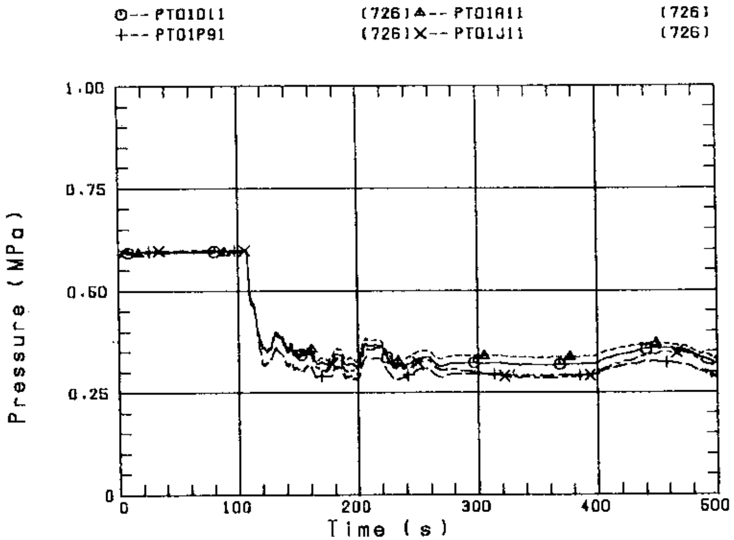

FIG. B-39 PRESSURE IN PV (J - TOP OF PV, D - CORE CENTER, A - CORE INLET, P - BELOW COLD LEG NOZZLE IN DOWNCOMER)

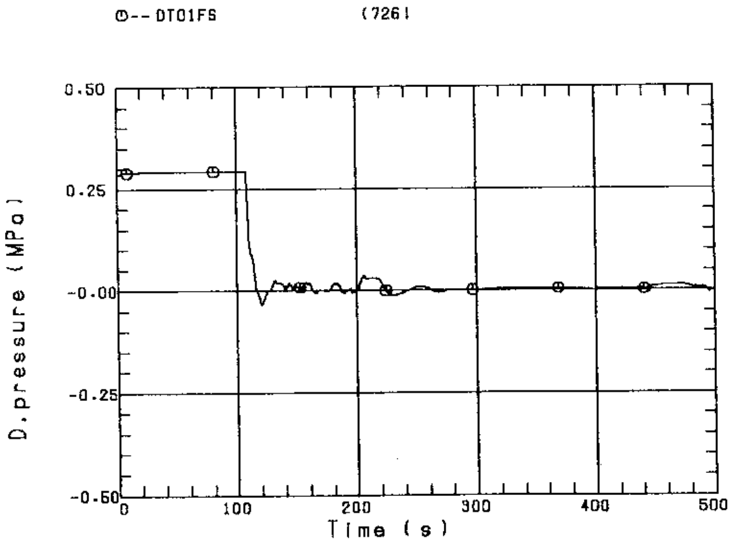

FIG. B-38 DIFFERENTIAL PRESSURE OF BROKEN COLD LEG - PV SIDE, DOWNCOMER - CONTAINMENT TANK-I

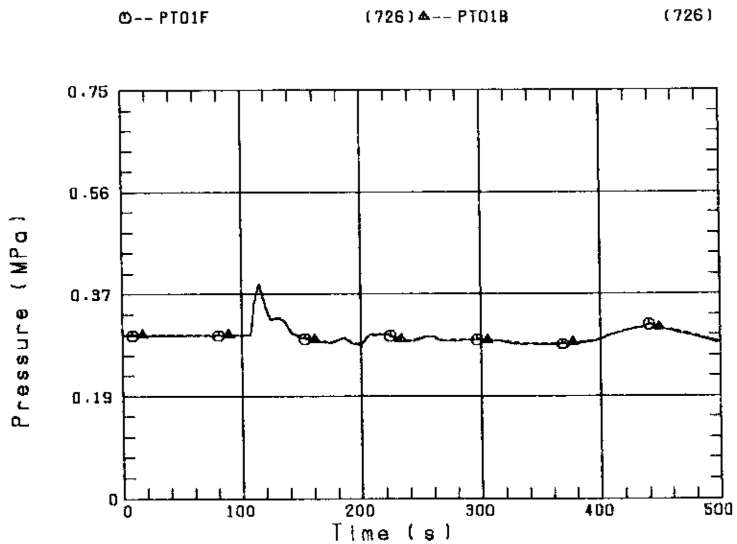

FIG. B-40 PRESSURE AT TOP OF CONTAINMENT TANK-I AND CONTAINMENT TANK-II (F-CONTAINMENT TANK-I, B-CONTAINMENT TANK-II)

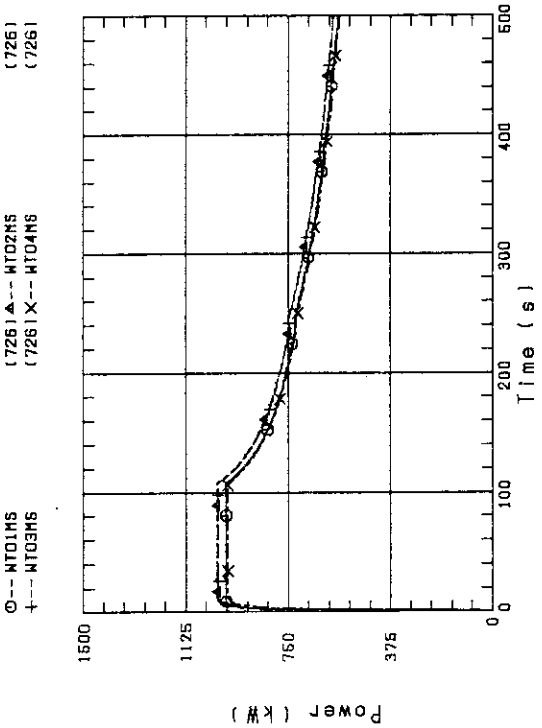

FIG. B-41 BUNDLE POWER (BUNDLE 1,2,3,4)

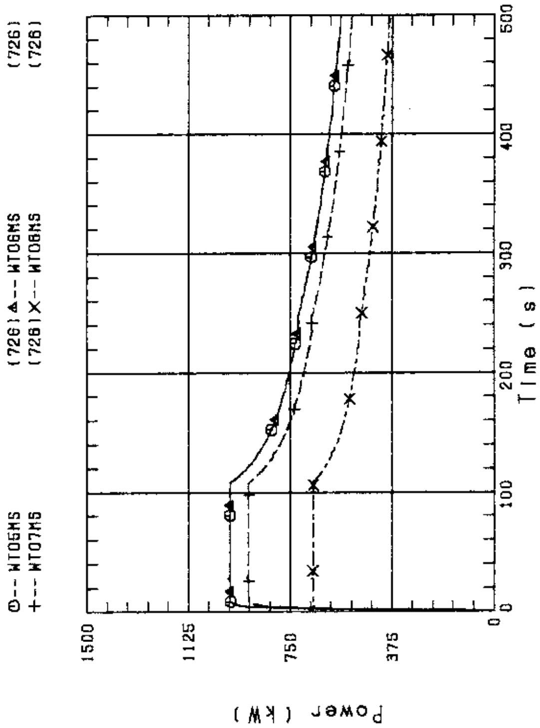

FIG. B-42 BUNDLE POWER (BUNDLE 5,6,7,8)

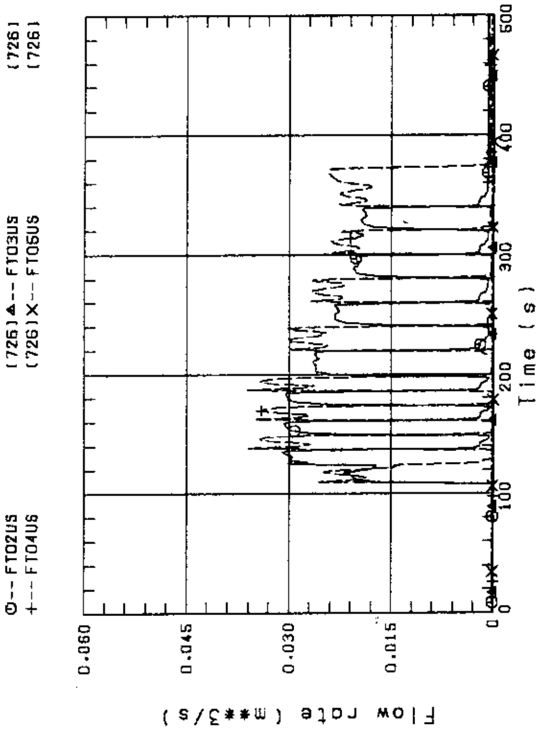

FIG. B-43 FLOW RATE OF UCSP INJECTION LINE-1(BUNDLE7,8),LINE-2(5,6),LINE-3(3,4),LINE-4(1,2)

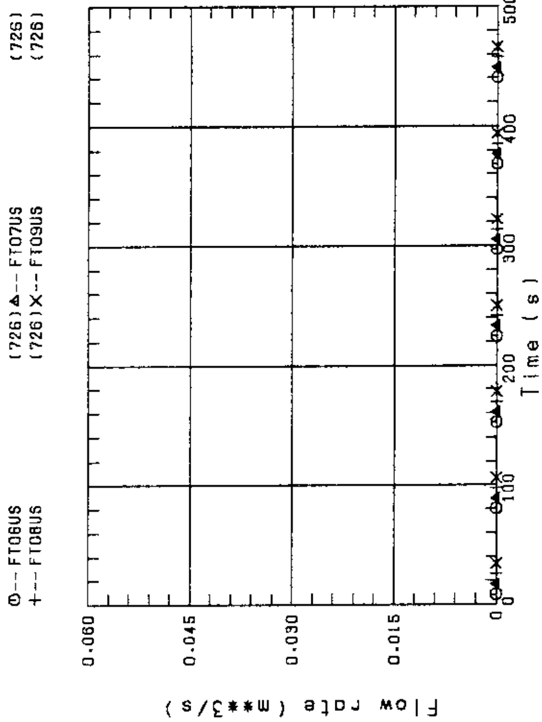

FIG. B-44 FLOW RATE OF UPPER HEAD INJECTION LINE-4(BUNDLE1,2),LINE-3(3,4),LINE-2(5,6),LINE-1(7,8)

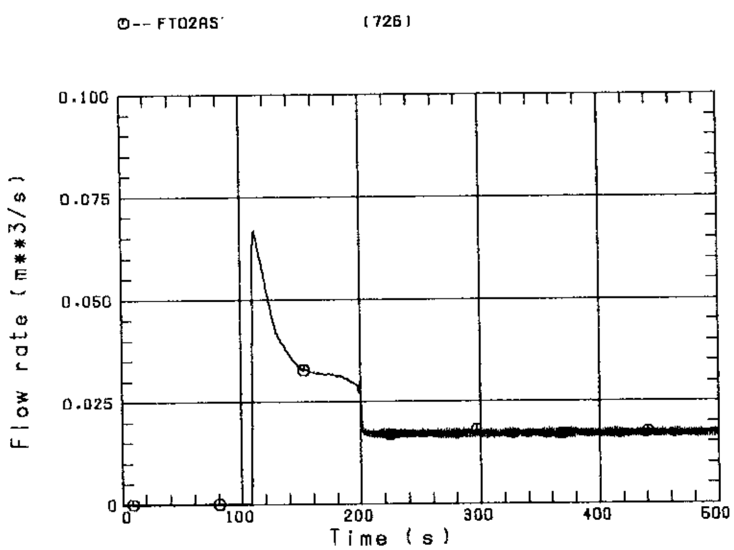

FIG. B-45 FLOW RATE OF ECC WATER (01-LOWER PLENUM, 02-INTACT COLD LEG, 03-BROKEN COLD LEG)

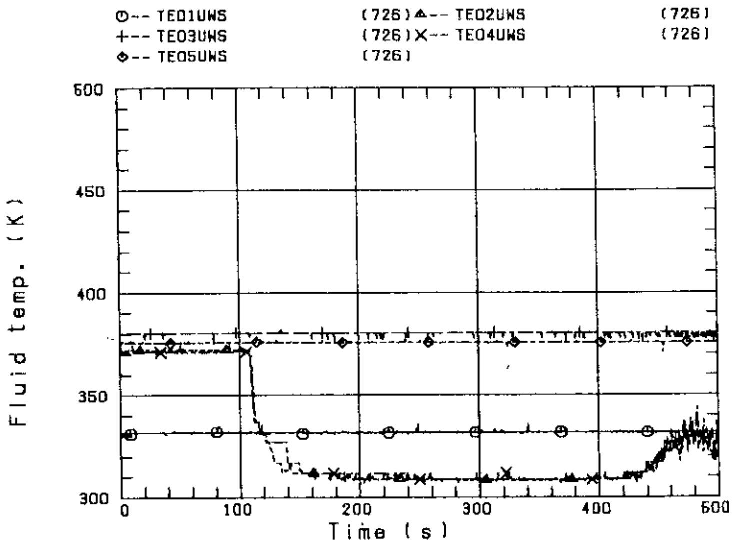

FIG. B-47 FLUID TEMPERATURE IN UCSP INJECTION LINE, 02(BUNDLE7,8),03(5,6),04(3,4),05(1,2),01(LOWER PLENUM)

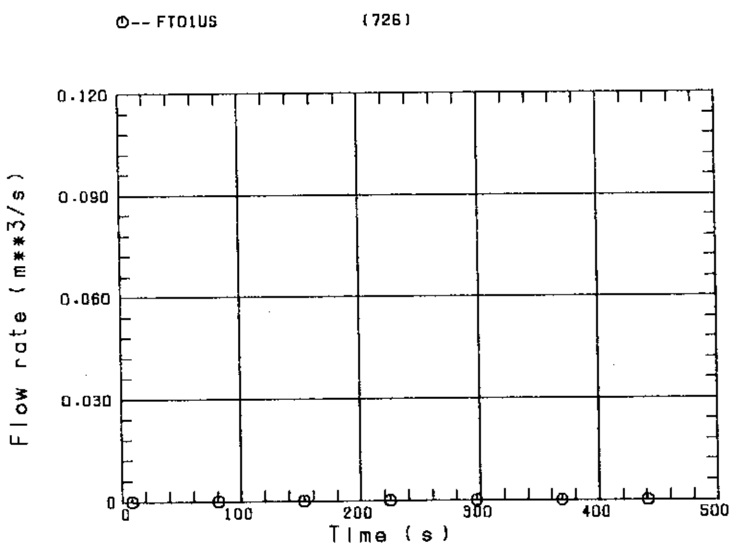

FIG. B-46 FLOW RATE OF LOWER PLENUM INJECTION WATER (ACC HEADER LINE)

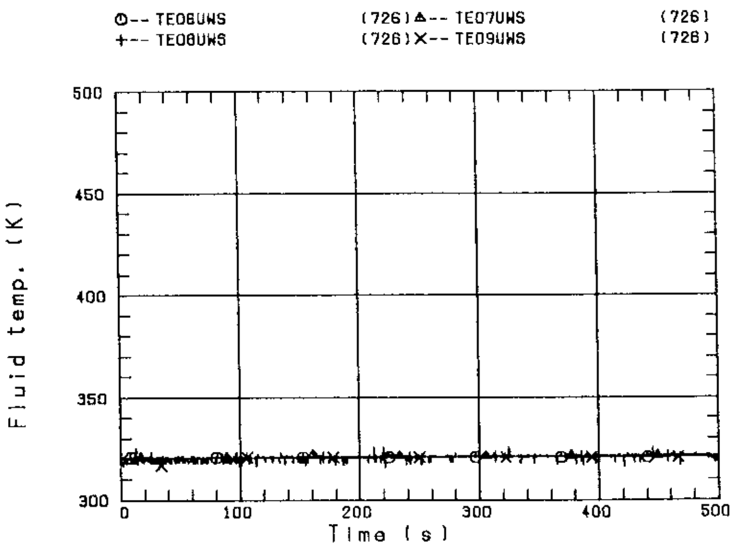

FIG. B-48 FLUID TEMPERATURE IN UCSP INJECTION LINE, LINE-4(BUNDLE1,2),LINE-3(3,4),LINE-2(5,6),LINE-1(7,8)

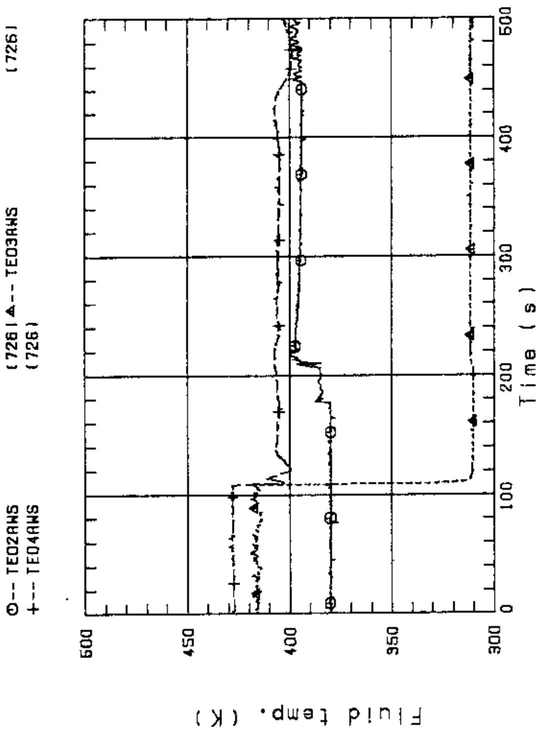

FIG. B-49 FLUID TEMPERATURE IN ECC INJECTION PORT
HOT LEG, IC LEG, BC LEG